ECOHYDROLOGICAL MODELING OF BEAVER DAMS

A Thesis Submitted to the
College of Graduate and Postdoctoral Studies
In Partial Fulfillment of the Requirements
For the Degree of Master of Science
In the Department of Geography and Planning
University of Saskatchewan
Saskatoon, Canada

By
Ignacio José Aguirre Belmar

PERMISSION TO USE

In presenting this thesis in partial fulfillment of the requirements for a Postgraduate degree from the University of Saskatchewan, I agree that the Libraries of this University may make it freely available for inspection. I further agree that permission for copying of this thesis/dissertation in any manner, in whole or in part, for scholarly purposes may be granted by the professor or professors who supervised my thesis work or, in their absence, by the Head of the Department or the Dean of the College in which my thesis work was done. It is understood that any copying or publication or use of this thesis/dissertation or parts thereof for financial gain shall not be allowed without my written permission. It is also understood that due recognition shall be given to me and to the University of Saskatchewan in any scholarly use which may be made of any material in my thesis/dissertation.

DISCLAIMER

Reference in this thesis to any specific commercial products, process, or service by trade name, trademark, manufacturer, or otherwise, does not constitute or imply its endorsement, recommendation, or favoring by the University of Saskatchewan. The views and opinions of the author expressed herein do not state or reflect those of the University of Saskatchewan and shall not be used for advertising or product endorsement purposes. Requests for permission to copy or to make other uses of materials in this thesis in whole or part should be addressed to:

Head of the Department of Geography and Planning
117 Science Place
University of Saskatchewan
Saskatoon, Saskatchewan S7N 5C8 Canada

OR

Dean
College of Graduate and Postdoctoral Studies
University of Saskatchewan
116 Thorvaldson Building, 110 Science Place
Saskatoon, Saskatchewan S7N 5C9 Canada

ABSTRACT

Beavers (*Castor canadensis and C. fiber*) are expanding in their native range in North America and Eurasia and are expanding their range into urban environments and the Arctic tundra. Outside their natural range, they are also in Southern Patagonia because of historic releases in the fur industry. Given the broad geographical span of this expansion, it is critical to understand and predict the hydrology of beaver-dominated landscapes. Beavers build dams that modify the water balance and modulate streamflow through different flow states, which might result in drought and flood mitigation. To date, four published hydrological models have been developed to predict these impacts; however, these models were unable to represent dam variability and dynamics. In this study, a model specific to beaver dams was developed to predict the impacts of beaver dams on hydrology by including the flow state dynamics and the heterogeneity of dams and ponds. First, through the instrumentation of the montane peatland of Sibbald Fen in the Canadian Rocky Mountains, I determined that flow state changes of beaver dams are dynamic on a much shorter scale than previously documented. The shifts from one flow state to another happen regularly, have limited synchronicity within dam sequences, and can be predicted. In Sibbald, 66% to 80% of the flow state changes coincided with rainfall-runoff triggers and no changes were associated with biota using the dams. Following this flow state dynamic, I then developed an open-source model called BeaverPy in Python to simulate key features of dams and their impact on hydrology. Five single flow states and mixed combinations were included to identify their dynamics using a vector-based modeling approach, which accounted for changes in dam structures. Simulating individual and in-sequence dams from Sibbald Fen demonstrated that BeaverPy successfully models streamflow modulation by beaver dams, water storage in ponds, and flow state changes. Metrics for simulated vs. measured behavior for streamflow showed a good agreement in root mean squared error (g in beaver-dominated environments, thereby enhancing the understanding of how to incorporate beaver dams into flood mitigation and stream restoration projects and climate change initiatives.

ACKNOWLEDGEMENTS

LIST OF CONTENTS

LIST OF TABLES

LIST OF FIGURES

LIST OF ABBREVIATIONS

FN	False negative results (confusion matrix)
FP	False positive results (confusion matrix)
FV	Field visits
KGE	Kling-Gupta efficiency
MB	Model Bias
MDv5a	MegaDetector version 5a
MDv5b	MegaDetector version 5b
MLE	Mean log error
NDP	Non-determined periods. Refer to periods of flow state change that could be determined because of vegetation obstructing the lens.
NRMSE	Normalized Root mean square area
NSE_m	Modified Nash-Sutcliffe efficiency
RMSE	Root mean square area
SD	Standard deviation
SE	Southeast section of Sibbald Fen
TN	True negative results (confusion matrix)
TP	True positive results (confusion matrix)
V-A-h	Relationship between volume-area-water level

LIST OF NOTATIONS

A_c	Area of a cross-section
A_x	Area of a porous media
C_b	Proportion of flow state changes coincident with biota able to perform the shift divided by C_v
C_g	Dam gapflow discharge coefficient
C_h	Proportion of flow state changes coincident with precipitation divided by C_v
C_o	Dam overflow discharge coefficient
c_p	Specific heat of air
C_t	Number of flow state changes without exclusions
C_v	Number of flow state changes excluding periods with data
D_g	Division of a dam into G-1 and G-2
D_h	Hydrologically effective height of a beaver dam
D_l	Dam length
D_p	Position of dam in a sequence
D_w	Dam width
e_a	Actual vapor pressure
g	Gravitational constant
e_s	Saturation vapor pressure
$G-1$	Water transmitted by gaps (gapflow state)
$G-2$	Water transmitted by a large gap at the top of the dam (gapflow state)
GW_{ei}	Additional inflow to a linear reservoir when the storage is over the maximum
GW_o	Outflow of a linear reservoir
GW_s	Storage of a linear reservoir
h	Water level in a beaver pond
h_0	Unit height of water surface
h_{max}	Maximum pond depth
H_w	Head (water) above a weir
i	Each pair (simulated/measured) of data
I	Inflow
I_{GW}	Groundwater inflow
I_p	Precipitation over ponds
I_{rp}	Water volume added by precipitation for a specific time
I_s	Surface inflow
J	Water level above D_g
j_e	Outlier weight coefficient in NSE_m
K_g	Permeability of a dam in gapflow state
k_{gw}	Linear reservoir constant
K_{hx}	Saturated hydraulic conductivity of a porous media

K_r	Travel time of the flood wave during routing (Muskingum)
K_s	Permeability of pond sediments (seep flow state)
K_{th}	Permeability of a dam in throughflow state
K_u	Permeability of the lower section of a dam (underflow state)
L_p	Precipitation falling over a pond for a specific time
L_w	Length of a weir
M_1	Modification of flow state by biota using their mechanical abilities
M_2	Modification of flow state change by biota using their weight
n	Manning roughness coefficient
N_f	Number of flow channels (seep flow state)
N_l	Number of equipotential lines (seep flow state)
n_m	Sample size to calculate the metrics
O	Outflow
O_{bd}	Outflow from dams
O_{etp}	Pond evapotranspiration
O_m	Observed/Measured results (BeaverPy)
O_{sp}	Seepage from ponds to aquifers
p	Morphometry coefficient for V-A-h
P_a	Pond area
P_{ma}	Pond maximum area
P_{mv}	Pond maximum volume
P_v	Pond volume
Q	Outflow/Discharge
Q_c	Discharge through a stream cross-section
Q_x	Discharge to the x-direction
R	Hydraulic radius
r_a	Air resistance
R_g	Length of G-2 contracted weir (gapflow state)
R_g	Soil heat flux
R_n	Net radiation
s	Scaling coefficient for V-A-h
r_s	Surface resistance
S_c	Stream slope
S_m	Simulated/Modeled results (BeaverPy)
S_{max}	Maximum storage of a linear reservoir
s_t	Slope of the saturation vapor pressure-temperature curve
t	Time interval
u	Hydraulic depth
U_{et}	Evapotranspiration from vegetation-covered areas.

U_p	Precipitation over vegetation-covered areas
w	Width of a channel
W	Average velocity through a cross-section
X_r	Weight of the outflow during the Muskingum routing
y	Downstream water level
α	Priestly-Taylor coefficient
$\Delta\beta$	Difference between h and y
$\dfrac{\Delta h}{\Delta x}$	Gradient of the total hydraulic head
ΔE	Difference between h and D_h
ΔGF	Difference between h and D_g
ΔS	Change in storage
ΔS_{bd}	Change in storage in beaver ponds
ΔS_v	Change in storage in the vegetation-covered areas
Δt	Change in time
ΔUF	Difference between h and D_t
$\lambda_v E$	Latent heat of vaporization
ρ_a	Air density
σ_S / σ_O	Standard deviation of simulations / observations
γ	Psychrometric constant
μ_S / μ_O	Simulation / observation mean

1. INTRODUCTION

The population of beavers (*Castor canadensis and C. fiber*) is expanding inside and outside their native range. In their native range, beavers have been densifying throughout North America (Hood & Bayley, 2008; Naiman et al., 1988) and Eurasia (Graham et al., 2022; Halley et al., 2012; Neumayer et al., 2020; Pollock et al., 2015), and outside of this territory beavers are spreading to urban settings (Bailey et al., 2019; England & Westbrook, 2021; Westbrook & England, 2022), the Arctic tundra (Foster et al., 2022; Tape et al., 2018, 2021, 2022a, 2022b) and, as consequence of historic fur farming, to Southern Patagonia (García et al., 2022; Huertas Herrera et al., 2020, 2021; Skewes et al., 2006; Westbrook et al., 2017). As a result of the extensive distribution of beavers, it is critical to understand and predict the hydrology of beaver-dominated environments. Beavers build dams that modify water balance and modulate the streamflow, which leads to increased surface and groundwater storage (Johnston & Naiman, 1990; Karran et al., 2018; Westbrook et al., 2006), attenuation of high flows (Puttock et al., 2020; Westbrook et al., 2020) increased precipitation-to-peak flow lag time (Nyssen et al., 2011), and augmentation of low flows (Westbrook et al., 2006). How beaver dams modify the water balance is not fully understood, as beaver dams have high variation in their physical structure (Hafen et al., 2020), which changes over beaver occupancy cycles (Hood, 2020a). A key element to understanding the alteration of hydrological processes by beaver dams is their flow state (Ronnquist & Westbrook, 2021; Woo & Waddington, 1990), which refer to the ways that water flows past each dam structure. For instance, the water can flow over a dam, which is termed "overflow", or through gaps with the flow state termed "gapflow". This approach provides context for an assessment of the dynamics and triggers of change from one flow state to another. It also provides the basis needed to formulate predictions, which can be best performed using models. This thesis addresses this challenge by developing the question of: *How dynamic is the behavior of beaver dams, and how should this dynamism be represented in a hydrological model?*

Beavers build dams to increase water depth until ponds are large enough to serve as a refuge for the beaver colony (Gurnell, 1998). Ponds keep the beaver lodge entrance underwater, thereby increasing access to food resources for the beavers, especially in wintertime (Hood, 2020b). As a result, because beavers adapt construction techniques for different environments, the influence of beaver dams on hydrological processes is not universal. There

is an existing hydrological classification for beaver dams to describe backwater effects, while the flow paths that streamflow takes past a beaver dam are explained by an existing hydrological classification of beaver dams using flow states (Ronnquist & Westbrook, 2021; Woo & Waddington, 1990). Flow state changes can be trigger by biotic, hydrologic, or geomorphic elements (Ronnquist & Westbrook, 2021). These key mechanisms and their dynamics have not yet been incorporated into hydrological models, which limits the prediction capabilities of these models in beaver-dominated environments. Previous attempts to simulate the impacts of beaver dams using models (Beedle, 1991; Caillat et al., 2014; Neumayer et al., 2020; Noor, 2021) only used one flow state, and the shifts from to another were not implemented. Modeling the impacts of beavers on hydrology is needed to understand and quantify the alteration to water budgets from beaver activities, and our ability to measure how beaver dams in particular increase the resilience of catchments (Auster et al., 2021; Brazier et al., 2021). More recently there is a need to understand how beaver dams can be used in climate change mitigation initiatives (Jordan & Fairfax, 2022).

The overarching goal of this thesis is to examine how beaver dams can be incorporated into hydrological models to develop accurate hydrological predictions. There are two questions asked in the thesis to meet this goal. The first one asks how dynamic flow state changes are, and which variables are driving this change. The objectives to address this question relate to quantifying the temporal variability of flow states using field data and camera traps following the classification of Ronnquist & Westbrook (2021) and Woo & Waddington (1990) and are to: 1a) quantify the temporal variability of flow state of beaver dams; and 1b) assess the relative importance of rainfall vs. biotic drivers in regulating flow state changes of beaver dams. The second question builds on the outcomes from question one and focuses on how to represent streamflow modulation and water storage dynamics of beaver dams and their flow states using a physically based modeling approach. The objectives to answer this question are to: 2a) build an open-source model to route streamflow through beaver-dominated landscapes; and 2b) demonstrate the model using individual and in-sequence dams.

1.1 THESIS ORGANIZATION

This research was written in manuscript style, and it is comprised of five chapters. Chapter 1 includes the Introduction and Objectives. Chapter 2 is a literature review covering beavers, dam construction, flow states, hydrological impacts of beaver dams, and previous modeling approaches. Chapter 3 focuses on question one, the short-term dynamics of beaver dam flow states based on research conducted in Sibbald Fen, a montane peatland in the Canadian Rocky Mountains. Chapter 4 focuses on question two, model representation of streamflow routing through beaver-dominated environments. Neither Chapter 3 or 4 were published at the time of thesis defence. Finally, the thesis concludes with Chapter 5, which synthesizes the research and its main implications.

2.   LITERATURE REVIEW

This literature review provides insight into beaver behaviors and synthesizes the current understanding of how beavers impact catchment water balances. The review then describes the simulation of beaver impacts into hydrological models and their limitations.

2.1. BEAVERS

2.1.1. Background on beavers

Beavers are semi-aquatic mammals of the order Rodentia (Hood, 2020b). There are two species of beaver with different geographic distributions. The North American beaver (*Castor canadensis*) is endemic to North America and the range of the Eurasian beaver (*C. fiber*) extends from the British Isles, across northern Europe, into Mongolia (Hood, 2020b). On average, beavers weigh around 30 kg and are approximately 120 cm long. It is the second large rodent after capybara of South America (Hood, 2020b).

According to Ernest Thompson Seton, there were around 60 to 400 million beavers in North America pre-European contact (Naiman et al., 1988); then, numbers began to decline since the 17th century because of over-harvesting during the fur trade. Today, with environmental regulation and a relative absence of predators, their populations have increased considerably, reaching an estimated 6 to 12 million in the 1980s with continued increases globally (Hood, 2011; Naiman et al., 1988; Whitfield et al., 2015)

Beavers are herbivores with a central-place foraging strategy of browsing and consuming plants, stems, twigs, buds, and leaves (Hood, 2020b). Their diet is broad, and they consume several plant species that provide necessary micronutrients. Poplar (*Populus sp.*) and willow (*Salix sp.*) are preferred forage species in many parts of its range (Hood, 2020b). Beavers do not eat wood, instead they store woody stems, from which they eat the bark and stems, at the entrance of their lodges to create a winter food cache (Hood, 2020b).

Due to their ability to change the aquatic environments in which they live, they are called ecosystem engineers. They are also identified as a keystone species because of their disproportionate effect on the ecosystem, above even their own needs (Hood, 2020b; Rosell et al., 2005; Touihri et al., 2018). According to Paine (1966, 1969), the loss of a keystone

species generates a decay in the ecosystem and a loss of diversity. Currently, both species of beavers are central to several aquatic ecosystem conservation efforts, including monitoring, habitat protection, and management (Gibson & Olden, 2014; Hood, 2011, 2020b).

2.1.2. Beaver behavior and associated models

Beavers build dams as a strategy to increase water depth until they create ponds large enough to serve as a refuge (Gurnell, 1998). Beavers choose to live in sites with as high as fourth-order streams (Westbrook et al., 2006) and waterways with a depth generally less than 68 cm (Swinnen et al., 2019). Mainly, wood, mud, and stones are used to build the dam, and the proportion of these materials depends on their availability in each place (Ronnquist & Westbrook, 2021). Building a beaver dam is based on the principle of reducing water velocity to facilitate its construction and begins with an anchor point such as fallen trees or downed logs (Beedle, 1991). Then, beavers continue to place branches roughly perpendicular to the flow direction, thereby reducing flow velocity and continuing until the beaver dam often acquires a U-shape in the upstream direction (Beedle, 1991; Ronnquist, 2021)

Beaver dams can be directly on the watercourse (in-channel) or disconnected (off-channel). There may be as few as one dam per stream in the former case or there may be more than ten dams per km under the optimum conditions (Woo & Waddington, 1990). These systems or sequences of dams may offer greater capacity for flood mitigation, although the breach of one dam could generate problems downstream (Westbrook et al., 2020). Isolated beaver ponds can occur more than 2 km away from the watercourse, for example in peatlands (Stoll & Westbrook, 2020), although other variables such as distance to food sources, slope, and percentage of grassland must be considered (Hood, 2020a).

Macfarlane et al. (2017) developed the Beaver Restoration Assessment Tool (BRAT) model to predict where beavers could build dams and their spatial range considering distance to water source, vegetation useful to dam building, channel size, and topographical gradient. Stoll & Westbrook (2020) used this model in Riding Mountain National Park, Manitoba, Canada, and the algorithm of Karran et al. (2017) to conclude that the park can support 24,690 beaver dams and hold between 8.2 and 12.8 million m^3 of water in beaver ponds.

2.2. EFFECTS OF BEAVERS ON THE HYDROLOGY OF RIVER CORRIDORS

The hydrology of stream systems is altered by beaver dams. Beaver dams and their associated ponds increase the depth, duration, and extent of surface inundation (Morrison et al., 2015; Westbrook et al., 2006). Ponding of water behind beaver dams raises the hydraulic head of the stream reach which generates enhanced surface and subsurface water exchange of the stream with its floodplain (Janzen & Westbrook, 2011; Lautz & Siegel, 2006). The effect of this is maintained or elevated water tables in the riparian area. In addition, beaver dams can trigger overbank flooding during high flows. In broad valleys, some of this water can flow kilometers downstream before the flow returns to the channel (Westbrook et al., 2006). In this way, beavers play an important role in the maintenance of wetland conditions in riparian areas (Hood & Bayley, 2008; Westbrook et al., 2006).

Beaver dams are different from human-constructed earthen dams in terms of their form and the way they influence stream hydrology. Earthen dams are built by compacting successive layers of sediments with more impervious sediments at the core/foundation of the dam and more permeable materials on the outer faces that permits seepage (Talukdar & Dey, 2019). In contrast, beaver dams are built by beavers using a variety of local materials including wood (logs, branches, twigs), channel and bank sediment, and rocks (Gurnell, 1998). Many earthen dams are accompanied by a spillway to protect against catastrophic washout. Because of their differences in form, beaver dams and earthen dams affect streamflow differently (Auster et al., 2022; Czerniawski & Sługocki, 2018). For example, beaver dams are permeable, and have temporally variable outflow mechanisms (Woo & Waddington, 1990) where water can flow over the dam, through the dam, under the dam, or a mixed combination, the heterogeneity within the structure (i.e., a wide range of shapes, varying width, lengths, and materials). In contrast, (here give a sentence on how streamflow is affected by earthen dams given that the goal of building them is create a water pool upstream).

By enhancing open water extent (i.e., surface water storage), beaver dams can increase evapotranspiration both in stream channels and in riparian areas. For example, Woo & Waddington (1990) studied the water balance of two catchments, one with a beaver dam at its outlet and another without a dam in northern Ontario, Canada. They determined that the dammed basin had greater evaporation. Burns & McDonnell (1998) used isotope-tracers to

show higher summer evaporation in streams with beaver dams, with the greatest differences occurring at high flows rather than low flows. Fairfax & Small (2018) studied the influence of beaver damming on evapotranspiration in Nevada, USA using the Penman-Monteith equation and a modelling (METRIC) approach. They showed that riparian evapotranspiration was higher in areas near beaver dams by between 50 and 150%.

Beaver dams also modify the streamflow regime. Streamflow modulation consists mainly of the paradoxical attenuation of high flows and increase in low flows (Green & Westbrook, 2007; Nyssen et al., 2011). These effects are particularly noticeable in flooding or drought (Hood & Bayley, 2008; Westbrook et al., 2006, 2020). For example, Nyssen et al. (2011) documented how beaver dams create a one-day delay in the peak flow and increased the streamflow from 0.6 m^3s^{-1} to 0.88 m^3s^{-1} in a 317 km^2 basin in Belgium. In England, Puttock et al. (2020) described changes in flow regimes since the reintroduction of beavers at four sites in England and compare both spatial and temporal variation. Using a Before-After-Control-Impact (BACI) methodology, they observed a reduction in flow of 17% in the dry season and 62% during the wet season after beaver reintroduction. Additionally, they observed that the presence of beaver dams reduced both stormflow and flashiness and increased lag time, which is explained by an increase in storage in the basin. In Canada, Westbrook et al. (2020) studied the fate of beaver dams and the ability of dams to attenuate streamflow during the largest (at the time) flood event. They rejected two long-held hypotheses about the response of dams to extreme rainstorms. First, they showed that dams do not have limited attenuation capacity; instead, storage was considerable, especially in dam sequences, and second, they determined that the majority of dams did not fail.

Figure 2-1 represents a synthesis of the studies mentioned. The figure highlights the scale issues (space and time) of the impact of beaver activities on water balance following the framework developed by Blöschl & Sivapalan (1995). From a spatial perspective, most of the studies I reviewed address small scales between 100 m and 1000 m, using research basins where certain processes can be measured with high-resolution observations such as Sibbald Fen in the case of Janzen & Westbrook (2011), Streich & Westbrook (2020), and Westbrook et al. (2020). Nevertheless, some researchers use broader scales, such as Hood & Bayley (2008) and Stoll & Westbrook (2020), who utilized a landscape scale. From a temporal viewpoint, most studies use scales between one hour and one day, such as Burns &

McDonnell (1998), Nyssen et al. (2011), and Woo & Waddington (1990); although some studies are more focused on seasonal variations like Westbrook et al. (2006).

Assessing the influence of beavers on hydrology requires a small spatial scale where water table, evapotranspiration, streamflow, and storage can be measured in detail. Research questions related to flow modulation in flooding scenarios apply to smaller temporal and spatial scales, while studies focused on drought opt for larger spatial and temporal scales. Hourly time steps allow the quantification of effects such as delay-to-peak, peak channel storage, and peak discharge, thus enabling calculations related to the effects of beaver dams during and after storms.

1.	Neumayer et al. (2020)	8.	Westbrook et al. (2020)
2.	Fairfax & Small (2018)	9.	Westbrook et al. (2006)
3.	Janzen & Westbrook (2011)	10.	Hood & Bayley (2008)
4.	Ronnquist & Westbrook (2021)	11.	Puttock et al. (2017)
5.	Woo & Waddington (1990)	12.	Puttock et al. (2020)
6.	Streich & Westbrook (2020)	13.	Burns & McDonnell (1998)
7.	Stoll & Westbrook (2020)	14.	Nyssen et al. (2011)
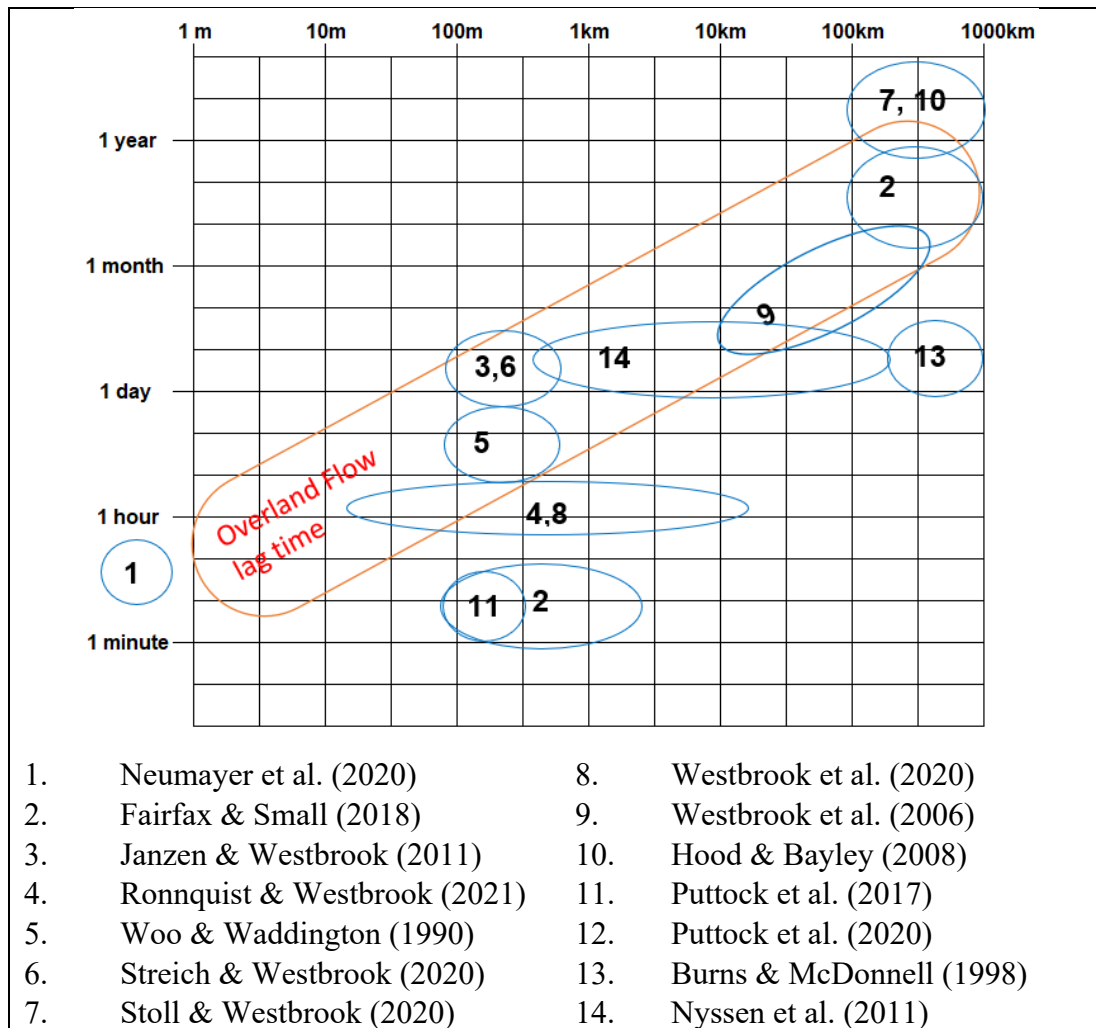
Figure 2-1 Focus of studies of beaver hydrology, overlaid on the time-space framework of Blöschl & Sivapalan (1995). Overland flow is presented as a reference (Blöschl & Sivapalan, 1995).

Regulating dam backwater effects (Burchsted et al., 2010; Ronnquist & Westbrook, 2021) and the flow paths that streamflow takes past a dam (Brazier et al., 2021) is in part regulated by dam water tightness. Aspects of dam structure like wood-to-sediment ratio influence its water tightness (Woo & Waddington, 1990). Streamflow can move past a dam by overtopping it (overflow), funneling through gaps in it (gapflow), seeping through its pores (throughflow) or leaking through its base (underflow) (Woo & Waddington, 1990; Figure 2-2). Ronnquist & Westbrook (2021) observed that streamflow could also move past a dam by looping beneath it through the hyporheic zone (seep flow) or flowing past it via simultaneously flowing along two or more of the paths previously described (mixed) (Figure 2-2). Each path interrupts downstream water transmission in different ways that we are just beginning to understand.

Woo & Waddington (1990) explained that path differences were due to the physical condition of the beaver dam as impacted by the degree of beaver maintenance. In their framework, the primary driver of changes in the flow state of beaver dams is beaver activity and, therefore, newly built dams are the overflow type, with an active role of beavers in dam maintenance. As dams become older, they might occasionally sustain small breaches during high flows and transiently be in the gapflow type until the holes are repaired by beavers. Alternatively, the base of the dam might weaken, permitting a change to underflow type. When dams are abandoned by beavers, they decay and the interstitial mud becomes washed away, thereby permitting water flow through the entire dam structure (throughflow type). Ronnquist & Westbrook (2021) broadened this perceptual model by hypothesizing that various mechanisms can also affect the way water moves past a beaver dam on much shorter time scales. Their perceptual model included a hydrological mechanism that increases (rainfall) or decreases (evaporation) pond levels, a hydrogeomorphic mechanism (dam erosion during high flows), and a biological mechanism (beaver activity). To reflect that dam flow types are dynamic, shifting over the beaver occupancy cycle of a dam and also hypothetically shifting over the course of a summer, the hydrological classification is referred to as the *flow state* of a beaver dam (Ronnquist & Westbrook, 2021; Woo & Waddington, 1990).

Overflow	Gapflow	Through flow

Underflow	Mixed	Seep
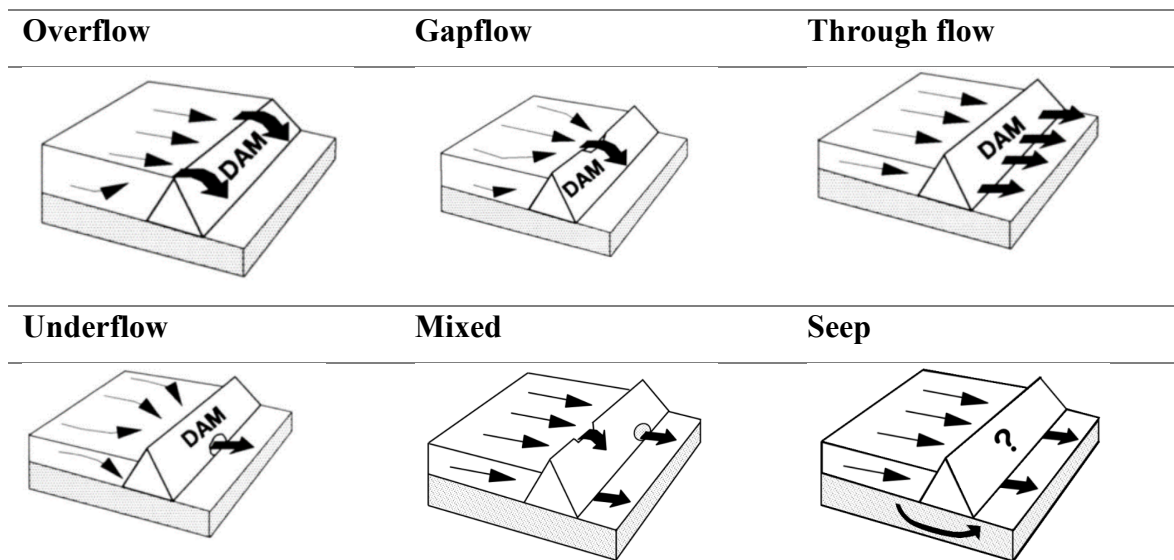
Figure 2-2 Flow states for beaver dams. Overflow, gapflow, through flow and underflow were defined by Woo & Waddington (1990) and mixed and seep flow were developed by Ronnquist & Westbrook (2021). Source: Ronnquist (2021). Table modified from the original.

2.3. ECOHYDROLOGICAL MODELING OF BEAVER DAMS

Representing beaver dams in ecohydrological models is a formidable challenge because their influence on ecohydrological processes is not universal (e.g., Figure 2-2). There is not a direct equivalent of water routing through beaver ponds in hydraulic engineering (Beedle, 1991). Given the complexity of this endeavor, there have only been four attempts thus far, beginning with Beedle (1991), then Caillat et al. (2014), Neumayer et al. (2020), and Noor (2021). Each of the approaches used in these studied is briefly reviewed and compared.

Beedle (1991) developed the first model using the Modified Puls method, executed within a PC spreadsheet. Beedle simulated the effect of 44 dams on runoff at the catchment outlet. The inflow was calculated from a 5-year storm event near the watershed and processed with a triangular-shaped hydrograph. Outflows were calculated by considering beaver dams as broad crest spillways, meaning that all dams were modeled as being in the overflow state (Ronnquist & Westbrook, 2021; Woo & Waddington, 1990). In the overflow state, discharge occurs only if the pond water level is higher than the dam height, with the beaver dam represented as an impermeable barrier. Using this approach, Beedle developed a single relationship between storage and outflow. As a result, the inflow and outflow hydrographs

shared the same shape for every beaver dam, i.e., the lag time to peak flow ranged between 10 and 15 min, and the peak flow attenuation was 5.3%. To examine the influence of multiple beaver dams in sequence, Beedle simply considered a direct relationship between the reduction in peak flow and the number of ponds. Two important shortcomings of the approach used by Beedle (1991) included that: 1) field observations indicate it is not realistic to represent storage-outflow links with a single relationship given that six flow states of beaver dams have been described (Ronnquist & Westbrook, 2021; Woo & Waddington, 1990); and 2) seepage and evapotranspiration, both which have been shown to be important along beaver dam sequences (Larsen et al., 2021), are ignored.

Caillat et al. (2014) and Noor (2021) used a different approach from that employed by Beedle (1991) to simulate the influence of beaver dams on streamflow. They first ran the BRAT model (Macfarlane et al., 2017) to determine the capacity of the stream network to support beaver dams. They followed beaver dam capacity modelling with simulation of beaver dam impacts on streamflow using HEC-HMS (U.S. Army Corps of Engineers, 2022). Both studies set a fixed rate for seepage and evapotranspiration in the modeling. Caillat et al. (2014) modeled 42 dams on the Jemez Watershed, where there is a current beaver population, and reported a 5 to 30% attenuation of peak flow in spring and summer. Given that all dams were numerically represented the same way in the model, all simulated output hydrographs had the same shape and timing, varying only in magnitude based on streamflow inputs. Noor (2021), using the same methodology, modeled 42 dams on the Milwaukee River and reported an average peak flow reduction between 11% and 48% and a peak volume reduction between 15 and 48%.

Neumayer et al. (2020) introduced a different approach to those used previously in modelling the influence of beaver dams on streamflow. Neumayer et al. began by conducting a photogrammetric survey to assess the stream and beaver dams and determined that sequences contained between two and eight dams. All dams were modeled as in-stream leaky barriers without explicitly representing upstream water storage in beaver ponds. The solution to simulate beaver dam leakiness was to use many small, round, unobstructed culverts (up to 70 per dam), placed parallel to the flow direction, to create a way to vary dam permeability. Effectively, the Neumayer et al. approach involved representing beaver dams in the throughflow state and the throughflow plus overflow flow states (Ronnquist & Westbrook,

2021; Woo & Waddington, 1990). There were two modeling scenarios: 1) fully maintained dams characterized by low permeability and a freeboard between 0.05 m and 0.15 m, and 2) rarely maintained dams characterized by high permeability and a freeboard between 0.35 m and 0.45 m. Neumayer et al. (2020) observed no significant effects of beaver dams on peak and peak delay on return periods greater than two years. Simulations with beaver dams showed larger flooded areas (>300%) than simulations without beaver dams. The peak attenuation was calculated up to 13.1%, and the peak delay was ~3 h.

The four beaver dam implementations described above used platforms developed for general purposes even though Beedle (1991) acknowledged that a direct equivalent of water routing through beaver ponds in hydraulic engineering does not exist. For example, three of the studies used modules created to represent human-made reservoirs even though the associated human-made dams have a static structure, whereas beaver dams have a dynamic structure owing to beaver rearrangement of branches, sediment accumulation on the upstream face of the dam or becoming lodged in the interstitial space, high flows mobilizing dam materials, or the biotic action of animals other than beaver compressing or removing dam materials (Ronnquist & Westbrook, 2021). While the previously mentioned models were able to creatively adapt existing engineering hydrology tools to represent beaver dams, they were unable to represent key dynamic features of beaver dams, such as the change between flow states and the role of biotic drivers (Ronnquist & Westbrook, 2021).

In addition, these four model implementations examined only one type of beaver dam scenario – dams built on stream channels–, and it is needed to recognize that beavers build dams in a variety of habitats, including the damming of seepage. Moreover, beaver dams exhibit a broad range of conditions that affect their impacts over the catchment. For instance, beavers in peat-dominated conditions (Ronnquist & Westbrook, 2021; Westbrook et al., 2020) drive a significant exchange of groundwater-surface water (Streich & Westbrook, 2020), which is different for beaver in mineral-dominated conditions or karst (Cowell, 1984). Another example is how dam height is considered in models. Dam height has been set to local conditions, between 0.12 m and 0.9 m (Noor, 2021) or 0.37 m to 1.18 m (Beedle, 1991). However, many studies have reported beaver dam heights exceeding 2.0 m (Demmer & Beschta, 2008; Hafen et al., 2020; Karran et al., 2017; Ronnquist & Westbrook, 2021). Therefore, modelling efforts need to include a more realistic range in beaver dam height.

2.4. RESEARCH GAP

Recent efforts to represent the hydrological impacts of beaver dams on streamflow and water storage have culminated in four models (i.e., Beedle, 1991; Caillat et al., 2014; Neumayer et al., 2020; Noor, 2021). These studies have provided invaluable base knowledge; however, they were unable to incorporate key dynamic characteristics of beaver dams such as variable dam flow states (Ronnquist & Westbrook, 2021; Woo & Waddington, 1990). They were also not able to capture the heterogeneity of dams and ponds (Hood, 2020b; Hood & Larson, 2015; Karran et al., 2018). They used hydrologic platforms developed for general purposes, although Beedle (1991) recognized the lack of equivalent for water routing through beaver dams in hydraulic engineering. For example, Beedle (1991), Caillat et al. (2021), and Noor (2021) used a module written to simulate human-made reservoirs regardless that reservoirs have a static structure in contrast to a beaver dam, which experiences a continuous change in their structure (Hafen et al., 2020) which is ultimately linked to occupancy cycles (Hood, 2020). The path that streamflow takes past a beaver dam is hypothesized to be influenced by factors such as structural changes made by animals such as beavers, hydrological events like rainfall-runoff, and hydrogeomorphic events like erosion of sediment and/or woody material during flood events (Ronnquist & Westbrook, 2021). These previous modeling attempts also needed to adapt their approaches with resourcefulness, such as Neumayer et al. (2020) which to represent the throughflow state set up non-obstructed round culvert throughout the dam (up to 70).

The models selected by Beedle (1991), Caillat et al. (2014), Neumayer et al. (2020), and Noor (2021) were limited to represent the heterogeneity of ponds, thus leading to inaccurate pond volume assessment. Hood (2020a) and Hood & Larson (2015) have reported the broad variability of beaver ponds, both active (i.e., with beaver presence/maintenance) and inactive, which can be accurately determined using the methodology developed by Karran et al. (2017). Another example is dam height, which Noor (2021) reported as ranging from 0.12 to 0.9 m and Beedle (1991) reported as ranging from 0.37 to 1.18 m. However, several field-based studies have reported dams with heights exceeding 2.0 m (Demmer & Beschta, 2008; Karran et al., 2018; Ronnquist & Westbrook, 2021). Overall, previous model implementations have taken a limited worldview of beaver dams – small ones built on stream channels that have a set path that streamflow can take past them.

One potentially fruitful approach to more realistically representing beaver dams in (eco)hydrologic models is to use a physical-based model that considers dam heterogeneity and flow state dynamics. Flow states are reported in the literature as dynamic (Woo & Waddington, 1990), with the shifts from one to another linked to beaver occupancy cycles (Johnston & Naiman, 1987, 1990). Further, it has been hypothesized that shifts in the flow state of beaver dams can also occur on much shorter time scales via biotic, hydrologic, and geomorphic factors. Whether the flow state of beaver dams change over the course of a the ice-free period has yet to be studied, which limits our ability to determine the best way to represent beaver dams in hydrological models. Having a model capable of predicting flow regulation by beaver dams will allow for the evaluation of the effects of beaver dams on river restoration and mitigation plans in a more realistic way.

3. ARTICLE I: SHORT-TERM DYNAMICS OF BEAVER DAM FLOW STATES[1]

3.1. INTRODUCTION

Stream practitioners have newfound interest in implementing beaver- (*Castor canadensis and C. fiber)* based stream restoration (Conlisk et al., 2022; Pollock et al., 2015; Whitfield et al., 2015) and climate change mitigation initiatives (Jordan & Fairfax, 2022). This is because beavers build dams that modify the water balance in ways that increase catchment resilience, with positive benefits to the ecosystem and communities (Auster et al., 2021; Brazier et al., 2021; Charnley et al., 2020; Jordan & Fairfax, 2022; Larsen et al., 2021; Thompson et al., 2021). During high flows, beaver dams attenuate the flow and increase the lag time (Nyssen et al., 2011), even during large storms (Westbrook et al., 2020). During low flow, beaver dams increase groundwater recharge and baseflow (Westbrook et al., 2006). Beaver dams also augment basin water storage (Woo & Waddington, 1990), open water availability (Hood & Bayley, 2008), and local evapotranspiration (Fairfax & Small, 2018). How beaver dams modify components of the water balance is not fully understood as beavers have a broad geographic range and beaver dams have high variation in physical structure (Hafen et al., 2020), which changes over beaver occupancy cycles (Hood, 2020a) and influences the ways that water flows through each dam structure (Ronnquist & Westbrook, 2021; Woo & Waddington, 1990)). Without a clear understanding of the flow state dynamics of beaver dams, it is difficult to understand the impact they have on the hydrology of river systems.

Beaver dams are built to increase water depth until ponds large enough to serve as a refuge are created (Gurnell, 1998). The pond keeps the beaver lodge entrance underwater. This increases beaver access to food resources especially in wintertime (Hood, 2020b), providing

a secure method to feed their families while increasing their survival rate when hunted by their main predators (wolves (Canis lupus; Gable et al., 2016; 2018a, 2018b; Gable & Windels, 2018) and wolverines (*Gulo gulo*; Scrafford & Boyce, 2018)). Beavers prefer streams as high as fourth-order (Naiman et al., 1988; Westbrook et al., 2006) and shallow, gently-sloping waterways (Swinnen et al., 2019) as places to build dams. Beaver dams can also be located off-channel in wetlands (Johnston & Naiman, 1990; Naiman et al., 1988; Stoll & Westbrook, 2020), on lakeshores (Gurnell, 1998), in ponds (Hood & Bayley, 2008), and in human-built drainages (Bailey et al., 2019). Dams are composed mainly of wood, soil, and stones; the exact proportion of each building material depends on their local availability and landscape setting (Beedle, 1991; Ronnquist & Westbrook, 2021).

The process of dam building on a waterway begins by establishing an anchor point, for example, coarse woody materials already present in the channel. Then, beavers continue to place branches in the same flow direction, which reduces flow velocity that continues until the beaver dam acquires a U-shape in the upstream direction (Beedle, 1991). Once built, the structures can passively capture woody materials and sediment entrained in the flowing stream (Blersch & Kangas, 2014). In peatlands, beavers tend to excavate soil and pile it in berm-like fashion to construct a dam that intercepts groundwater flow (Karran et al., 2018). While beaver dams are highly diverse in physical form and are dynamic structures in terms of how water is routed past them, beaver dams can be characterized by their physical and/or hydrological properties. Beaver dams were originally categorized according to their capacity to hold water and the degree to which beavers participate in dam maintenance (Johnston & Naiman, 1987, 1990; Johnson-Bice et al., 2022). Dams were categorized in this way because the degree to which beavers maintain dams has been associated with the probability of their failure. Dams that are actively maintained by beavers tend to have a lower chance of breaching during high discharge events, whereas dams no longer being maintained by beavers have a higher probability of breaching during high discharge events (Butler & Malanson, 2005).

Woo & Waddington (1990) categorized beaver dams by their hydrology. They suggested four categories based on the path that streamflow takes as it passes by a dam: water flowing over the top of the dam (overflow), water flowing through gaps (gapflow), water flowing through the base of the dam (underflow), and water flowing through the dam pores

(throughflow). Ronnquist & Westbrook (2021) added two categories to the Woo & Waddington categorization: water flowing beneath the dam structure (seep flow) and water flowing past the dam via two or more categories (mixed flow). Woo & Waddington (1990) further proposed a succession of flow types as dams age. In their framework, the primary driver of changes in the flow state of beaver dams is beaver activity and, therefore, the flow state change of beaver dams aligns with beaver site occupancy. Newly built dams are the overflow type, with an active role of beavers in dam maintenance. As dams become older, they might occasionally sustain small breaches during high flows and transiently be in the gapflow type until the holes are repaired by beavers. Alternatively, the base of the dam might weaken, permitting a change to the underflow type. When dams are abandoned by beavers, they decay and the interstitial mud becomes washed away, permitting water flow through the entire dam structure (throughflow flow type). Neumayer et al. (2020) noted that younger dams can effectively impound water and modulate discharge; however, as dams age, their capacities to alter the streamflow and storage are diminished.

Ronnquist & Westbrook (2021) challenged the conceptualization of the mechanisms that drive flow state changes for beaver dams. They proposed three mechanisms that trigger a change between one flow state and another: biotic activity, specifically the dam building and repair actions of beavers; geomorphic activity, such as erosion or sedimentation processes; and hydrologic activity, for instance, the occurrence of rainfall- or snowmelt-runoff events that increase stream discharge and pond water level. Other researchers have also made statements suggestive of a hydrological trigger of dam flow state change. For example, Butler & Malanson (2005) and Devito & Dillon (1993) described streamflow as exceeding the dam crest during rainfall-runoff events. Although Ronnquist & Westbrook (2021) described only beavers as biota that influence dam structure, beaver dams serve as important ecological corridors for a variety of mammals to traverse water barriers (Hood, 2023; Wikar & Ciechanowski, 2023). It is plausible that some of the mammals that traverse beaver dams have a sufficiently heavy paw/hoof print (Lundmark & Ball, 2008), for example bears (*Ursus americanus*) and moose (*Alces alces*), to modify beaver dam structure in ways that could trigger a change in the flow state. If hydrological or biotic activity can trigger changes in the flow state of beaver dams, it is likely that beaver dams change flow state much more frequently than simply among the different occupancy stages of a beaver dam site.

Given the widespread interest in using beavers to assist with mitigating climate change impacts and restore stream function (Jordan & Fairfax, 2022), it is imperative to understand and predict the magnitude of influence beaver dams have on streamflow mitigation better. As each dam flow state interrupts downstream water transmission in different ways and leads to different water retention capacity and flow mitigation potential (Ronnquist & Westbrook, 2021), it is also critical to quantify the hydrological behavior of beaver dams in relation to their flow state (Brazier et al., 2021). This study evaluated how often changes in the flow state of beaver dams occur and possible triggers for those changes. This study evaluated how often changes in the flow state of beaver dams occur and possible triggers for those changes. It was hypothesized that the flow state of beaver dams could change multiple times over the ice-free period in response to rainfall-runoff events, beaver modification of dam structure, and wildlife crossings.

3.2. METHODS

3.2.1. Study area

The study was conducted on a sequence of three beaver dams in Sibbald Fen, a montane peatland in the Canadian Rocky Mountains approximately 70 km west of Calgary, Alberta (Figure 3-1; Westbrook & Bedard-Haughn, 2016). Sibbald Fen is 2.1 km long, 0.4 km wide on average, varies 34 m in elevation from north to south, and is adjacent to forested foothills (Streich & Westbrook, 2020). The fen is capped by peat, which is thin (<0.5 m) in the northern zone of the fen, and deeper (up to 6.5 m) peat in the central zone (Streich & Westbrook, 2020). The regional climate has a strong seasonal component with warm summer temperatures, variable rainfall, lower humidity and cold winters with abundant snowfall and higher humidity. In winter, large temperature swings can occur due to Chinooks (warm dry winds) coming from the west (Streich & Westbrook, 2020). Bateman Creek, a third-order tributary of Jumpingpound Creek, drains the fen and flows into Jumpingpound Creek and the Bow River.

Based on air photo analysis, beavers reoccupied in this peatland by 1958 following the fur trade (Karran et al., 2018). They intermittently occupy and abandon dam sites depending on

hydroclimate conditions and riparian vegetation availability (Westbrook et al., 2020). At the time of this study there was an active beaver colony in the southeast drainage of the fen.
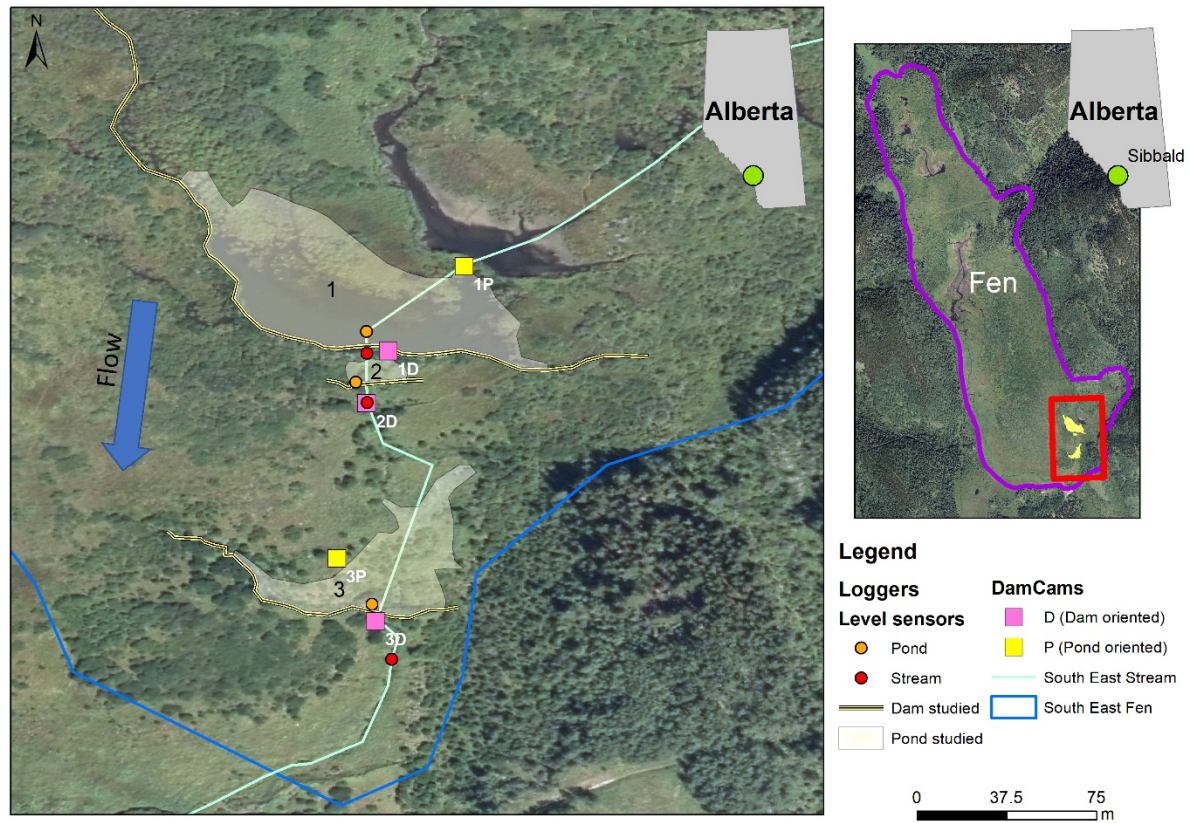
Figure 3-1 Map of the study area. The map depicts the southeast portion of Sibbald Fen, showing the three dams in this study and their ponds numbered from upstream to downstream. Each camera trap is represented with a square, pink for cameras oriented to capture the dam's key hydrological features (D) and yellow for cameras oriented to capture the pond's wildlife interactions (P). Level sensors are represented with circles, red for ones located on the stream, and orange for others on the ponds. The watershed boundaries were delineated with a 1.0 m resolution LIDAR imagery collected on June 16, 2022 by members of the Centre for Hydrology of the University of Saskatchewan. The blue arrow indicates the flow direction of the SE stream. The inset map shows the beaver dam sequence (yellow) studied within the Peatland (purple). Both maps include the Canadian province of Alberta and the location of Sibbald within the Canadian Rocky Mountains (green dot).

The southeast drainage of the fen is 10.4 ha, based on 1 m LIDAR delimitation collected on June 16, 2022, and the stream has a contributing area of 228.1 ha. Beavers have extensively modified this drainage, and there were >25 beaver dams at the time of the study. Three dams were selected in sequence for the study, all of which were built with a varying mud, peat, and branches across the stream channel (Table 3-1; Figure 3-1).

Table 3-1 Description of beaver dams in the study. The area of the pond was obtained from the 1 m LIDAR imagery collected on June 16, 2022. The other variables were obtained from field observations in June 2022. Effective beaver dam heights were determined using the method from Ronnquist (2021). The elevations were measured using a center-point pond elevation approach. Dam widths were measured by the top of the dam.

	Dam #1	Dam #2	Dam #3
Pond area [m^2]	3438	143	1448
Dam length [m]	91	22	68
Dam width [m]	1.1	0.5	1.3
Observable length of the pond by the camera-trap [m]	7	5	7
Camera height [m]	0.7	0.75	1.1
Effective dam height* [m]	1.0	0.8	1.8
Dam height [m]	1.5	1.2	2.1
Elevation [m.a.s.l.]	1490	1488	1480

*Effective dam height is the difference in water depth difference upstream vs downstream of the dam.

3.2.2. Site instrumentation

Five camera traps were installed to record wildlife presence at the three beaver dams and the daily flow state of each beaver dam. Cameras were a mix of RECONYX HyperFire 2 and HyperFire X600. Three of the cameras were positioned facing the dam at key outflow points (Table 3-1). These cameras were installed on May 25, 2022, and were programmed to record images when motion triggered. The cameras were also programmed to record an image every 8 hours (i.e., 08:00, 16:00 and 00:00 MST). Camera D1 was located 2 m downstream of Dam #1, camera D2 8 m downstream of Dam #2, and camera D3 4 m downstream of Dam #3 (Figure 3-1). On July 13, 2022, two more cameras were added with the intent to record wildlife use of the beaver ponds. These camera traps were set to record 10-s video each time motion was detected (Figure 3-1). Images and videos were saved on a memory card that was downloaded approximately monthly during the study. Cameras were mounted on a length of angle iron or fence post that was secured by two lengths of rebar installed in an X pattern (Figure 3-2). The vegetation in the camera's line of sight was trimmed using hedge trimmers when vegetation obscured the lens. The camera traps were removed from the site on September 27, 2022.

The water level of each beaver pond was continuously measured using a level sensor (Leverlogger, Solinst, ON) installed in a PVC standpipe. As well, level sensors were installed in the stream directly downstream of each studied dam to continuously measure stream stage (Figure 3-1). All level sensors were programmed to collect data at 15-minute intervals and were secured inside the standpipes using chains. The standpipes were perforated along the entire length and securely wrapped with fiberglass mesh, thus allowing water to flow freely while avoiding excess sediment collection in the pipe. Stream level data were converted to discharge using on-site measured rating curves collected using the velocity-area method (Dingman, 2015). A flow meter (OTT MF Pro) was used to measure the cross-sectional flow velocity. An inlet station was installed at the beginning of the SE stream to capture streamflow upstream the beaver impacts.

Sibbald Fen is equipped with a meteorological station (51.056°N, 114.868°W, 1490 m.a.s.l.) that collects hydrometeorological data all year (Westbrook & Bedard-Haughn, 2016); it is part of the Canadian Rockies Hydrological Observatory (https://research-groups.usask.ca/hydrology/science/research-facilities/crho.php). This study used the rainfall measurements for 2022, which were collected with a Texas Electronics TE525 tipping bucket rain gauge (0.2 mm resolution; Streich & Westbrook, 2020). A barometric pressure sensor (Barologger, Solinst, ON) was installed at the meteorological station to correct water level data for fluctuations in barometric pressure.
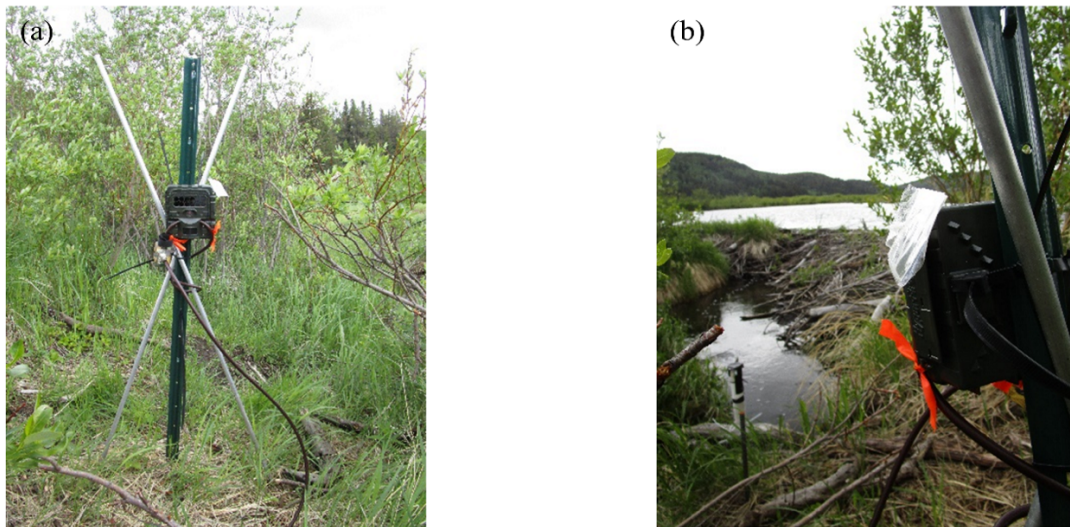
Figure 3-2 Illustration of the camera trap set-up for Dam #3. (a) image shows the camera installed in a three-part-rebar structure, and (b) has an overview behind the camera. Photo credit: Chelsea Cook, used with permission.

3.2.3. Image catalogue

A catalogue of the images and video recorded by the camera traps was created. Each image and video were given a unique, human-readable id that included the study site, the key target of the camera (dam or pond), the download date, and the original RECONYX id. This process was designed to avoid repeated names in the registry as RECONYX cameras have a limited name identifier. The file re-naming process was automated using a custom Python 3.8 (Van Rossum & Drake, 2009) script (Appendix A), following the main data strategies outlined by Fennell et al. (2022) and Niedballa et al. (2016).

3.2.4. Flow states identification

The daily flow state of each beaver dam was determined by using the time-triggered images from the camera traps that faced the beaver dams (D cameras in Figure 3-1). A set of guidelines (Table 3-2) was developed to consistently catalog flow states based on the diagrams and descriptions of Ronnquist & Westbrook (2021) and Woo & Waddington (1990). The guidelines refer to the perspective of an observer downstream of the dam. Flow state classification started with the 08:00 image; if it was not clear, it was followed by the

16:00 image; if that image was not clear, it used the 00:00 image. The accuracy of the guidelines was validated on five field visits (FV) to minimize bias, in which dams were observed from multiple perspectives, including upstream and lateral positions.

Some flow states were easier to identify on the images than others. For example, the overflow state was relatively easy to identify as water can be seen over the top of a beaver dam. In contrast, identifying the seep flow and mixed flow states were especially challenging. Seep flow has no or minimal surface water transmission (Ronnquist & Westbrook, 2021) and so it was the default category if the images lacked evidence of other flow states. Mixed flow refers to two or more flow states present simultaneously. For instance, Dam #1 was classified as being in the mixed flow state in late June and early July as there was water flowing under the dam simultaneously through gaps in the main dam body (Table 3-2). The images obtained during those times were classified as being in the mixed state to indicate both characteristics of overflow and gapflow. The throughflow flow state was not observed in any image

Table 3-2 The beaver dam flow state characterization, as published in the literature (Ronnquist & Westbrook (2021) and Woo & Waddington (1990)), and guidance used to field-identify beaver dam flow state. The right-hand column shows images from camera traps, except the throughflow image captured in Sibbald Fen during the 2022 field season.
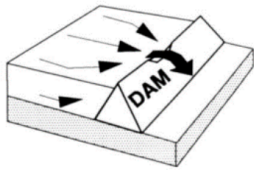
Flow state	Schematic representation	Camera trap image
Overflow Beaver dams in overflow state show water flowing over the top of the dam while the dam body acts impervious to flow (Woo & Waddington, 1990). The overflow area does not need to span the entire dam length to be considered overflow (Ronnquist, 2021).		
Gapflow Beaver dams in gapflow state concentrate the flow over gaps (Woo & Waddington, 1990) distributed across the entire body of the dam. The minimum threshold for a hole is 0.02 m, and there is no limitation on the number of gaps (Ronnquist, 2021). Gaps can be in the top of the dam (Ronnquist, 2021) producing an analog to a contracted rectangular weir.		

Table 3-2 (Continued)
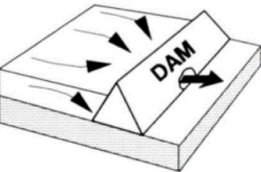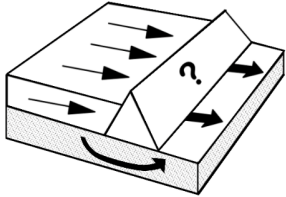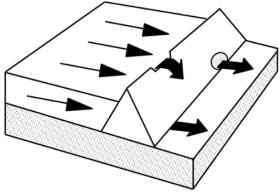
Flow state	Schematic representation	Camera trap image
Throughflow Beaver dams in throughflow state transmit flow from the entire pervious body of the dam (Woo & Waddington, 1990, Ronnquist, 2021). Dams in this flow state can exhibit gaps below the threshold of 0.02 m. In the three dams observed, there was no registry of throughflow. The corresponding image is a new dam built downstream, which shows water flowing through the mud and holes within sticks (smaller than 0.02 m).		
Underflow Beaver dams in underflow state transmit water on the bottom of the dam (Woo & Waddington, 1990). The flow path must be located below the top of the dam (Ronnquist, 2021). Dams classified as underflow showed surface path flows ending near the downstream water level.		

Table 3-2 (Continued)

Flow state	Schematic representation	Camera trap image
Seep flow Beaver dams in seep flow state do not exhibit surface flow paths; instead, the water is transmitted around the dam or through the sediments below (Ronnquist, 2021). Dams in seep flows must not show any other flow state. In the field, it is possible to observe the flow path merging downstream.		
Mixed Beaver dams in mixed flow state exhibit more than one flow state (Ronnquist & Westbrook, 2021). Ronnquist (2021) recorded field observations where two and three flow states were observed simultaneously, and that most combinations included gapflow. The image shows a mixed flow state formed with gapflow and underflow.		

A binary method was developed to assess image quality. Good-quality images enabled the observation of flow states, while poor-quality images did not. Poor-quality images were associated with vegetation covering the lens or fog which affected visibility (Table 3-3). The rapid growth of the vegetation in the summer exceeded the height of the camera covering the lens. This challenge was solved by trimming the vegetation within the camera's view (see Table 3-1) on August 10 to 12. Those images were discarded and marked those days in the image catalog as having no valid images for analysis. Also, morning fog affected the images on some days, which prevented observation of flow state; thus, the other images from that day were used to determine the flow state.

Flow states were analyzed by counting the number of changes from one flow state to another (C_v), excluding the periods without information because of unusable images. For instance, a change from overflow to underflow counts as one change, but a change from an unusable image to underflow were not counted. Total changes (C_t), including unusable periods, were counted, but all statistical analyses were performed with C_v.

Table 3-3 Illustration of some typical challenges encountered while using camera traps and procedures adopted for mitigating them.

Issue	Camera trap image
Vegetation covering the lens Images with the view obscured by vegetation were unusable as the beaver dam was unobservable. To mitigate blocking of images by vegetation, plant trimming is recommended. The vegetation was trimmed in front of the camera traps on August 10-12, 2022, using hedge clippers. This procedure resolved the challenge.	
Foggy images Images with the view obscured by fog led to too poor of image quality to reliably identify flow state. Foggy images occurred primarily on the 8:00 am time-triggered images. To ensure there is at least one usable image captured each day, images should be captured more than once per day using the set time interval option to ensure image redundancy.	

3.2.5. Animal and human detection

Wildlife use of dams was assessed using both motion-triggered and time-lapse images. The workflow was divided into three steps: (1) wildlife detection, (2) species identification, and (3) the assessment between the presence of wildlife at a time of flow state change of a beaver dam.

3.2.5.1. Wildlife detection

All images in the registry were analyzed for presence/absence of wildlife using an automated approach. Images were processed through two machine-learning software: *MegaDetector*

(Beery et al., 2019) and *CameraTrapDetectoR* (Tabak et al., 2022). *MegaDetector* is a Python-based machine-learning software developed with a generalized detector and specific classifiers able to identify animals, humans, and vehicles (Beery et al., 2019). Identifying animals has been reported to have an accuracy of 0.96 (Fennell et al., 2022) and a precision between 0.82 and 0.99 (Fennell et al., 2022; Vélez et al., 2022). The two models available on version 5 of *MegaDetector* were used: MDv5a and MDv5b, which differ in their training datasets (Osner, 2022). MDv5a and MDv5b were run using a Conda environment on Windows 10 laptops and on Google Colab (https://colab.research.google.com/) with a GPU-enabled workspace. *CameraTrapDetectorR* (Tabak et al., 2022) is an R-based machine-learning software that identifies animals, humans, and vehicles. For animals, *CameraTrapDectorR* can also identify three taxonomic categories: class, family, and species; the software was developed with training datasets mainly from North America. Tabak et al. (2022) reported a precision of 0.96 for the binary presence of an animal and 0.8 for the taxonomy category of species. The version 0.1 shared on May 27, 2022, on https://github.com/TabakM/CameraTrapDetectoR was used in R v.4.1.2 (R Core Team, 2023) with the option to identify animals, humans, and vehicles. It was not used any additional detailed taxonomy classification.

The classification quality was evaluated with a random sample of the images viewed manually using the software *Timelapse* (Greenberg, 2020; Greenberg et al., 2019). The analysis was focused only on wildlife, not people. There is no vehicle traffic at the study site. The sample size was calculated with the total number of images per camera, a confidence level of 99.9%, and a margin of error of 5%. Then, it was built a confusion matrix following Vélez et al. (2022) and calculated the correctly identified results or true positive results (*TP*), the false positive (*FP*), the false negative (*FN*), and true negative (*TN*). To compare the different results, precision, accuracy, and recall were calculated using the following equations (Vélez et al., 2022):

$$Precision = \frac{\sum TP}{\sum TP + FP} \qquad\qquad (3\text{-}1)$$

$$Recall = \frac{\sum TP}{\sum TP + FN} \tag{3-2}$$

$$Accuracy = \frac{\sum TP + TN}{\sum TP + FP + FN + TN} \tag{3-3}$$

3.2.5.2. Animal species identification

The results of MDv5a, MDv5b, and *CameraTrapDetectoR* were merged and selected the images for which at least two of the software detected animals. Instead of providing binary discrimination of the images, both software returns a detection confidence/certainty value ranging from 0 (low confidence) to 1 (high confidence) (Fennell et al., 2022). The suggested confidence value for each software were used, 0.2 for MDv5 (Beery et al., 2019) and 0.5 for CameraTrapDetectoR (Tabak et al., 2022). All the images selected after this filter were identified manually in Timelapse (Greenberg, 2020; Greenberg et al., 2019). A database was developed with the common name of the animal, the date and time of capture, and the animal's location in relation to the dam: on the dam, downstream of the dam, upstream of the dam, and other (e.g., flying over the dam).

The database was completed by adding the scientific name, family, and average adult weight of the identified animals, excluding insects. The weight of each identified animal was estimated to determine if it was likely capable of compressing the dam (i.e., weight above 20 kg) and, therefore, changing the flow state of the beaver dam. Animal weights were retrieved from the R Package *traitdata* (https://github.com/RS-eco/traitdata, accessed on March 10, 2023), using R v.4.2.2 (R Core Team, 2023). The primary sources for biota information were Myhrvold et al. (2015) and Wilman et al. (2014), and the secondaries were Cloutier (1950), Johnsgard (2009), Nature Alberta (2018), and St. Clair (2003). Each *Timelapse* template used is available in Appendix B; the animal names, families, and weights in the catalog are available in Appendix C.

3.2.5.3. Evaluation of wildlife at the time of flow state change

It was evaluated whether flow state changes occurred coincident with the recording of wildlife. Based on field observations, animals have two mechanisms to change the flow state

of beaver dams. Some animals can directly modify dams, such as beavers and river otters (coded M_1). Other animals can change the flow state by the action of their weight pressing down on the structure (coded M_2). While the minimum paw/hoof force to elicit a change in beaver dam structure is unknown, any animal weighing > 20 kg was considered to have a sufficient paw/hoof force to alter dam structure when traversing it. The occurrence of the M_1 mechanism to drive flow state change was evaluated with a binary approach, assigning a value of 1 to any day with at least one image with beavers or river otters present on the dam and 0 otherwise. The presence of the M_2 mechanism was assessed with a binary approach, assigning a value of 1 to any day with at least one image of any animal >20 kg present on the dam and 0 otherwise. The results from evaluating these two mechanisms were merged, assigning a value of 1 to any day with either M_1 or M_2 equal 1, and otherwise a value of 0 to the absence of both for each day. A metric, C_b, was established to describe the proportion of observed flow state changes triggered by animals as:

$$C_b = \frac{Flow\ states\ on\ beaver\ dams\ changes\ triggered\ by\ animals}{Total\ number\ of\ flow\ state\ changes\ (C_v)} \qquad (3\text{-}4)$$

3.2.6. Rainfall triggered flow state changes

The occurrence of rainfall events in driving changes in the flow state of beaver dams was assessed. Rainfall from the on-site tipping bucket was first aggregated to a daily time step after verifying that the precipitation occurred as rain using daily images recorded by the RECONYX camera located at the meteorological station. The difference in rainfall and snowfall over beaver ponds is given by the time of liquid release into the pond because snowfall is only incorporated into streamflow after it melts while rainfall is incorporated immediately. The correspondence between flow state changes of beaver dams and rainfall was analyzed through a binary approach. A value of 1 was assigned to any change of flow state coincident with a rainfall event >1 mm that day or the previous and 0 otherwise. A metric, C_h, was established to describe the proportion of observed flow state changes triggered by rainfall as:

$$C_h = \frac{N\ of\ changes\ in\ the\ flow\ state\ of\ beaver\ dams\ triggered\ by\ rainfall}{Total\ number\ of\ flow\ state\ changes\ (C_v)} \qquad (3\text{-}5)$$

3.3. RESULTS

3.3.1. Flow state changes

Each beaver dam studied displayed temporal variation in its flow state. Changes in flow state were not synchronous amongst the beaver dams despite being positioned in sequence (Appendix D). Dam #1, located in the upstream position of the beaver dam sequence, experienced six changes in flow state (i.e., C_t and $C_v = 6$) during the study period (Figure 3-3). The dam was in the underflow state at the beginning of the study period and changed to mixed state on June 13, with both underflow and gapflow states observed (Figure 3-3 image 1). On June 28, the dam returned to the underflow state but changed back to the mixed state on July 16 (combination of underflow and seep states). It remained in the mixed state for 20 days until it returned to the underflow state on August 5 (Figure 3-3 image 2). On August 21, the dam changed to the mixed state with both underflow and gapflow states observed. Five days later the dam switched back to the underflow state in which it remained until the end of the study period (Figure 3-3 image 3). The average duration for each flow state was 14.8 days ($SD = 7.2$ days). The most frequent flow state for Dam #1 was the underflow state which occurred for 71% of 139-day study period. Dam 1 was in the mixed state for 28% of the study period and was divided equally between gapflow and underflow states and underflow and seep states. Underflow, by itself or combined with the others flow states, was present during the entire study period on this dam. There were no observations of water flowing over the top of the dam during field visits or in the images collected by the camera traps. Flow state, as a categorical variable, was correlated with pond water level, as indicated by a significant Kruskal-Wallis (KW) test ($H = 103.6$, $p < 0.001$).
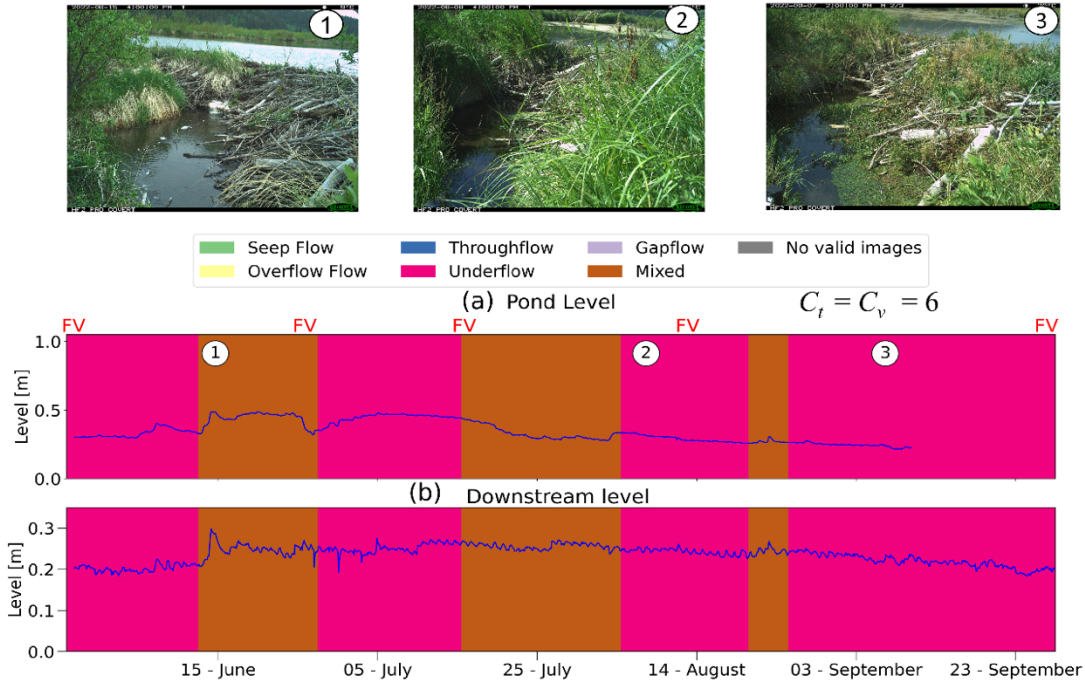
Figure 3-3 Flow state identification for Dam #1 in relation to pond level and downstream water level. The numbers on the pond level plot correspond to the camera trap images at the top of the figure. Image 1 was captured on June 15 when the dam was classified as having a mixed flow state (underflow and gapflow states). Images 2 and 3 shows underflow states and were captured on August 8 and September 7. On September 10, some animals move the logger and there are no valid recordings after that date.

Dam #2, located in the middle of the studied beaver dam sequence, had a C_t of 7 and a C_v of 5 (i.e., 2 non-determinable periods) during the study period (Figure 3-4). The dam was in the seep flow state (Figure 3-4, image 4) at the beginning of the study period until June 6 when the dam changed to the overflow state (Figure 3-4, image 5). The overflow state persisted until July 10 when vegetation obscured the camera's view of the beaver dam. On August 10, the vegetation was trimmed, and it was observed that the dam was in the underflow state, remaining in that state for 11 days (Figure 3-4 image 6). On August 22, the dam changed to the overflow state for three days, returning to the underflow state for another two days, and back to the overflow state for two days. The dam returned to the underflow state on August 29 until the end of the study period. The average duration of each flow state was 10.5 days (*SD= 14.2 days*). The most frequently occurring flow state was the underflow state which occurred for 40% of the study period. The overflow state occurred for 29% of the study period, and the seep flow state occurred for 8% of the study period. Flow state could not be determined from the camera trap images for 23% of the study period due to vegetation obscuring the camera's view of the beaver dam. This dam did not present any mixed flow

state, and each flow state was clearly observable. Flow state was correlated with pond water level ($H = 906$, $p < 0.001$).
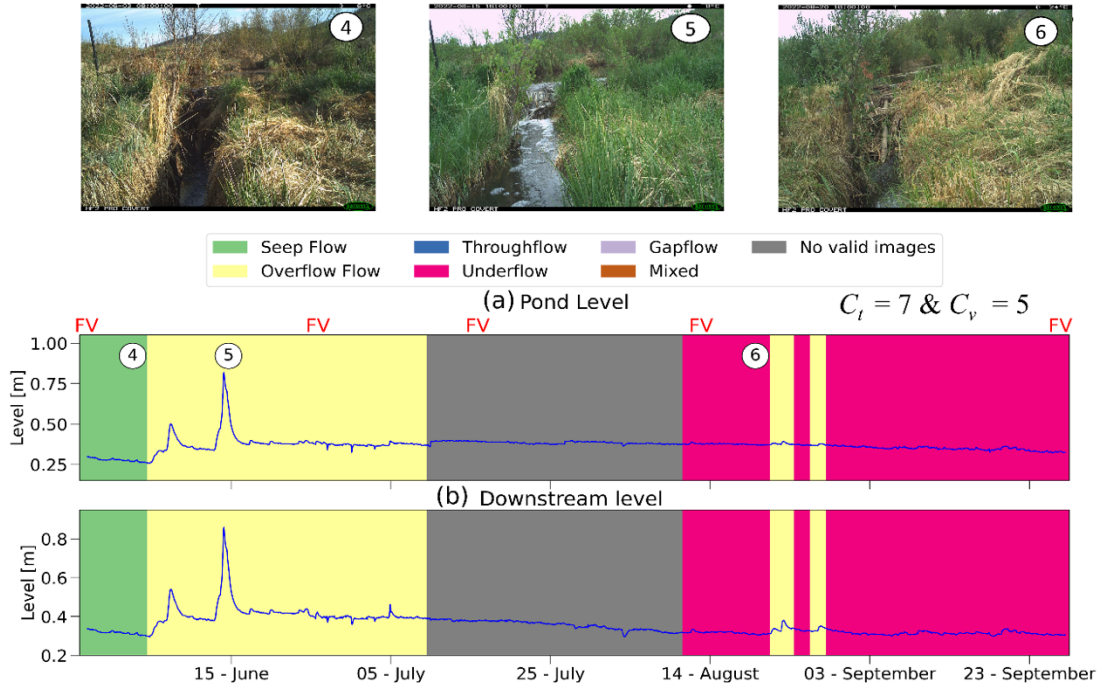
Figure 3-4 Flow state identification for Dam #2 in relation to pond level and downstream water level. The numbers on the pond level plot correspond to the camera trap images at the top of the figure. Image 4 was captured on June 2 where the dam was classified as seep flow. Image 5 was captured on June 15 where the dam's flow state was identified as overflow state. Image 6 was captured on August 20 where the dam was identified as the underflow state.

Dam #3, located in the downstream position of the beaver dam sequence, had a C_t of 18 and a C_v of 12 (i.e., 6 non determinable intervals) during the study period (Figure 3-5). The dam was in the gapflow state at the beginning of the study until June 5, when it changed to the overflow state. On June 8, the flow state changed for one day to gapflow, followed by overflow for two days and then gapflow (Figure 3-5 image 7) for two days. On June 12, the dam changed to the overflow state for six days and on June 18, the dam changed for one day to a mixed flow state (combination of overflow and gapflow states), returning the next day to the overflow state (Figure 3-5 image 8). Between June 21 and July 5, the flow state of Dam #3 changed between the mixed, overflow and gapflow states. On July 6 the camera's view of the beaver dam was obscured by vegetation. Field visits on July 9 and 10, and from July 13 to 15, indicated the dam was in the gapflow state. The vegetation in the camera's view was trimmed on August 10, and it was observed that the dam was in the underflow state.

34

On August 23 the dam changed to the mixed state (combination of gapflow and underflow) for two days and returned to the underflow state (Figure 3-5 image 9) until the end of the study period. The average duration for each flow state was 3.0 days (*SD = 2.5 days*). The most frequent flow state was the underflow state which occurred for 44% of the study period, followed by the gapflow state at 14%, the overflow state for 12%, and the mixed state for 9%. The flow state could not be determined for 21% of the study period when vegetation obstructed the camera's view of the beaver dam. Flow state was correlated with pond water level (*H = 1428, p < 0.001*). Of note, beavers built a dam on June 27 (coded Dam #4) downstream of Dam #3, which raised the stream stage immediately downstream of Dam #3 and reduced stream velocity from 0.107 m^{s-1} to 0.03 m^{s-1}. Dam #4 was mainly composed of mud, peat and thin (diameter less 0.05m) branches. Dam #4 was removed on August 9; however, beavers rebuilt it overnight and not attempt to modify it again were made (Figure 3.5b).
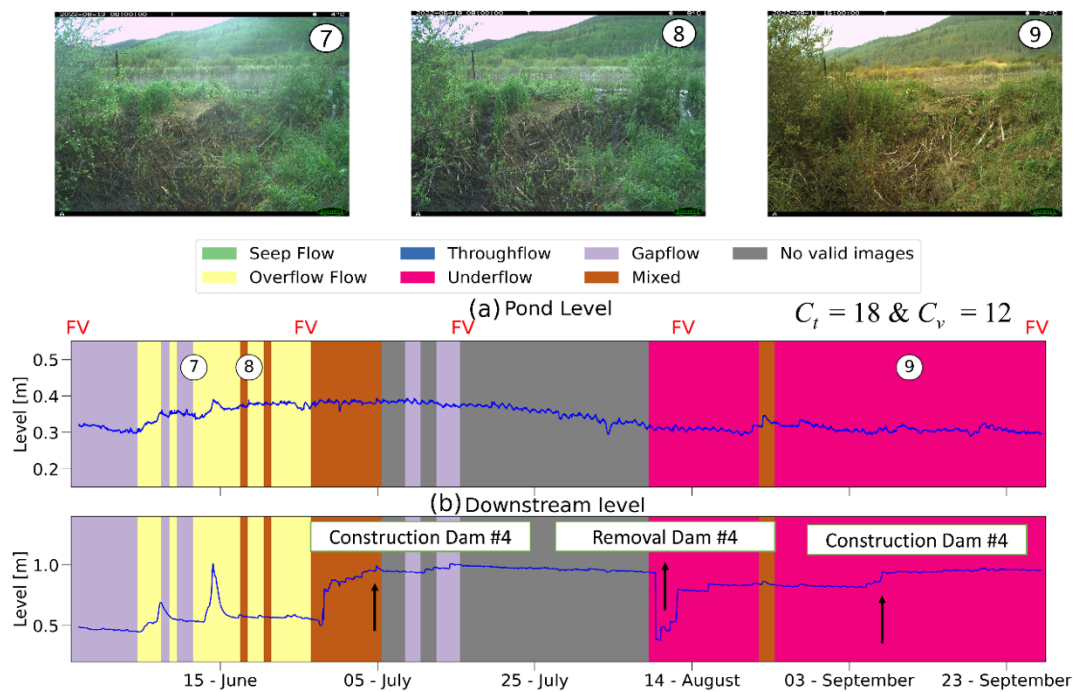
Figure 3-5 Flow state identification for Dam #3 in relation to pond level and downstream water level. The numbers on the pond level plot correspond to the camera trap images at the top of the figure. Image 7 was captured on June 13 where the dam was classified as gapflow. Image 8 was captured on June 19 where the dam's flow state was identified as overflow state. Image 20 was captured on September 11 where the dam was identified as the underflow state.

3.3.2. Animal triggered flow state change

The three cameras facing the beaver dams recorded 182,537 images, and the three cameras facing the beaver ponds recorded 642 images and 178 10-second videos during the 139-day study period. Only 0.4% of the total images recorded animals (Table 3-4); the remaining images were triggered by vegetation movement. Most of the animals were observed on a dam (47%) or downstream of a dam (41%) (Table 3-4). There were no animals in any of the images and videos from cameras P1 and P3, so these cameras were excluded from further analysis.

The accuracy of the detection of animals by machine learning software was manually evaluated with a random sample of 3,206 images. For camera D1, 233 were sampled of the 1,608 images, for camera D2 1479 were sampled of the 65,325 recorded images; and for camera D3 1,494 were sampled of the 115,604 recorded images. All the people present in the images were researchers within the team who worked carefully when close to the dams so that they did not trigger any flow-state change. Regardless, dates of field visits were marked with FV to assess if any flow-state changes in beaver dams occurred coincident with researcher visits. A confusion matrix (Vélez et al., 2022) was built for the random sample of images, and from it was calculated precision, recall, and accuracy (Table 3-5). In terms of accuracy, the best model was MDv5b with 0.96, and in terms of precision, the best model was MDv5a with 0.47. The three models detected with high accuracy the animal presence; however, they also detected a significant number of false positives resulting in low precision values, which was in line with Beery et al. (2019).

Table 3-4 Total abundance of animals, key species, and their location relative to a beaver dam per camera for the 139-day study period as identified with machine learning and manual identification of species. Note that the percentages for species do not add to a 100 as images with insects are not reported. The last rows include the location of the identified species within the dam. The total number of images with biota was set to 100% for each dam, and the percentages from rows 4 to 11 were computed using that reference.

		Dam1		Dam2		Dam 3	
		Number	%	Number	%	Number	%
Images	Images with biota	462	100%	261	100%	41	100%
Species	Most recorded species	Mallard (60%)		White-tailed deer (72%)		Great-blue heron (73%)	
	Images with avian species	425	92%	35	13%	38	93%
	Images with mammal species	32	7%	226	87%	1	2%
	Images with beavers	2	0%	0	0%	0	0%
Location	Downstream of a dam	98	21%	187	72%	28	68%
	Upstream of a dam	58	13%	1	0%	8	20%
	On a dam	287	62%	70	27%	3	7%
	Other	18	4%	3	1%	2	5%

Table 3-5 Metrics to evaluate the performance of the MDv5a, MDv5b and CameraTrapDetectoR machine learning algorithms for detecting only animals in three cameras oriented to capture key hydrological features (Cameras D).

Model	Metric	D1 Camera	D2 Camera	D3 Camera	Average
MDv5a	Precision	0.05	0.78	0.64	0.49
	Recall	0.86	1.00	0.75	0.87
	Accuracy	0.85	1.00	0.97	0.94
MDv5b	Precision	0.07	0.70	0.57	0.45
	Recall	0.57	1.00	0.67	0.75
	Accuracy	0.93	1.00	0.96	0.96
CameraTrapDetectoR	Precision	0.07	0.47	0.27	0.27
	Recall	0.21	1.00	0.50	0.57
	Accuracy	0.97	0.99	0.91	0.95

There were 426 images of animals recorded at Dam #1 (Figure 3-6a), most of which (62%) were on the dam. Mallards were the most frequently recorded animal (Figure 3-6 image 10). There were only two days when cameras recorded animals with the ability to change the beaver dam flow state, i.e., M_1 (Figure 3-6b). In both cases, the animal was a beaver. Neither recording of the beaver corresponded to a change in flow state of the beaver dam. This dam therefore had no biotic-triggered flow state change, with a C_b of 0.
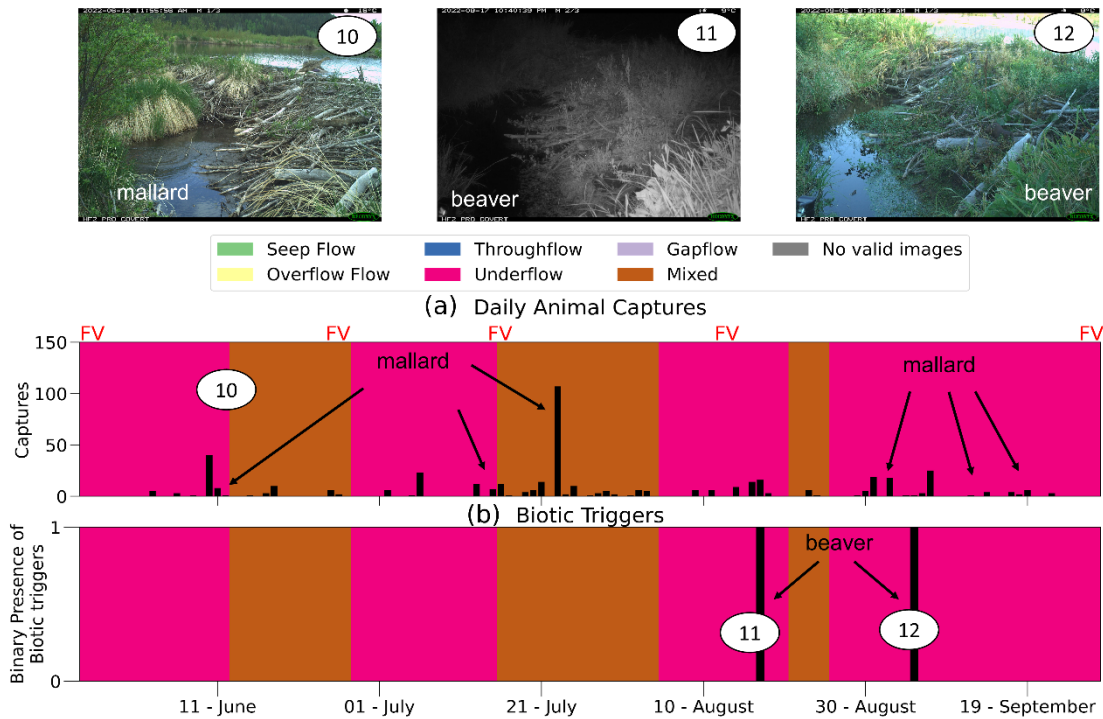
Figure 3-6 Animal identification for Dam #1. (a) shows the number of daily animals captured after manual validation, and the arrows present the most frequently observed animal. (b) shows the binary presence of biotic triggers, which were two beavers in late summer. The three images illustrate relevant observed animals. Image 10 shows a mallard (captured on June 12), 11 shows the first beaver observation on August 17; 12 shows the last beaver observation on the dam on September 5.

There were 261 images of animals recorded at Dam #2 (Figure 3-7a), most of which (27%) were on the dam. The first observed animal was a songbird (Figure 3-7 image 13). On only two days were animals with sufficient weight (>20 kg) to modify the flow state of beaver dams recorded (Figure 3-7b). One of the animals was a white-tailed deer on the dam (Figure 3-7 image 14) observed on August 28, one day after the flow change (underflow to overflow). On September 3, another white-tailed deer on the dam was recorded (Figure 3-7 image 15).

In both cases, no coincident change in the flow state of the beaver dam was observed. As a result, the *Cb* index is 0.
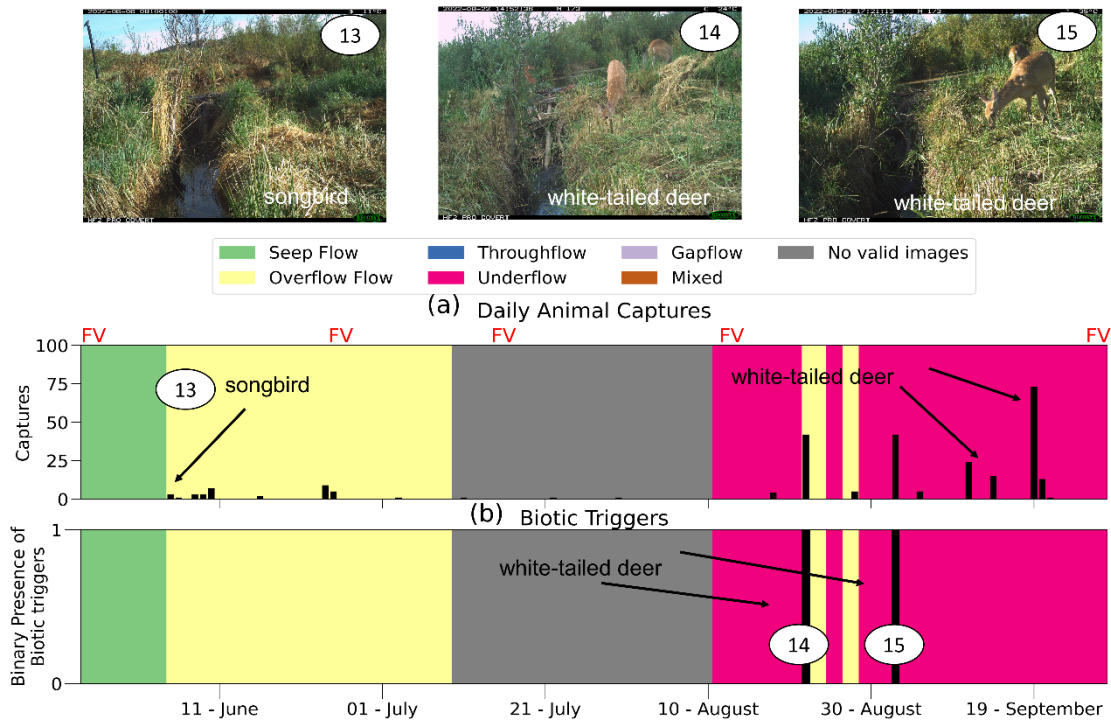
Figure 3-7 Animal identification for Dam #2. (a) shows the number of daily animals captured after manual validation, and the arrows present the most frequently observed animal. (b) shows the binary presence of biotic triggers, which were two white-tailed deer. The three images illustrate relevant observed animals. Image 13 shows a songbird (captured on June 6), 14 shows the first white-tailed deer observation on August 22; 15 shows the last white-tailed deer observation on September 2.

There were 41 images of animals recorded at Dam #3 (Figure 3-8a), most of which were avian species, such as mallard ducks and great-blue herons. In no cases did the cameras record an animal capable of modifying the beaver dam structure (M_1) nor did cameras detect

any animals that weighed > 20 kg (M_2). Therefore, there were no recorded instances of a biota-triggered change in beaver dam flow state (i.e., $C_b = 0$).
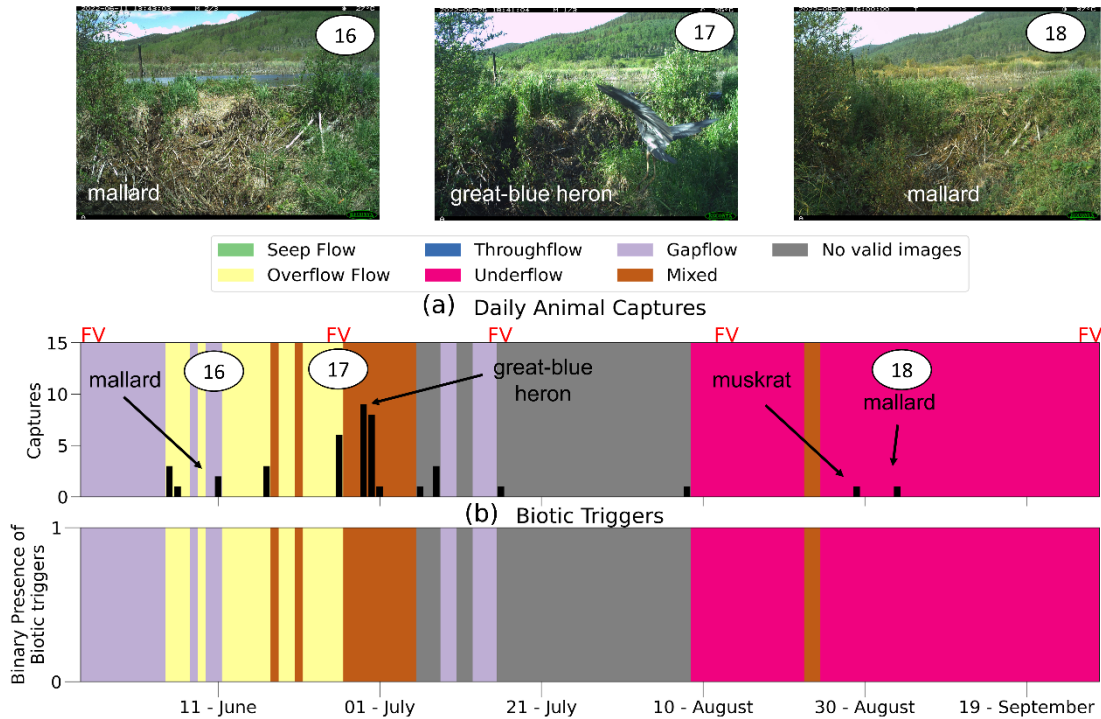
Figure 3-8 Animal identification for Dam #3. (a) shows the number of daily animals captured after manual validation, and the arrows present the most frequently observed animal. (b) shows the binary presence of biotic triggers, which were absent for this dam. The three images illustrate relevant observed animals. Image 16 shows a mallard (captured on June 11), 17 shows a great blue heron on June 26; 18 shows a mallard observed on September 3.

3.3.3. Rainfall triggered flow state change.

The role of rainfall events as a hydrological trigger of flow-state changes was evaluated for the three beaver dams in this research. From May to October 2022, there was 310.2 mm of rain, occurring on 51 days (37%). Mean daily rainfall was 2.2 mm (SD = 6.3 mm, Figure 3-9). The largest event was 96.2 mm occurring June 12-15, and the second largest event was 47.7 mm on June 4-6.
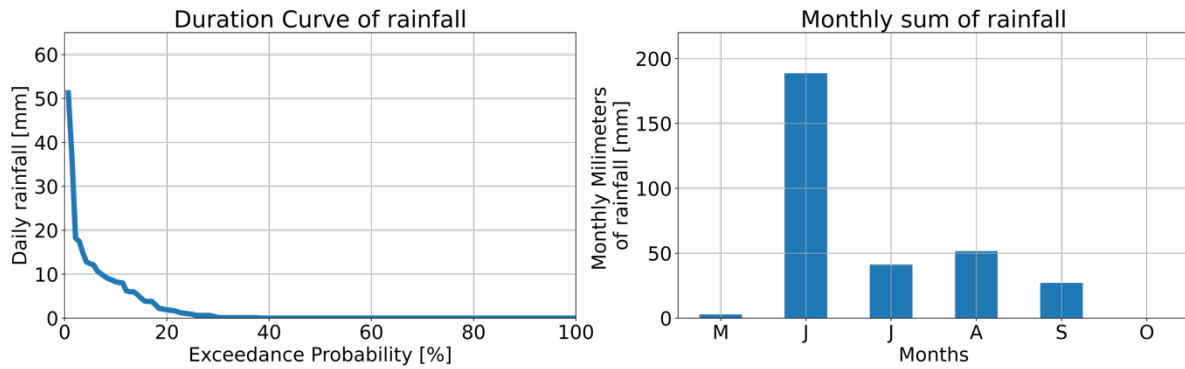
Figure 3-9 Analysis of the rainfall registered during the 139-day-study period. (a) shows a duration curve of rainfall built with daily data, which shows a few storms up to 55 mm/day and most days without rainfall. (b) shows the monthly sum of rainfall, where it can be observed that most are concentrated in June, followed by August.

For Dam #1 (Figure 3.10a), 67% of the six flow-state changes coincided with rainfall events ($C_h = 4/6$). Rainfall during these events averaged 12 mm (SD = 21.1 mm). For Dam #2 (Figure 3.10b), four of the five valid flow-state changes (80%) were coincident with rainfall events with an average of rainfall of 9.4 mm (SD = 9.1 mm; Figure 3.10b). The remaining event had negligible rainfall (only 0.1 mm). For Dam #3 (Figure 3.10c), eight of the 12 valid (C_v) flow-state changes (67%) were coincident with rainfall ($C_h = 8/12$). These rainfall events averaged 5.2 mm (SD = 7.7 mm).
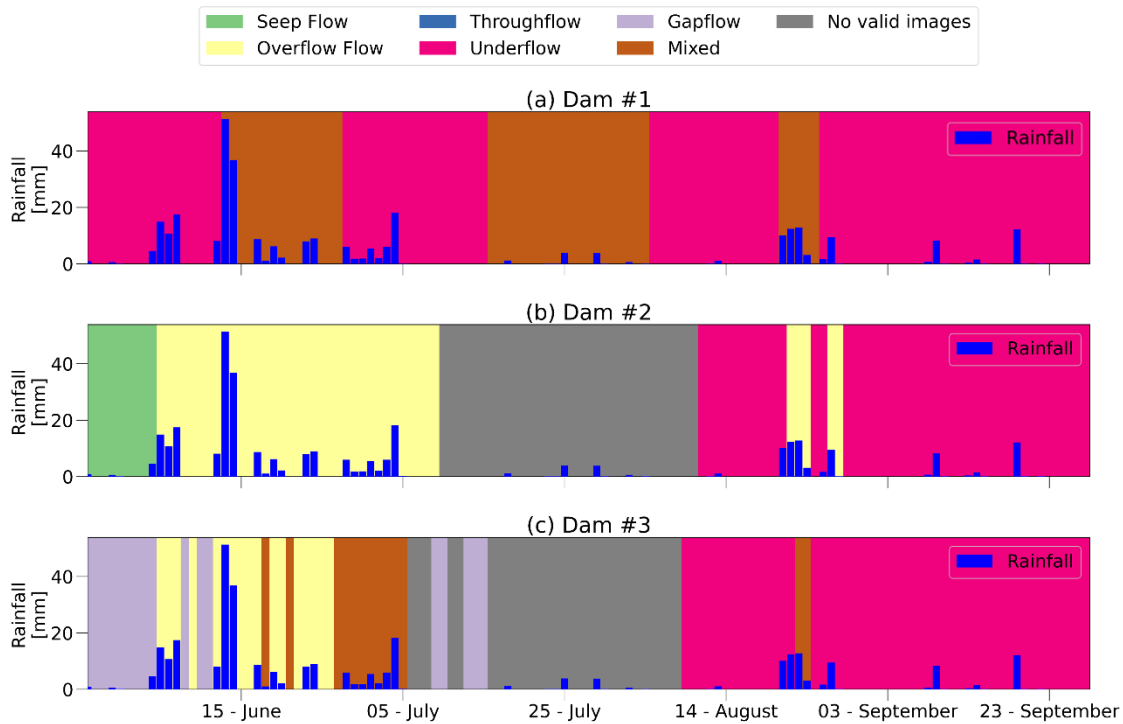
Figure 3-10 Timing of rainfall (mm) in relation to temporal variations in beaver dam flow state during the study period (May to October 2022). Dams are ordered from an upstream position (Dam #1) to a downstream position (Dam #3).

3.4. DISCUSSION

Flow state changes of beaver dams have previously been linked to the beaver occupancy cycle (Neumayer et al., 2020; Woo & Waddington, 1990); however, the results indicated that the shift from one flow state to another can occur multiple times over the course of a summer. Camera traps were invaluable to identifying changes in the flow state of beaver dams. Consistent with our hypothesis, the majority of flow state changes were due to rainfall-runoff events. In contrast with the proposed hypothesis, no flow state changes occurred in response to beaver actions or coincident with recorded wildlife crossings of beaver dams. The findings have implications for how beaver dams should be represented in ecohydrological models.

The majority (more than two-thirds) of observed changes in the flow state of the studied beaver dams occurred in response to rainfall. The variations in the proportion of flow state changes driven by rainfall across the three dams can be explained by total and available pond storage. Total storage is important as the smallest pond (Dam #2) presented several more

43

rainfall-runoff triggered shifts in flow state than the other studied dams. A smaller pond often has a lesser capacity to mitigate event runoff than a larger pond simply because it has a lesser volume at capacity. The available storage at the time of an event is also key as it regulates how much water can be stored before a pond spills its banks (Westbrook et al., 2020). Assuming a theoretical, empty pond formed by a beaver dam in a gapflow state, the pond level must increase to at least the height of the gaps to generate flow. For instance, Dam #3, which generated a larger pond, changed to a mixed state formed by gapflow-underflow (i.e., activation of gaps) to release the August 23-25 stormflow due to minimal available pond storage. The pond level at Dam #1 increased by 0.08 m with the first recorded rainfall, with no corresponding shift in flow state. The dynamic, seasonal variation of beaver pond volumes (i.e., fullness) observed is a reasonably common phenomenon. Peak pond volumes at the study site were reached during spring, corresponding with the timing of the rainfall peak, which is consistent with previous observations at some sites (Devito & Dillon, 1993; Ronnquist & Westbrook, 2021) but is in contrast with observations of an autumn peak at other sites (Clifford, 1978; Nyssen et al., 2011; Scheffer, 1938).

Flow state changes of beaver dams had limited synchronicity, even during rainfall events. There was no flow state change that was shared by all three dams, but two changes (June 5 and August 25) were shared between Dams #2 and #3. Both dams shifted to the overflow state in response to rainfall-runoff (Figure 3-10, Appendix D). The lack of further synchronicity might be explained by the cascade effect of the studied beaver dam sequence. During a storm, the upstream dam (e.g., Dam #1) releases the excess water downstream, accumulating water in the following ponds, which might elicit a change the flow state to address the excess. This cascade mechanism might also explain why the downstream dams exhibited a greater number of flow state changes than the most upstream dam. Cascade effects are common in human-made multi-reservoir systems (Wang et al., 2019). Ultimately, the factors will determine if a beaver dam releases water to another in a more downstream position are the size of the pond and its degree of fullness prior to a rainfall-runoff event (i.e., its capacity to mitigate increased inputs). Other potentially important but less studied factors are dam materials (i.e., dam permeability), and the opportunity for other pathways of water dispersion such as floodplain activation (Westbrook et al., 2006, 2020). Understanding synchronicity in flow state changes in response to rainfall-runoff events, or lack of it, within

beaver dam sequences will be helpful in predicting the floodwater mitigation potential of beaver dams, as Westbrook et al. (2020) demonstrated.

While flow state changes were not observed in a successional pattern, for example, all dams in the sequence changing to the same flow state after reaching a specific rainfall threshold, there was some predictability in dam responses. Larger rainfall events tended to change the flow state of the beaver dams to the overflow state, in which there is relatively quick release of excess water in the pond to the downstream environment. It was detected that the changes between flow states during storms generally corresponded to an increase in the water transmission potential, transitioning from the seep flow state, characterized by a very limited capacity to transmit the excess water, to the overflow state, characterized by rapid water transmission at relatively high volume. In addition to the transmission potential mechanism, the structural properties of the dam must be considered in predicting changes in flow state. For instance, a beaver dam can only change to the gapflow state if it has gaps with a diameter >0.02 m (e.g., Dam #1). Likewise, for a dam to be in the throughflow state, it must have sufficient permeability to allow water to noticeably flow through it. Throughflow state was absent in this study and in the Ronnquist & Westbrook (2021) study which was regional in the same geographical area. If a dam is well-maintained by beaver and does not have gaps, or alternatively, has low permeability, it is likely be functioning primarily in the underflow state.

Camera traps are a non-invasive way to study animals and their behavior, and several studies have successfully recorded beaver activity at dams and in ponds, for example, Dytkowicz et al. (2023) and Swinnen et al. (2014, 2015). Although 764 images of animals were captured near the dams, only two images contained beavers (near Dam #1). Neither beaver observation occurred coincident with change in the flow state of the dam. Beavers are responsible for building and maintaining beaver dams and therefore have been identified as the primary agent of flow state change (Johnston & Naiman, 1987, 1990; Naiman et al., 1988; Woo & Waddington, 1990). Camera traps though are imperfect detectors, and a number of reasons exist as to why beavers were not recorded, even potentially when present. Empty frame recordings can occur even when a beaver triggers a camera because of a lag time in movement of an animal and the start of a camera (Swinnen et al., 2014). Beavers have been reported to

swim at an average speed of 0.64 m s^{-1} (Allers & Culik, 1997), and while the cameras used have a short (0.2 s) trigger speed, which is faster than beavers could likely swim out of the camera view, beavers have a low profile in the water and can submerge quickly. Further, the camera traps were positioned to capture changes in the flow state of beaver dams and therefore may not have been ideally placed to observe wildlife use of the beaver dams. Also, camera views did not include the entire dam length and beavers may have interacted with Dams #1 and #3 along the sections not captured by the cameras. Additionally, while there is not yet literature guidance on the ideal camera distance from a beaver dam to capture beaver activity, only the pond-facing cameras were located at the upper end of the camera's detection range of 30 m. Camera installation height was set for a full view of the outflow point of each beaver dam, and Jacobs & Ausband (2018) report no difference in animal detection rate between cameras set between 0.6 and 3.0 m height. It is suggested that researchers interested in augmenting their hydrometric observations with camera traps at beaver dams deploy at least two camera traps – one pointed toward the dam to obtain data on flow states, and another closer to the dam to obtain information on animal use and modification of the beaver dam.

In addition to the two recordings of beavers at Dam #1, 762 images of other animals were recorded. None of these animal sightings occurred coincident with a change in dam flow state. However, only a small proportion of these images were of animals with a sufficient hoof weight to cause structural changes to a beaver dam (i.e., white-tailed deer and cattle). The images show these animals were drinking from the pond or crossing the stream by a path other than across a dam. The majority of animals observed on the dam were birds (e.g., mallard or great-blue heron), consistent with the literature (Medin, 1990). Birds in this region do not weigh enough to cause changes in beaver dam structure. While birds can pick up woody material from the dams by their talons or beaks, this behavior was not observed in the recorded images.

A small, but not insignificant, proportion of the flow state changes recorded (20-33%) did not correspond to a rainfall-runoff event or dam use by biota. Rather, these changes tended to coincide with periods of pond level decrease. Beaver ponds can have dynamic levels (Larsen et al., 2021) and during the study period it was documented up to 0.56 m of change in pond level. At Dam #1, for example, it was observed a change from underflow to the mixed

state driven by an accumulated 15% pond level decline (Change 3, Appendix D). In the absence of rainfall or snowmelt inputs, the hydrological mechanisms by which pond levels can decline are evaporation (Woo & Waddington, 1990) and non-meteorological events such as lateral water seepage into riparian soil and vertical recharge groundwater (Fairfax & Small, 2018; Feiner & Lowry, 2015; Graham et al., 2022; Wang et al., 2018). A decline in pond level has previously been documented to elicit a change in flow state. For instance, Ronnquist & Westbrook (2021) reported that a decrease in beaver pond level led to a flow state change from gapflow to seep flow. Therefore, the presence and quantification of these triggers must be accounted for in understanding system behavior.

This research documented that flow state changes are dynamic, changing up to 12 times over a six-month period (i.e., every ~10 days). This rate of change is much faster than is reported by Woo & Waddington (1990) in their perceptual framework. Rather than changing on short time scales, Woo & Waddington reported that flow states primarily change over the beaver occupancy cycle of a dam site (Naiman et al., 1988). Therefore, this study expands this framework by including short-term changes in the flow state of beaver dams (Figure 3-11). This new understanding of flow state change potentially enables prediction of how beaver dams will mitigate flooding events, given that it has been established that flow state changes are a key mechanism to control the impacts of large storms (Ronnquist & Westbrook, 2021; Woo & Waddington, 1990) along with floodplain activation (Westbrook et al., 2006, 2020). The study should therefore generate further dialogue about how flood attenuation by beaver dams is modeled (Graham et al., 2022; Neumayer et al., 2020). Current ecohydrological modeling approaches that include beaver dams assume they have a permanent flow state, often the overflow state (Beedle, 1991; Caillat et al., 2014; Noor, 2021). Although, Neumayer et al. (2020) considered dams to have a mixed state between throughflow and overflow. These results indicate that representing beaver dams in models as having one unique flow state, particularly the overflow state, is unrealistic. Because the flow state of beaver dams is dynamic on short time scales, ecohydrological models must be flexible and include a parameterization of all flow states of beaver dams explicitly. Model parameterizations must also consider the mechanisms that can trigger these flow state changes (Ronnquist & Westbrook, 2021), especially rainfall-runoff events.
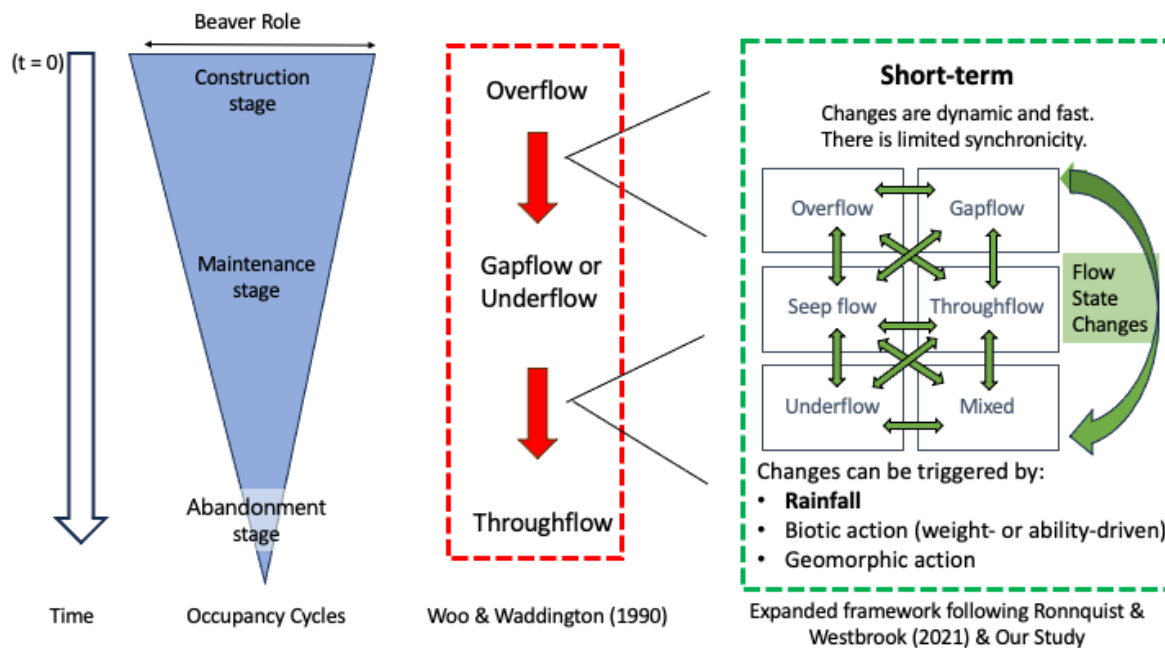
Figure 3-11 Expanded flow state framework. This figure synthesizes how long-term flow state changes, as viewed by Woo and Waddington (1990) in red, are related to short-term flow state changes (this research) depicted in green. During each stage in the long-term linked to the beaver occupancy cycles (blue polygon), in the short-term (days/months), there are dynamic, fast, predictable changes happening, which are being triggered by three mechanisms described by Ronnquist & Westbrook (2021). The size of the blue polygon shows the beaver role, which is higher during the construction stage and lower during the dropout period when dams become relics. Time is depicted by the left arrow starting from the time of beaver dam construction (t=0). The arrows in the short term are shows as reference as the shifts can happen from many flow states.

3.5. CONCLUSION

Communities and practitioners are incorporating beaver dams in flood mitigation, stream restoration, and climate change adaptation plans (Auster et al., 2021; Brazier et al., 2021; Charnley et al., 2020; Jordan & Fairfax, 2022; Larsen et al., 2021; Thompson et al., 2021). Therefore, they need to be able to understand and predict the magnitude of the streamflow modulation by beaver dams. Flow states of beaver dams are critical to understanding how beaver dams regulate streamflow behavior (Ronnquist & Westbrook, 2021; Woo & Waddington, 1990). The hypothesis that flow state changes are dynamic on short time scales, triggered by rainfall and biotic agents, was tested to improve prediction capabilities. Through the utilization of camera trap imagery and hydrometric data, it was concluded that flow state changes in beaver dams are highly dynamic, occurring regularly over a period of months. In

the study site, 67% to 80% of the flow state changes were triggered by rainstorms; none were triggered by biota. One-third of the flow state changes could be explained by other hydrological mechanisms that led to declining pond levels, potentially groundwater-surface exchange or evapotranspiration. There was limited synchronicity in flow state change amongst the three studied beaver dams despite that they occurred in sequence. That said, there was predictability of the beaver dam system. For instance, a flow state can only shift to gapflow if it has a structural predisposition (i.e., gaps larger than 0.02 m). Therefore, the succession of the flow state can be predicted by observing several features.

This work therefore expands the Woo & Waddington (1990) flow state framework by adding a short-term component of dynamic flow state changes; changes were fast, reasonable predictable, and occurred primarily in response to rainfall. As practitioners consider the positive benefits of beaver dams on landscapes and how these dams enhance the resilience to droughts and floods(Fairfax & Whittle, 2020; Jordan & Fairfax, 2022; Pollock et al., 2015; Westbrook et al., 2020; Wohl, 2021), they need to be able of anticipate the impacts of beaver damming. Understanding flow state changes, including the role of rainfall and biota, is vital for integrating beaver dams into hydrological models in a realistic and process-based approach, enabling local and regional assessments.

4. ARTICLE II: BEAVERPY: A PHYSICAL-BASED MODEL TO REPRESENT FLOW MODULATION BY BEAVER DAMS[2]

4.1. INTRODUCTION

Beavers (*Castor canadensis* and *C. fiber*) are densifying in their native range in Eurasia (Graham et al., 2022; Halley et al., 2012; Neumayer et al., 2020; Pollock et al., 2015) and North America (Hood & Bayley, 2008; Naiman et al., 1988), and increasing in number in urban environments (Bailey et al., 2019; England & Westbrook, 2021; Westbrook & England, 2022). At the edge of their native range, beavers are encroaching into new environments, specifically into Arctic tundra (Foster et al., 2022; Tape et al., 2018, 2021, 2022a, 2022b); there is also a population of introduced beavers in southern Patagonia that is expanding northward (García et al., 2022; Huertas Herrera et al., 2020, 2021; Skewes et al., 2006; Westbrook et al., 2017). Given the expansion of beaver populations globally, it is critical to understand and predict the hydrology of beaver-dominated landscapes. Prediction of the hydrology of beaver-dominated landscapes is challenged by there not being a direct equivalent of water routing through beaver ponds in hydraulic engineering (Beedle, 1991). As a result, most hydrological models do not have the capability to address the wide-ranging impacts of the effect of beaver dams on hydrological processes. To be useful for predicting the hydrology of beaver-dominated environments, hydrological models must be capable of explicitly representing the diverse impacts of beaver dams on the water budget (Addy & Wilkinson, 2019; Keys et al., 2018; Larsen et al., 2021; Neumayer et al., 2020; Ronnquist & Westbrook, 2021; Wade et al., 2020, and Chapter 3).

Beavers build dams to increase water depth until the associated pond is large enough to serve as a refuge from predators (Gurnell, 1998). Beaver dams change key components of the water

---

balance, including storage and flow dynamics. For example, beaver dams alter stream and wetland ecosystems by increasing surface and groundwater storage (Johnston & Naiman, 1990; Karran et al., 2018; Westbrook et al., 2006). Beaver dams also mitigate high flows and flooding (Puttock et al., 2020; Westbrook et al., 2020), increase the precipitation to peak streamflow lag time (Nyssen et al., 2011), and augment low flows (Westbrook et al., 2006). Since beavers adapt their techniques for constructing dams in different environments, the form and composition of beaver dams are highly variable. As a result, the influence of beaver dams on hydrological processes is not universal. There is an existing hydrological classification for beaver dams to describe backwater effects and the flow paths that streamflow takes past a beaver dam (Ronnquist & Westbrook, 2021; Woo & Waddington, 1990).

There have been four previous implementations of beaver dams in hydrological models. Beedle (1991) simulated peak flow discharging over a series of 44 beaver dams using a modified Puls method to determine detention storage effects on Kuiu Island, Alaska, USA. Caillat et al. (2014) used the model HEC-HMS to simulate the impact of 42 dams on streamflow in the Jemez Watershed, New Mexico, USA. Noor (2021) applied the same methodology as Caillat et al. (2014) to model streamflow past 42 beaver dams in the Milwaukee River, Wisconsin, USA. Neumayer et al. (2020) coupled the rainfall-runoff model WaSim with the hydraulic model HYDRO_AS-2D to represent 51 dams in 12 sequences in the Otterbach and Glonn basins, Germany. These implementations used three multipurpose platforms to simulate the impacts of beaver dams on catchment outflows. However, these platforms were limited in that they could not represent the observed heterogeneity of beaver dams nor their effects on hydrological processes.

There are several limitations of previous beaver dam modeling approaches that likely contributed to the mismatch between simulated and observed data. First, beaver dams have varied structural composition and are built across a wide geographic range. Therefore, ponds can have concave, convex, or conic morphology (Karran et al., 2017). The model platforms previously mentioned do not have parameters to represent the variety of dam and pond morphometry; consequently, dams and ponds have been represented as having the same shape irrespective of location. Second, beaver dams have six flow states; each differently

influences the way in which water flows past a dam (Ronnquist & Westbrook, 2021; Woo & Waddington, 1990). Both Aguirre et al. (Chapter 3) and Ronnquist & Westbrook (2021) showed that the flow state of beaver dams is dynamic on short and long-time scales. Flow state change can occur via biotic, geomorphic, or hydrologic triggers (Ronnquist & Westbrook, 2021; Chapter 3). Existing models do not have modules to represent the flow state of beaver dams or changes in the flow state. Third, the model platforms that have been used to simulate the impacts of beaver dams on streamflow are not open source. This limits the use of the models and is not aligned with FAIR principles (Barker et al., 2022).

To overcome these limitations, what is needed is a physically based ecohydrological model that can address the complex interactions between ecosystem processes and the storage and flux of water in beaver-dominated environments. Such an ecohydrological model should be written with open-source code to ensure reproducibility of model results by a broad community of users and align with FAIR principles. To address this challenge, introduced is BeaverPy. The model, described in section 4.2.1, combines a bucket-based approach with current understanding of the heterogeneity of beaver dams in morphometry and environment to simulate runoff at the catchment outlet, level at all beaver ponds in the series, and the flow state of the beaver dams. A beaver-dominated catchment in the Canadian Rocky Mountain foothills, Sibbald, was chosen as the case study to calibrate and validate the model. This catchment is well-studied (Westbrook & Bedard-Haughn, 2016) and existing datasets are augmented with additional field data.

4.2. METHODOLOGY

4.2.1. Model Description

The BeaverPy model is an ecohydrological 1-D hydraulic model that explicitly includes flow states of beaver dams and changes between them to simulate runoff at the catchment outlet in beaver-dominated environments. The philosophic approach is centered on providing a physically based and field-informed model, i.e., an understanding of the processes (i.e., system physics) rather than identifying 'perfect' metrics, following Fang et al. (2013), Pomeroy et al. (2007), and Shook et al. (2021). There were five design principles adhered to in the development of BeaverPy.

1. The model explicitly handles dams made by beavers, thereby recognizing the natural variability of beaver dams, as driven by physical processes and the biotic actions of beavers.

2. BeaverPy focuses on representing water storage dynamics and streamflow modulation in beaver-dominated environments. First, it handles, through a 1-D hydraulic model, the streamflow simulation by beaver dams and ponds, by calculating pond storage, dam outflow, and dam flow state. Second, it tracks the water storage in areas other than beaver ponds, for example uplands, using a simplified ecohydrological model. However, BeaverPy purposely does not provide rainfall-snowfall-runoff algorithms. BeaverPy can be coupled with surface hydrological models to represent the complete hydrological cycle. Modeling the contributing area of the basin with a regionally suitable surface hydrological model and modeling flow through beaver-dominated areas with BeaverPy (Figure 4-1) is suggested.

3. Beaver dams experience structural changes over time which influences the way in which water flows past a beaver dam (Ronnquist & Westbrook, 2021; Woo & Waddington, 1990). BeaverPy captures this variability by parametrizing all variables as vectors (i.e., time-dependent variables) instead of fixed, single values.

4. The model is determinist. The same equations with the same parameters will always provide the same results.

5. The program is open source to encourage ecohydrologists to test, modify, and use it accordingly.
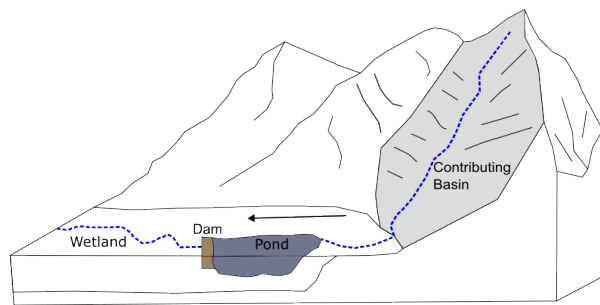
Figure 4-1 Depiction of proposed coupled framework. Modeling the contributing basin (gray) with models developed for that purpose and modeling the beaver-dominated area with BeaverPy is suggested. The arrow denotes the flow direction that goes from the contributing area of the basin to the wetland (upstream to downstream). Catchment schematics are not drawn to scale.

The BeaverPy model has a bucket-based approach where there are control volumes (buckets) to represent beaver ponds, aquifers, and vegetation-covered areas. Each bucket can receive, store, and discharge water. All the equations are presented in their conservative form given that it was assumed a constant water mass density of 997.0 kg m^{-3}. Every modeled element, such as dams, ponds, streams, and upland zones, can be represented by parameters with unique values to account for the heterogeneity observed in the field, following a semi-distributed approach, unlike a lumped approach where the entire wetland would have the same values (See Hrachowitz & Clark (2017) for an in-depth discussion on model discretization).

The BeaverPy model only tracks water volume, not momentum or energy, and its mathematical foundation is given by the continuity principle defined as follows:

$$\frac{I}{\Delta t} - \frac{O}{\Delta t} = \frac{\Delta S}{\Delta t} \qquad (4\text{-}1)$$

where, I (m^3) is the flow entering the control volume during the time Δt, O (m^3) is the flow leaving the control volume during the same time Δt, and ΔS (m^3) is the change of storage over that period. This principle was applied to all scales from the entire modeling domain to each element. The inflows to the model domain, formed by all dams, ponds, streams, aquifers, and vegetation-covered zones are defined by:

$$\sum_{t=1}^{n} I_{t,j} = I_S + I_{GW} + I_p + U_p \qquad (4\text{-}2)$$

where, the sum of $I_{t,j}$ (m^3) is the addition of the inflows from all j elements from time step (t = 1) to the last time step (n), I_s (m^3) is surface inflow, I_{GW} (m^3) is groundwater inflow, I_p (m^3) is precipitation over the ponds, and U_p (m^3) is precipitation over vegetation-covered area. The outflows are described as follows:

$$\sum_{t=1}^{n} O_{t,j} = O_{bd} + O_{etp} + O_{sp} + U_{et} \qquad (4\text{-}3)$$

where, the sum of $O_{t,j}$ (m^3) is the addition of the outflows from all j elements from time step (t = 1) to the last time step (n), O_{bd} (m^3) is outflow leaving the ponds through the dams, O_{etp} (m^3) is pond evapotranspiration, O_{sp} (m^3) is seepage from ponds to the aquifer, and U_{et} (m^3)

is evapotranspiration from the unsaturated areas. As a result of considering inflows and outflows, the storages are described as follows:

$$\sum_{t=1}^{n} \Delta S_{t,j} = \sum_{t=1}^{n} I_{t,j} - \sum_{t=1}^{n} O_{t,j} = \Delta S_{bd} + \Delta S_v \qquad (4\text{-}4)$$

where, ΔS_{bd} (m³) is change in water stored in beaver ponds and ΔS_v (m³) is to change in water stored in the vegetation-covered areas. In the BeaverPy model, the water balance is calculated for each element for each time step from the elements upstream to downstream. All fluxes and buckets are summarized in a conceptual representation (Figure 4-2) to observe how they interact with the beaver pond and upland vegetation.
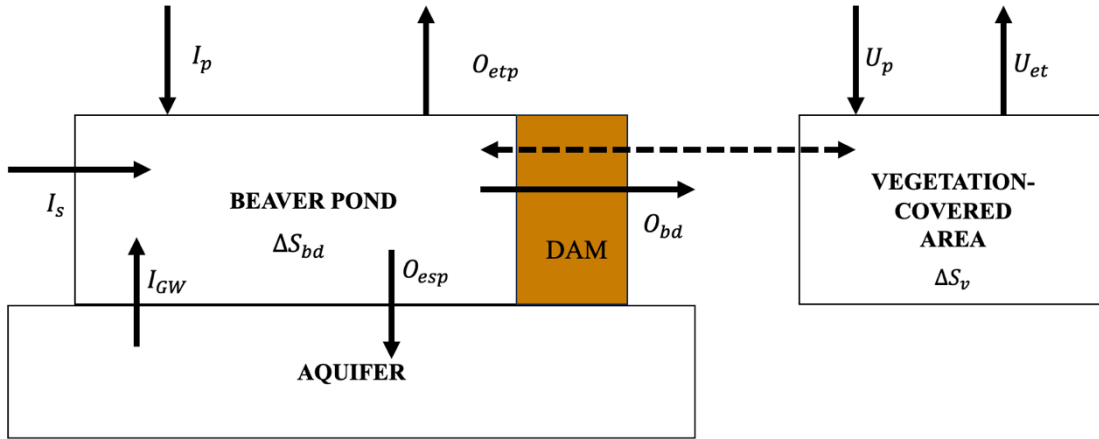
Figure 4-2 Conceptual representation of BeaverPy's modeling approach with control volumes for beaver ponds and vegetation-covered areas. The dotted line represented potential bidirectional water exchange between the beaver ponds and vegetation-covered areas which can be activated in the model if necessary. The symbols were described in equations 4-1 to 4-4. Drawings are not to scale.

The BeaverPy model was written in Python, developed to run in any recent version (>3.6) and tested in Windows (10/11), Linux (Ubuntu 22.01), and MacOS (Ventura). The code is open-source and can be installed with package-management software such as Python-Conda or Python Virtual Environment. It requires the following libraries to run: NumPy (Harris et al., 2020), Pandas (Pandas Development team, 2020), Matplotlib (Hunter, 2007), and tqdm (Costa-Luis et al., 2023). It is distributed under a GNU General Public License v3.0 and will be available at https://github.com/Ecohydrology-westbrook/beaverpy upon publication. (Appendix E). The model can be run on scripts or using Jupyter Notebooks (Kluyver et al., 2016) to enable easy reproducibility (Choi et al., 2021; Knoben et al., 2022). Included are

functions to save the model outputs in comma-separated files (CSV) or Parquet, methods to write a report with parameters and modeling decisions, and plotting utilities to show storage in ponds, inflows and outflows, and active flow states of beaver dams.

4.2.1.1. Beaver dam and pond parametrization

Beaver dams and ponds are heterogeneous in structure (Hood & Larson, 2015; Karran et al., 2017) over space and time (Ronnquist & Westbrook, 2021; Chapter 3). Changes to beaver dam structure can occur over the beaver occupancy cycle (Woo & Waddington, 1990) and over the span of days or months by the action of biological, hydrological, or geomorphic triggers (Ronnquist & Westbrook, 2021). To account for this broad range of structures, the BeaverPy model was designed as vector-based (one-dimensional arrays), instead of single-value-based.

Beaver dams were represented by their length D_l (m), width D_w (m) (Figure 4-3), position in the dam network D_p (counting from 1 to n starting upstream), and height D_h (m). Dams impound water behind them, thereby generating a pond that can be adequately represented by state variables such as its area P_a (m^2), volume P_v (m^3), and parameters such as maximum area P_{ma} (m^2), maximum volume P_{mv} (m^3), and a relationship among volume-area-water level (V-A-h; Karran et al. 2017). The pond water level at any moment t is denoted by h.
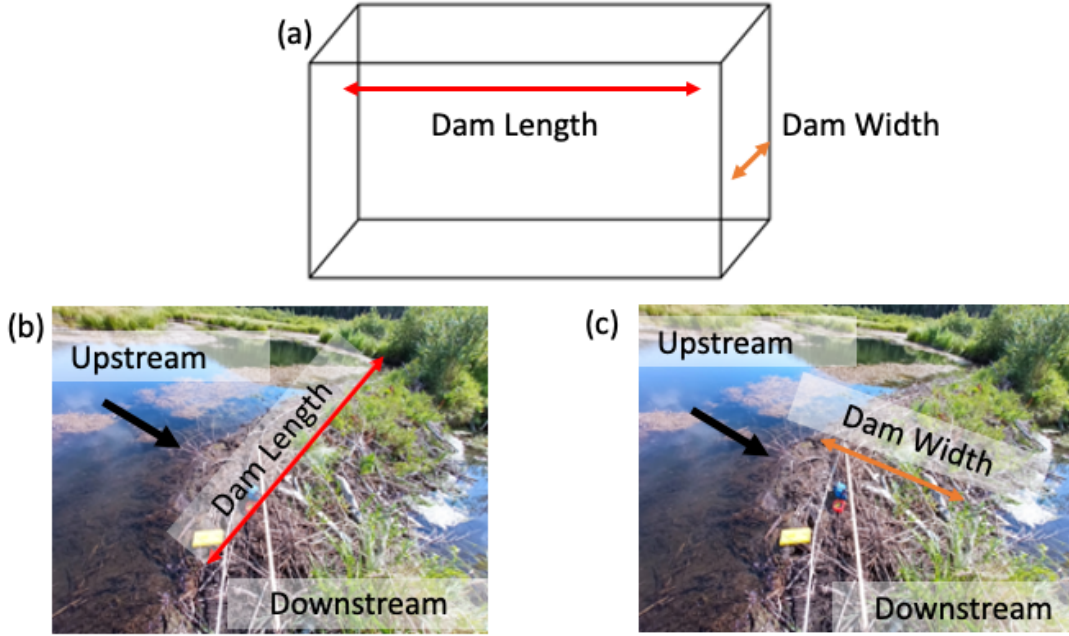
Figure 4-3 Dam length and width measurement approach. (a) shows a conceptual drawing where a red line depicts the dam length and an orange line the width (b) shows a field-captured image focusing on the dam length, which can be observed to be 90° to the flow (black line). Upstream represents the beaver pond, and downstream the stream where the dam delivers the outflow. (c) shows the same field captured image focusing on dam width in the same direction as the flow.

Two options were included for attaining the V-A-h relationship. One option is to provide a text file with bathymetry obtained from field observations. The second method is the Karran et al. (2017) algorithm, where the area ponded by a dam is calculated by:

$$P_a = s\left(\frac{h}{h_0}\right)^{\frac{2}{p}} \tag{4-5}$$

where, h_0 (m) is the unit height of the water surface (1 using SI units), s (m^2) is a scaling coefficient that represents the area of a circle with a radius of h_0, p is a dimensionless morphometry coefficient that denotes the shape of the bathymetric curve (i.e., a unique value describing the area-depth pond's relationship) The volume of a beaver pond is calculated by integrating all area profiles below h, as follows:

$$P_v(h) = \int_0^h s\left(\frac{h^*}{h_0}\right)^{\frac{2}{p}} dh^* = \left(\frac{s}{1+2/p}\right)\left(\frac{h^{(1+2/p)}}{h_0^{2p}}\right) \tag{4-6}$$

The pond area and volume are solved using fixed sequences of values every 0.1 m. To find intermediate values during the simulations, linear interpolation is used.

4.2.1.2.   Beaver dam outflow

The surface outflow (O_{bd}) released from a beaver dam is regulated by its flow state. There are six identified flow states: overflow, throughflow, underflow, gapflow, seep-flow, and mixed (Ronnquist & Westbrook, 2021; Woo & Waddington, 1990). In the BeaverPy model, each flow state is purposely represented by a unique equation to best represent the flow behavior observed in the field. During the evaluation of the surface outflow from a beaver dam, it was assumed that the pond water level is constant. To avoid large errors with this assumption, the default calculation time was set to 60 s.

The overflow state for beaver dams occurs when the water flows over the dam crest (Woo & Waddington, 1990). The overflow state is represented using a rectangular weir equation (Figure 4-3) as follows (Aydin et al., 2011; Bagheri & Heidarpour, 2010; Jain, 2001; Safarzadeh & Mohajeri, 2018; Shariq et al., 2022):

$$Q_{overflow}(h) = \frac{2}{3} C_o \sqrt{2g} D_l \Delta E^{\frac{3}{2}} \quad (h > D_h) \qquad (4\text{-}7)$$

where, $Q_{overflow}$ (m^{3}s^{-1}) is the outflow release from a dam in the overflow state, C_o is the dam overflow dimensionless discharge coefficient, g (ms^{-2}) is the gravitational constant with a value of 9.81 ms^{-2} (reference value consulted from Dingman (2015)), and ΔE is the difference between the pond water level (h) and the dam height (D_h). In this flow state, a dam is assumed impermeable. The equation is only valid if h is greater than the dam height; otherwise, the result would be 0 (Figure 4-4).
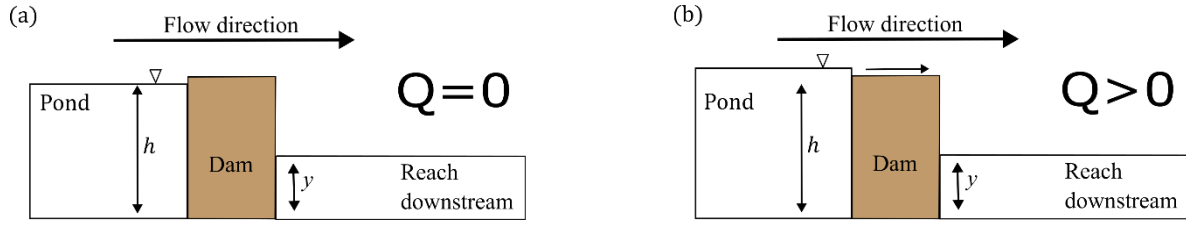
Figure 4-4 Schematic depiction of overflow flow state in beaver dams. (a) shows a pond with water level (h) below the dam's height; hence, it does not enable water transmission ($Q = 0$). (b) shows a pond with the water level above the dam's height, enabling water movement ($Q > 0$). In both cases, the dam is assumed as impervious. Dam schematics are not drawn to scale.

The throughflow state (Figure 4-5) occurs when streamflow passes through pores (i.e., diameter less than 0.02 m) in a dam. Therefore, beaver dams in the throughflow state were treated as a porous media. Flow through them is assumed to be laminar. The throughout flow state was represented with Darcy's Law, defined as (Dingman, 2015):

$$Q_x = A_x \times (-K_{hx}) \times \frac{\Delta h}{\Delta x} \qquad (4\text{-}8)$$

where, Q_x (m^{3}s^{-1}) is the discharge per unit area to the x-direction, K_{hx} (ms^{-1}) is the saturated hydraulic conductivity of a porous medium (e.g., a beaver dam) in the x-direction, A_x (m^2) is the area of the porous media and $\frac{\Delta h}{\Delta x}$ is the gradient of the total hydraulic head h of the fluid in the x direction.

For throughflow dams, a homogenous permeability is assumed for the entire dam structure (Figure 4-5b):

$$Q_{throughflow}(h) = (D_l \, \Delta\beta)K_{th}\frac{\Delta\beta}{D_w} \quad (h < D_h) \qquad (4\text{-}9)$$

where, $Q_{throughflow}$ (m^{3}s^{-1}) is the outflow resulting from a beaver dam in the throughflow state, K_{th} (ms^{-1}) is the permeability of the throughflow state, and $\Delta\beta$ is the difference between the pond water level (h) and the water level downstream y (m). The method for calculating the downstream water level is explained in section 4.2.1.3. The difference between the pond water level and the downstream water level (stream stage) drives the transmission of water (Figure 4-5a); hence, there is no transmission if both values are equal. In addition, the equation is only valid for cases where the pond water level is lower than the dam height.
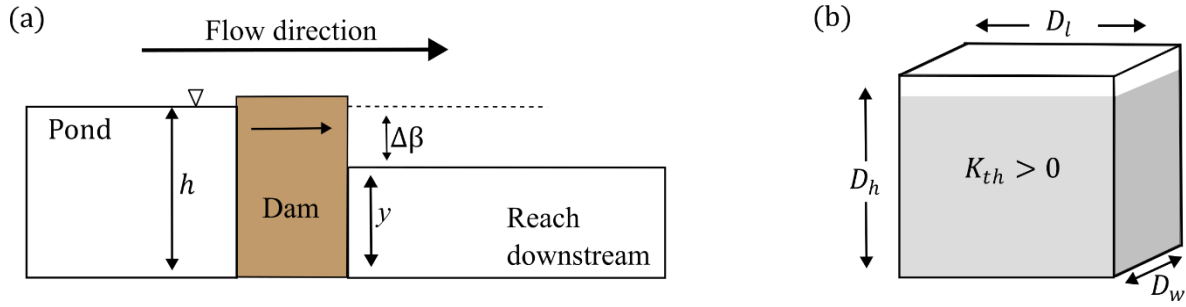
Figure 4-5 Schematic perspective of the throughflow flow state. (a) shows a lateral point of view with a flow direction from left to right. Pond level is represented by h, and the reach downstream level by y, the difference between both drives the water transmission ($\Delta\beta$). (b) shows a close-up perspective of dam, observed from upstream, the grey area has a homogeneous positive permeability enabling water movement. In (b), the white area shows the area without water transmission because the pond water level must be lower than the dam height. Dam schematics are not drawn to scale.

The underflow state (Figure 4-6) occurs when water is transmitted through the lower section of a beaver dam (Woo & Waddington, 1990). To represent this flow state, dam height, D_h, is divided into two sections by D_t: a lower section with a positive permeability (below D_t), and an upper section with a permeability of 0 (above D_t; Figure 4-6b). D_t is represented with a vector and can vary over time. The equation representing outflow when a dam in is the underflow state is:

$$Q_{underflow}(h) = (D_l \, UF) \, K_u \frac{\Delta\beta}{D_w} \quad (h < D_h) \tag{4-10}$$

where, $Q_{underflow}$(m³s⁻¹) is the outflow resulting from a dam in underflow state, K_u (ms⁻¹) is the permeability of the lower section of a dam during the underflow state, and ΔUF(m) is the difference between the pond water level and D_t:

$$\Delta UF = \begin{cases} h \; (h \le D_t) \\ D_t \; (h > D_t) \end{cases} \tag{4-11}$$

Like the throughflow state, the difference between the pond water level and downstream water level (stream stage) drives the transmission of water (Figure 4-6a), and the equation range is valid only if the pond water level is below the dam crest.
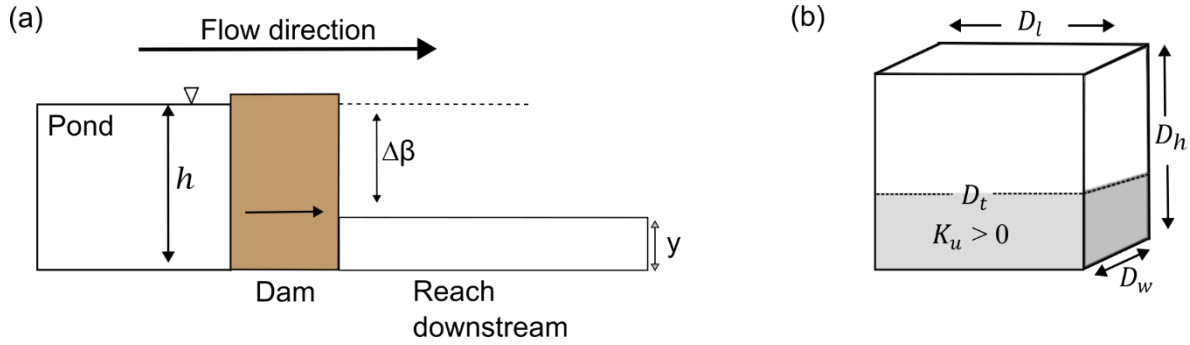
Figure 4-6 Schematic perspective of the underflow flow state. (a) shows a lateral point of view and the arrow notes the underflow area for water transmission. (b) shows the permeability of the dam observed from upstream, where the lower grey area has a positive homogeneous permeability, and above the D_t there is no water movement (permeability = 0). Dam schematics are not drawn to scale.

The gapflow state of beaver dams (Figure 4-7) occurs when the water is transmitted past a dam through gaps in it (Woo & Waddington, 1990). A gap in the dam is defined if the diameter of a hole is larger than 0.02 m (Ronnquist & Westbrook, 2021). As informed by field observations, there appear to be two gapflow schemes: G-1, which occurs when water is transmitted through gaps in the body of the dam structure, and G-2, which occurs when water is transmitted via a gap located in the crest of the dam, where the upper side of the gap is open to the atmosphere. G-1 and G-2 are independent and can be present at the same time. To represent this flow state, dam height D_h was divided into two sections by D_g (m): the portion where the water flows via the G-1 approach, and an upper portion where the water flows via the G-2 approach (Figure 4-7b). The G-2 approach was represented by a rectangular weir with two contractions as follows (Aydin et al., 2011; Bagheri & Heidarpour, 2010; Jain, 2001):

$$Q_{weir-gapflow}(h) = \frac{2}{3} C_g \sqrt{2g} \left(R_g - 0.2J\right)J^{\frac{3}{2}} \ (h < D_h) \qquad (4\text{-}12)$$

where, $Q_{weir-gapflow}$ (m³s⁻¹) is the outflow resulting from the G-2 approach, C_g is the dimensionless discharge coefficient of the gapflow weir, R_g (m) is the length of the contracted weir, and J(m) is the water level above D_g (Figure 4-7b). Then, the G-1 approach was represented following the same strategy as the throughflow state with a homogeneous permeability. The entire gapflow parametrization is the combination of both equations, defined as follows:

$$Q_{gapflow}(h) = Q_{weir-gapflow}(h) + [(D_l\,\Delta GF)\,K_g\,\frac{\Delta\beta}{D_w}]\,(h < D_h) \qquad (4\text{-}13)$$

where, $Q_{gapflow}(\mathrm{m^3s^{-1}})$ is the outflow resulting by a dam in gapflow state, $K_g(\mathrm{ms^{-1}})$ is the permeability of the dam during the gapflow state, and $\Delta GF(\mathrm{m})$ is given by the difference between the pond water level and D_g as follows:

$$\Delta GF = \begin{cases} h\,(h \le D_g) \\ D_g\,(h > D_g) \end{cases} \qquad (4\text{-}14)$$

The difference between the beaver pond and stream stage downstream of the beaver dam is key in driving water transmission (Figure 4-7a).
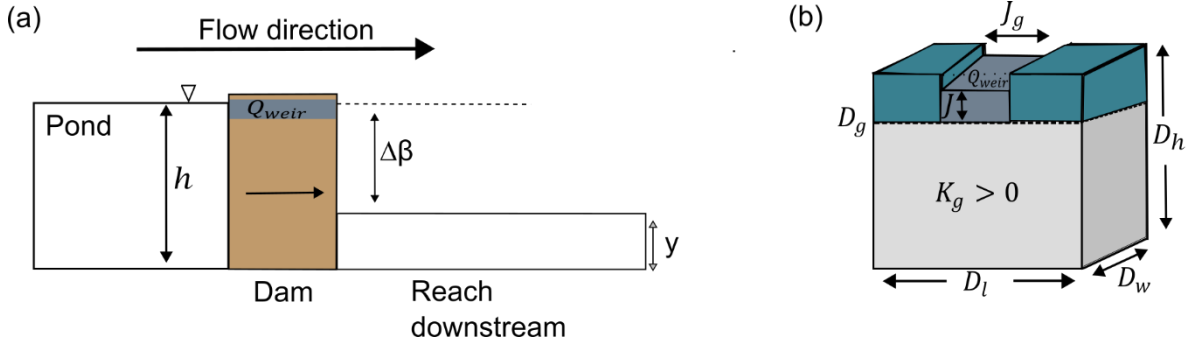
Figure 4-7 Schematic perspective of the gapflow state. (a) shows a lateral perspective where the main part of the dam is transmitting water by the gaps (G-1) and the upper part by the large gap (G-2, darker grey). (b) shows the dam from upstream, where the zone below D_g has a unique homogenous positive permeability (flow by gaps, G-1), and the zone above D_g shows the rectangular contracted weir (G-2, on darker grey). If the pond water level is higher than the zone parametrized by the weir, the water can flow by the turquoise zone. Dam schematics are not drawn to scale.

The seep-flow state occurs when surface water is transmitted to the downstream side of the beaver dam as hyporheic flow (Janzen & Westbrook, 2011; Ronnquist & Westbrook, 2021). The seep-flow state is represented with a Darcy-Forchheimer approach (Prieto, 2009):

$$Q_{seep\,flow}(h) = K_s\,\Delta\beta\,\frac{N_f}{N_l}\,D_w \qquad (4\text{-}15)$$

where, $Q_{seep\,flow}(h)\,(\mathrm{m^3s^{-1}})$ is the outflow resulting from a dam in the seep-flow state, K_s is the permeability of pond sediments, N_f is the number of flow channels, and N_l is the number of equipotential lines (Figure 4-8). Darcy-Forchheimer provides a physical-based solution

with variables that can be collected in hydrological studies in areas dominated by beaver dams, thereby avoiding over-parametrization.
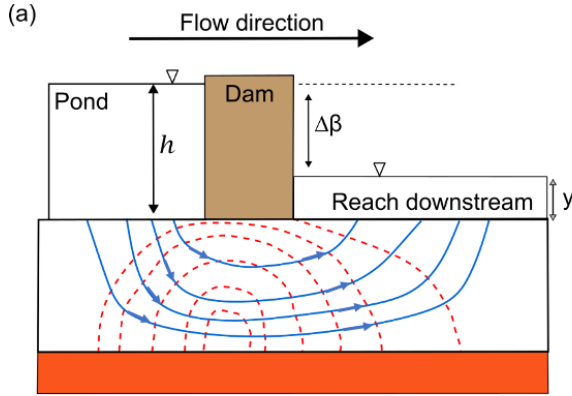
Figure 4-8 Schematic perspective of seep-flow state. The flow goes from left to right. The blue lines represent flow channels and the dotted red lines equipotential lines. The orange layer below can represent an impervious stratum or another aquifer layer. Dam schematics are not drawn to scale.

The mixed flow state (Ronnquist & Westbrook, 2021) is the existence of two or more flow states at the same time. In this first version of the BeaverPy model, combinations of only two different flow states with a unique code for each (see section 4.2.1.4 for the codes) are possible. The code could be improved in the future to include more than two flow states occurring at the same time. The flow states are given the same weight and therefore their mathematical representation is the sum between the flow states comprising the mixed state.

4.2.1.3. Stream stage downstream of a beaver dam

The channel water level (i.e., stream stage) downstream of the dam is solved using Manning's equation, assuming no backwater effects in the immediate vicinity of the dam downstream of it. The calculation considers the outflow of any channel (Jain, 2001):

$$Q = A \, W \tag{4-16}$$

where, Q (m³s⁻¹) is the discharge through a stream cross-section, A (m²) is the area of the cross-section, and W (ms⁻¹) is the average velocity through the cross-section. Stream velocity is for a steady uniform flow (Jain, 2001):

$$W = \frac{R^{2/3} \, S^{1/2}}{n} \tag{4-17}$$

63

where R (m) is the hydraulic radius determined by the cross-sectional area of flow divided by the wetted perimeter, S (m m^{-1}) is the stream slope, and n (s/[m$^{1/3}$]) is the Manning roughness coefficient. BeaverPy version 1.0 only provides simulation for streamflow for roughly rectangular-shaped channels given their common occurrence in the case study site (Shaw, 2009; see section 4.3). The hydraulic radius for a rectangular channel is (Jain, 2001):

$$R = \frac{w\,u}{w + 2u} \tag{4-18}$$

where w (m) is the width of the channel, and u (m) is the hydraulic depth of the water downstream. To find the hydraulic depth (u) in each iteration, referred to as the depth of water downstream (y) in 4.3.3, the following equation is iteratively solved using the discharge (Q_{t-1}) from the previous time step:

$$Q_{t-1} = \frac{(\frac{w\,u}{w + 2u})^{2/3}\, S^{\frac{1}{2}}\,(w\,2u)}{n} \tag{4-19}$$

Channel dimension can be customized to site conditions by altering equation 4-18.

4.2.1.4. Flow state of beaver dams

The flow state of a beaver dam is dynamic on time scales of days, months, and years. For example, in Chapter 3 it was shown that the flow state of beaver dams can change up to 12 times over a six-month period, triggered by the majority of the time by rainfall runoff. To represent the dynamic flow state of beaver dams in the BeaverPy model, a specific module was constructed. Each possible flow state was assigned a unique two-digit code (Table 4-1). Beaver dams in a single flow state, such as overflow, gapflow, throughflow, seep flow, and underflow, are represented by numbers between 11 and 15. Dams in a mixed-flow state (Ronnquist & Westbrook, 2021) are represented by numbers between 21 and 90. Codes from 90 to 99 represent other situations, such as modeling problems (90), periods without observed data (91), or unknown errors (99).

Table 4-1 Flow of beaver dams two-digit coding system. Single flow states are defined from 11 to 15 and mixed composed of two states from 21 to 30. Other situations regarding flow state are denoted with values from 90 to 99.

Category	Flow state of beaver dams	Code
Single flow states	Overflow	11
	Gapflow	12
	Throughflow	13
	Underflow	14
	Seep flow	15
Mixed flow states	Overflow – Gapflow	21
	Overflow – Throughflow	22
	Overflow – Underflow	23
	Overflow – Seep	24
	Gapflow – Throughflow	25
	Gapflow – Underflow	26
	Gapflow – Seep	27
	Throughflow – Underflow	28
	Throughflow – Seep	29
	Underflow – Seep	30
Others	Model output problem	90
	Observed data undefined flow state	91
	Unknown problem	99

The module checks every time step which flow state (Table 4-1) is occurring to calculate the surface outflow for each dam. There are three modeling choices for setting the flow state of a beaver dam: (a) set one flow state during the entire simulation, (b) set the flow state by reading a file (i.e., a hindsight approach), which allows use of observed flow state data, and (c) set the flow state by using conditions and rules to describe how flow state should change by calling other model variables (e.g., pond water level, total pond inflow, or discharge from the previous time-step). This last approach enables flow state forecasting by simulating periods without observed data using an understanding of the basin.

Modelers can configure a dam to run with the selected flow state plus the seep-flow to represent the ever-present water flowing below the dam through the sediments via gravity, as observed in peat-dominated environments. In addition, if a pond level is higher than the dam height, a flooding submodule activates, and the overflow state temporarily is used until the pond level falls to below the dam height. The flooding submodule is set to direct all excess water (i.e., water above the dam height) downstream (Figure 4-9a). This approach differs from field observations, which show that beaver ponds can also trigger overbank

flooding onto the floodplain (Figure 4-9b; Westbrook et al., 2006). Overbank flooding was not considered as it requires high-resolution (< 1.0 m) topographic imagery, which may or may not be available for all sites. By contrast, the approach employed is quick to configure and run, and does not require topographic data, which makes it easier to use in areas with scant data.
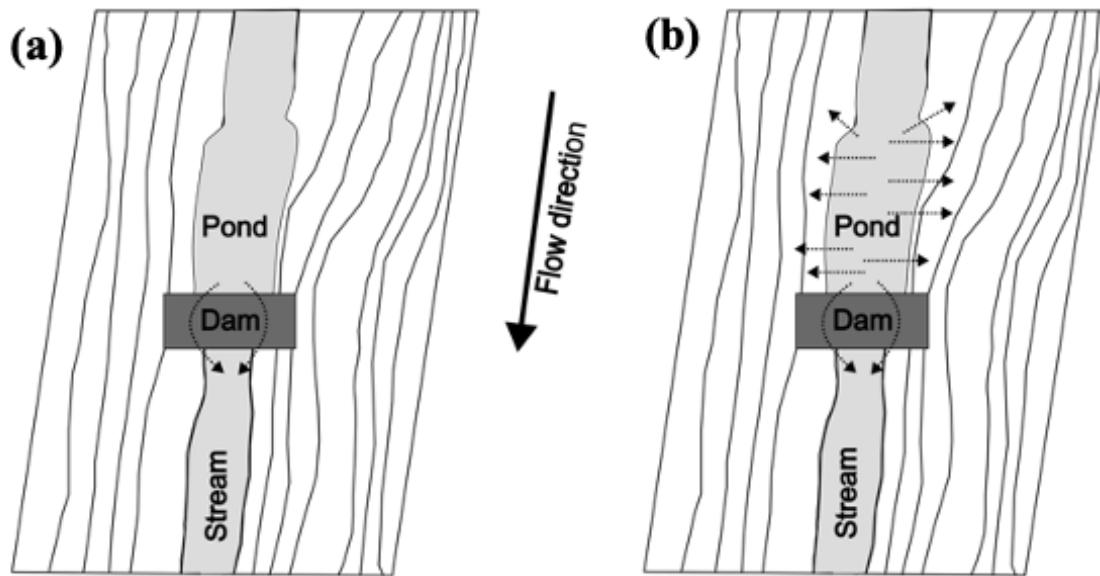
Figure 4-9 Flooding modeling approaches. Dotted arrows represent the overbank flooding direction, and solid black lines represent topographical contours. (a) shows the implemented approach where excess water is only directed downstream, and (b) shows observed flooding patterns where ponds inundate all directions onto the floodplain

4.2.1.5. Surface inflow

The BeaverPy model is a 1-D hydraulic model developed to route water through beaver dams and ponds. It therefore requires a forcing time series of surface inflow (m^3s^{-1}) to the beaver dam sequence. These forcing data must be complete (i.e., not missing data) and can be sourced from site streamflow, or alternatively, stream simulated from hydrological models.

To conduct research without an inflow streamflow gauge, the BeaverPy model can be coupled with a regionally suitable hydrological model. In this area the Cold Regions Hydrological Model (CRHM; Pomeroy et al., 2007, 2022) is one such example model platform, given its effectiveness in simulating hydrological processes in cold regions (Belvederesi et al., 2022), which is the type of environment beavers generally live in (Hood,

2020b). CRHM has modules to represent the redistribution of snow by the wind, snowmelt, evapotranspiration, avalanches, and runoff. CRHM was designed for ungauged catchments and does not require extensive calibration and produces a good representation of the dynamics of mountain basins (Ellis et al., 2010; Fang et al., 2013; Fang & Pomeroy, 2020). Annand (2022) coupled CRHM with the hydraulic model SWMM to represent hydrology of prairie ponds with excellent results, thus providing a path for CRHM + BeaverPy simulations.

4.2.1.6. Direct rainfall on beaver ponds

Beaver ponds can receive liquid and solid precipitation, depending on the geographic setting, which can increase the water level of the impoundment. Direct rainfall on beaver ponds is simulated via a routine (Neitsch et al., 2011):

$$I_{rp} = P_a L_p \qquad (4\text{-}20)$$

where, I_{rp} (m³) is the water volume added to the pond by precipitation for an instant t and L_p (mm) is the amount of precipitation (rainfall and snowfall) falling over the pond at the same time. The module uses the area of the pond P_a for that given time, calculated used the method described in section 4.2.1.1. If the precipitation over the vegetation-covered areas routine is active, the flows are handled by this module which uses the area of the zone and the same precipitation inputs.

4.2.1.7. Evapotranspiration from beaver pond and uplands

The BeaverPy model has two parametrizations for evapotranspiration: Penman-Monteith is used in unsaturated areas such as the uplands and vegetated areas of riparian wetlands where the water table is below ground. Priestly-Taylor is used in saturated areas such as beaver ponds. This dual evapotranspiration framework has been successfully used in different ecoregions, such as the Rocky Mountains (Fang et al., 2013), the Canadian Prairies (Cordeiro et al., 2017), and the Arctic (Krogh et al., 2017; Rasouli et al., 2014).

Penman-Monteith evaporation is calculated from net radiation, stomata resistance, and surface roughness as follows (Monteith, 1981):

$$\lambda_v E = \frac{s(R_n - R_g) + \rho_a \, c_p(\frac{e_s - e_a}{r_a})}{s + \gamma \, (1 + \frac{r_s}{r_a})} \tag{4-21}$$

where $\lambda_v E$ (MJ) is the latent heat of vaporization, s (kPa C^{-1}) is the slope of the saturation vapor pressure-temperature curve, R_n(MJ) is the net radiation, R_g(MJ) is the soil heat flux, ρ_a (kg m^{-3}) is the air density, c_p(MJ kg^{-1} C^{-1}) is the specific heat of air, e_s(kPa) is the saturation vapor pressure, e_a(kPa) is the actual vapor pressure, r_a(day m^{-1}) the air resistance, γ(kPa C^{-1}) is the psychrometric constant, and r_s(day m^{-1}) is the surface resistance.

Priestly-Taylor evapotranspiration is calculated using an energy balance with an empirical factor that accurately works the results in open water bodies (Krogh et al., 2017), defined by (Priestley & Taylor, 1972):

$$\lambda_v E = \alpha \frac{s \, (R_n - R_g)}{s + \gamma} \tag{4-22}$$

where α is a dimensionless empirical value accounting for the vapor pressure deficit and surface and aerodynamic resistance (Lhomme, 1997), with a value range from less than 1 (very humid conditions) to almost 2 (arid conditions). The BeaverPy model calculates evapotranspiration daily, and then the results are distributed (i.e., resampled) to the time-step of the model (as defined by the user) considering only active daylight. The Priestly-Taylor values are scaled to the actual area of the ponds and Penman-Monteith values are scaled to the upland values.

4.2.1.8. Groundwater fluxes

In wetlands with beaver activity, groundwater-surface interactions play a relevant role in the water budget (Feiner & Lowry, 2015; Streich & Westbrook, 2020; Westbrook et al., 2006), justifying the need to include them in BeaverPy. Groundwater inflow (I_{GW}) to each pond is represented with a linear reservoir approach in which each pond is associated with a groundwater bucket that releases water to the ponds. Linear reservoirs are conceptual representations that use a simple function for the outflow (Dingman, 2015; Fenicia et al., 2011). Classic implementations of linear reservoirs consider only one outflow at the bottom (Figure 4-10a); however, wetland water tables can rise above the land surface. To account

for surface flooding, the classic approach was modified, adding a second outflow at the top to release the surplus water (Figure 4-10b). The difference is given by the maximum storage parameter (S_{max}), which limits the bucket's storage. If the storage is below the maximum, the outflow is defined by the following equation:

$$GW_o = k_{gw}GW_s \quad (GW_s < S_{max}) \tag{4-23}$$

where, GW_o (m³s⁻¹) is the outflow of the linear reservoir and therefore the inflow to the pond; GW_s (m³) is the storage in the groundwater bucket, S_{max} (m³) is the maximum storage of the groundwater bucket, and k_{gw}(s⁻¹) is the reservoir constant (Dingman, 2015; Fenicia et al., 2011). If the storage is higher than the maximum, the outflow is defined by:

$$GW_o = (k_{gw}GW_s) + GW_{ei} \quad (GW_s \geq S_{max}) \tag{4-24}$$

where GW_{ei} (m³s⁻¹) is the additional inflow to the bucket once it reaches the maximum and it is directly transmitted as groundwater outflow from the bucket. In addition, the infiltration from beaver ponds to the aquifer (i.e., pond seepage) can be simulated by user choice of either the same linear reservoir with different parameters values or a fixed rate (mm/day).
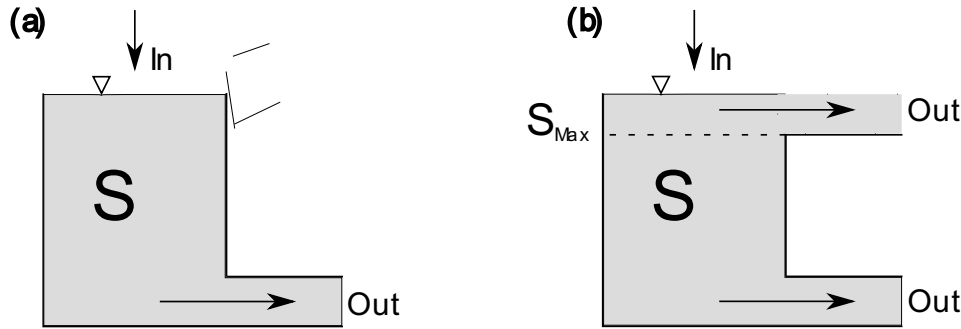
Figure 4-10 Linear reservoirs approaches for groundwater flow, where S refers to the storage. (a) shows the classic one outflow described by Dingman (2015) and Fenicia et al. (2011). (b) shows the two outflows implementation used on BeaverPy where S_{max} limits the storage.

4.2.1.9. Routing water from one beaver dam to another

For simulations with multiple dams, the BeaverPy model includes two approaches for routing water between beaver dams (streamflow routing): instantaneous and Muskingum. Instantaneous routing is defined as the outflow from the upstream dam being directly used as the downstream pond inflow. Muskingum (McCarthy, 1938; Perumal & Price, 2013)

routes the water and delays flood waves. The Muskingum parametrization starts with a finite difference approximation of the continuity principle (Equation 4-1) as follows:

$$\left(\frac{I_{t-1} + I_t}{2}\right) - \left(\frac{O_{t-1} + O_t}{2}\right) = \left(\frac{S_t + S_{t+1}}{2}\right) \qquad (4\text{-}25)$$

where the subscript t refers to the current timestep, and is solved using a travel time parameter as follows:

$$S_t = KO_t + KX(I_t - O_t) = K[XI_t + (1 - X)O_t] \qquad (4\text{-}26)$$

where, K (s) is the travel time of the flood wave routing through each stream reach and X (dimensionless) is the weight of outflow defined between 0 and 0.5.

BeaverPy is designed to simulate a wide range of beaver-dominated environments to which these two routing approaches are provided. Several authors suggest using Muskingum with basins larger than 2 km^2 to avoid unrealistic values within the time-dependent parameter K (Das, 2004; Gill, 1979; Nash, 1959; Singh & McCann, 1980). Similarly, smaller basins are modeled with an instantaneous routing approach. It is recommended to compute the travel time from one dam to another for all cases to evaluate the best routing modeling decision.

4.3. STUDY CASE

A beaver-dominated catchment, Sibbald, in the Canadian Rocky Mountain foothills west of Calgary, Alberta was chosen as the case study. Sibbald is described in detail in section 3.2.1 of this thesis. Considered was only the southeast (SE) section of Sibbald (Figure 4-11), a 0.10 km^2 beaver-dammed valley bottom that is drained by an unnamed stream, a tributary of Bateman Creek. The SE-section of Sibbald has an independent groundwater flow system based on the analyses of groundwater flow nets (Karran et al., 2018). There are approximately 26 beaver dams arranged in a network pattern (Chapter 3). Three beaver dams in sequence for study (Figure 4.10) were selected, given the availability of a rich 2022 dataset composed of daily flow state, with the drivers for each change, detailed field measurements, pond levels, and stream water level collected downstream of the dams (Chapter 3).

The stream channel in the SE part of Sibbald has a rectangular form (Shaw, 2009), which is common in peat substrates (Watters & Stanley, 2007). The water level downstream of each

dam was continuously measured using a level sensor (Leverlogger, Solinst, ON) installed in a PVC standpipe as described in section 3.2.2. Barometric pressure-corrected stream stages were converted to discharge using a site-specific rating curve. To construct the rating curves, stream velocity at 60% depth at three measurement points across the narrow channels measured using a magnetic-inductive 2-decimal precision flow meter (OTT MF Pro). Stream depth was measured at each point using a standard wading rod. In all, the rating curves were built from discharge measures obtained during five field visits between May and August 2022 (Appendix F).

In addition, a 1-m resolution LIDAR dataset was collected on June 16, 2022, by members of the Centre for Hydrology, University of Saskatchewan using a drone Rigel miniVUX2. Further, a detailed 1-m bathymetry and parameters for computing pond water volume via the V-A-h method of Dam #1 were available from previous fieldwork conducted by members of the Rocky Mountain Ecohydrology Research Group (C. Westbrook, unpublished data; Karran et al., 2017).

Meteorological data (rainfall, snow depth, temperature, wind, humidity, and solar radiation, and a camera trap to assist in differentiating snow from rain) obtained from the Sibbald weather station (51.056°N, 114.868°W at 1490 m.a.s.l.) were used as forcing data in the model. A detailed description of the station and its instruments is available at Streich & Westbrook (2020) and Westbrook & Bedard-Haughn (2016).
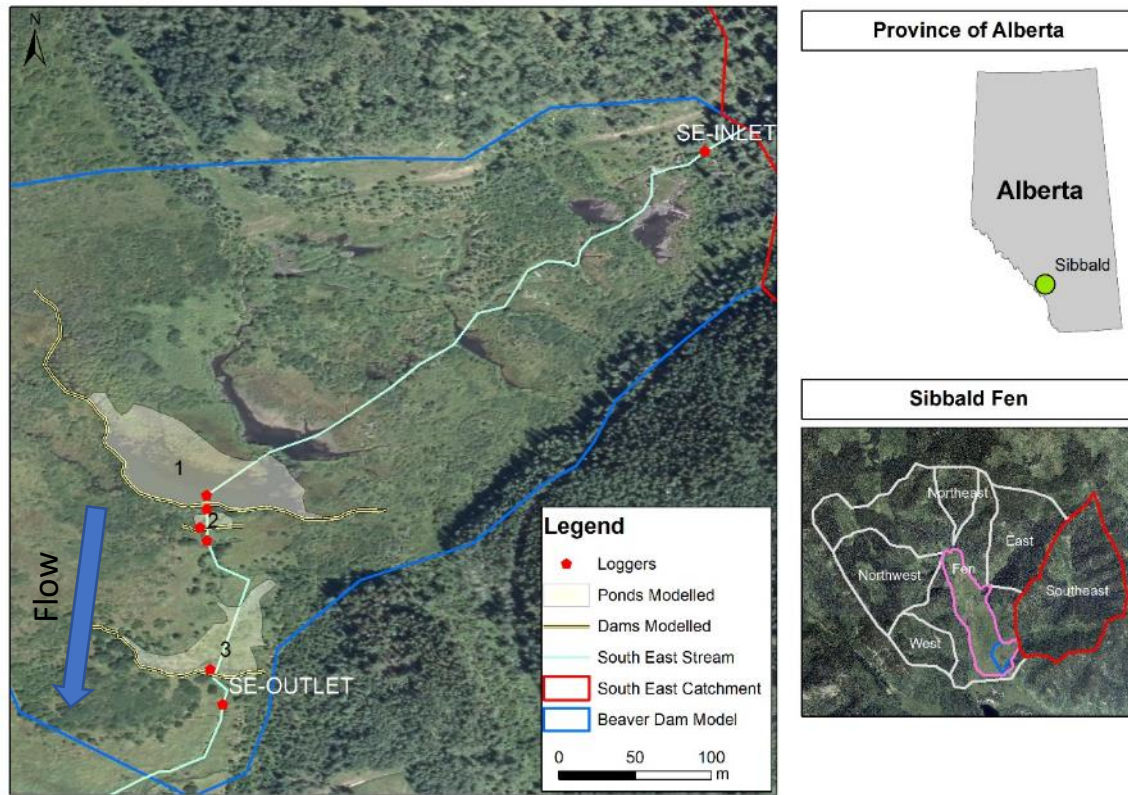
Figure 4-11 Map of the dams included in the BeaverPy demonstration. The principal map (left) depicts the southeast section of Sibbald Fen, showing the inlet station (SE-Inlet), the outlet station (SE-Outlet), and the three ponds included in the demonstration numbered from upstream to downstream. The boundaries were delineated with a 1.0-m resolution LIDAR imagery collected on June 16, 2022, by members of the Centre for Hydrology, University of Saskatchewan. The blue arrow indicates flow direction of the SE stream. The upper-right map shows the Canadian province of Alberta and the location of Sibbald Fen in the Canadian Rocky Mountains. The lower-right maps show the Bateman Creek catchment, which provides surface inflow to Sibbald Fen (in pink). The SE contributed basin is depicted in red, and the SE section of the fen in blue.

Several modeling decisions were adopted to conduct the simulation of the SE section of Sibbald Fen in BeaverPy. Given the basin size and a maximum travel time between the inlet and Dam #1 was <15 minutes, the routing approach chosen was instantaneous. The runoff from the upland area of each pond was not modeled, as the study case was focused on streamflow modulation by beaver dams. During the field study, there was no observed overbank flow from ponds to the vegetated riparian areas, making the separation (pond and upland area) possible and realistic. Owing to the lack of overbank flow, only pond evaporation, not vegetation evapotranspiration was considered. The pond evaporation was modeled using Priestly-Taylor.

I chose a process-based modeling approach to evaluate BeaverPy performance at the case study site, Sibbald Fen (See section 4.2.1). This means that parameter values were set based on field observations obtained between May and October 2022, or on previous research conducted at the site. The parameters used in the model are described in Table 4-2. There was therefore limited calibration of BeaverPy (see section 4.4). Calibration was performed only to establish the thresholds of change from one beaver dam flow state to another due to the short time series of beaver dam flow states observed in the field.

Table 4-2 Set of parameters used in the Sibbald Fen simulation and their source.

Sets of parameters	Source
Flow states of beaver dams	Chapter 3
Pond morphometry (length, width, height)	Measured during 2022 fieldwork using rulers.
Pond depth	For Dam #1 obtained from detailed bathymetry (See Figure 4-13). For Dam #2, measured manually with a ruler during June 2022 fieldwork. For Dam #3, assumed the same as Dam #1 given difficulties for measuring it during fieldwork.
Pond shape	Determined using LIDAR collected on June 16, 2022, by members of the Centre for Hydrology of the University of Saskatchewan.
Beaver dam characteristics (gaps size, gaps number, effective hydrologic height)	Fieldwork conducted during 2022 and the database generated by Ronnquist & Westbrook (2021)
Seep flow data	Janzen & Westbrook (2011)

4.4.   PARAMETER CALIBRATION

The BeaverPy modeling period was from May 28 to September 28, 2022 to match observed data. Internal calculations were computed using the default 60-second time step, and the results were analyzed using an hourly resolution. The changes from one flow to another were modeled using pond level-based rules. A minimum and maximum pond level was set for

each flow state, and if the pond level was computed outside of these limits, the flow state changed. For instance, if the pond level was close to the dam crest, the flow state could change to overflow. The flow state thresholds were defined independently for each dam, and the values were obtained through calibration (See section 4.3).

A limited calibration was performed to adjust the thresholds for each flow state of beaver dams. The values were modified only during the calibration period described below. The budget for simulations was set at 20 runs for each Dam. The objective function was RMSE, as it matched the average behavior of the hydrographs. As a result, each flow state threshold was adjusted. For instance, the overflow state threshold was set at 0.9 m for Dam #1, 0.8 m for Dam #2, and 1.2 m for Dam #3. The values set for individual runs were kept to the in-sequence simulation.

A calibration from May 28 to July 30 (62 days) and a validation period from July 31 to September 27 (61 days) were defined to evaluate the flow state threshold calibration. Five standard metrics were selected to assess model performance during calibration and validation periods – the root mean square area (RMSE), the range normalized root mean square error (NRMSE), the mean log error (MLE), the modified Nash-Sutcliffe efficiency (NSE_m), the Kling-Gupta efficiency (KGE), and the Model Bias (MB). RMSE (Willmott et al., 2005) was calculated as follows:

$$RMSE = \left(\frac{1}{n} \sum_{i=0}^{n} (S_i - O_i)^2 \right)^{\frac{1}{2}} \tag{4-27}$$

where S represented the simulated values, and O the observed ones. Each timestep was represented by the subindex i and n represents the total of time series (sample size). Results for this metric is provided in the same unit as the unit of the input data. NRMSE (Han et al., 2020; Pontius et al., 2008) normalized the RMSE range with the range compare within the results scale, and is defined by:

$$NRMSE = \frac{RMSE}{(\max(O_i) - \min(O_i))} \tag{4-28}$$

where max and min refer to the maximum and minimum observed value. MLE (Törnqvist et al., 1985) is described by:

$$MLE = \frac{1}{n}\sum_{i=0}^{n} \ln(\frac{S_i}{O_i}) \tag{4-29}$$

NSE_m (Krause et al., 2005) is a modified version of the NSE metric (Nash & Sutcliffe, 1970), which gives less weight to outliers and is calculated as follows:

$$NSE_m = 1 - \frac{\sum_{i=1}^{n}|S_i - O_i|^{j_e}}{\sum_{i=1}^{n}|O_i - \bar{O}|^{j_e}} \tag{4-30}$$

where, $\bar{O}$ refer to the mean of observed values, and j_e is the outlier coefficient weight set to 1 following Krauser et al. (2005). KGE (Gupta et al., 2009; Knoben et al., 2019) is defined by:

$$KGE = 1 - \sqrt{(r-1)^2 + \left(\frac{\sigma_S}{\sigma_o} - 1\right)^2 + \left(\frac{\mu_S}{\mu_O} - 1\right)^2} \tag{4-31}$$

where, r is the Pearson Correlation coefficient, σ_S is the standard deviation of simulations, σ_O is the standard deviation of observations, μ_S is the simulation mean, and μ_O the observation mean. MB (Fang et al., 2013) is computed as follows:

$$MB = \frac{\sum_{i=0}^{n} S_i}{\sum_{i=0}^{n} O_i} - 1 \tag{4-32}$$

Using different metrics thoroughly assesses key sections of the hydrograph, including trend representation, magnitude, and timing. For RMSE, MLE, and MB, close values to 0 are better. Positive values of MLE and MB suggest overestimation and negative underestimation of measured values. For NSE_m and KGE, closer values to 1 are better. NSE_m and KGE cannot be directly compared as their relationship is not unique, and it is linked to the coefficient of variation of measured values (Knoben et al., 2019). All metrics were computed using the HydroErr Python package (Roberts et al., 2018).

4.5.   RESULTS

4.5.1. Simulation of a single beaver dam in Sibbald Fen

The BeaverPy model was first run for a system containing a single beaver dam. Dam #1 (Figure 4-12). Dam #1 is 91 m long built with branches with a diameter of between 0.01 and

0.3 m placed over an initial layer of mud. It is located in an upstream position in the studied beaver dam sequence. It had an effective hydrological height (*sensu* Ronnquist & Westbrook, 2021) of 1.2 m (Chapter 3) and a single surface outflow. Its most frequent flow state was underflow, with changes from one flow state to another driven by rainfall the majority of the study period (Chapter 3). There was no water flowing over the top (i.e., overflow state) during the study period based on daily images acquired with a camera trap (Chapter 3) and observations during six field visits. Outflow from the dam flows into the peat-lined SE stream in a 1.27 m wide reach before flowing into another beaver pond.

Figure 4-12 Photograph of the outflow of Dam #1 in Sibbald Fen obtained on September 27, 2022, to illustrate the characteristics of this outflow. Most often, the water is transmitted using the underflow flow state (Chapter 3).

The pond generated by Dam #1 is surrounded by vegetation, primarily sedge and willow (*Salix* spp.). Pond bathymetry, measured on June 16 to 17, 2009 (C. Westbrook, unpublished data; Figure 4-13) indicated the maximum depth of the pond associated with Dam #1 was 1.69 m.

In BeaverPy, the V-A-h curves were used to compute pond storage for Dam #1 (Figure 4-12). Therefore, the field bathymetric data were used to parameterize the Karran et al. (2017) method to calculate pond storage. The pond at Dam #1 had $p = 0.7$ and $s = 331.4$ m^2. Then, it was compared the bathymetry-measured and computed curves obtained an R^2 of 0.99.
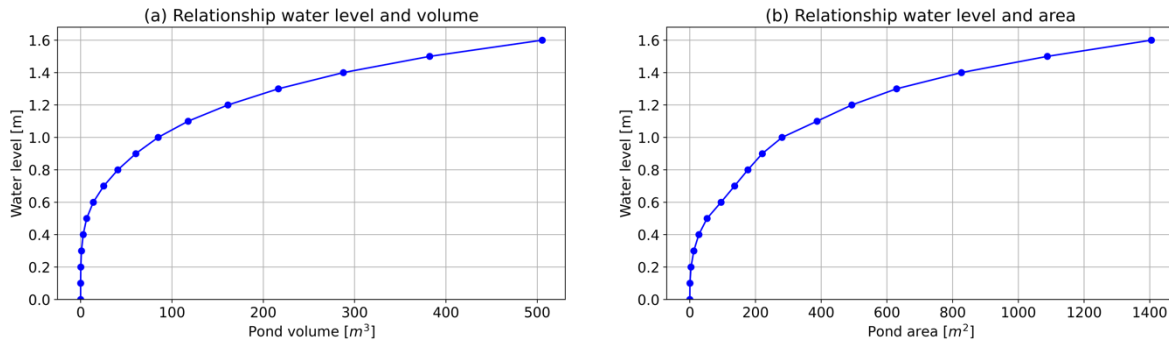
Figure 4-13 Relationship among pond water level (h), pond volume (V), and pond area (A) for Dam #1. (a) presents the relationship between water level and volume, and (b) shows the relationship between water level and area.

Figure 4-14 and Table 4-3 shows the measured and modelled stream discharge downstream of Dam #1. Simulated discharge was well matched in terms of event timing with observations. For example, the simulated peak discharge on June 14 in response to the 96.2 mm rainfall occurred within 11 hours of observed. As well, the simulated streamflow indicates peaks occurring after rainfall on July 4 and August 23, which are consistent in timing with observations. The simulated streamflow also shows diel cycles consistent with an evapotranspiration effect that match with observations (Figure 4-16 and 4-18). In general, simulated discharge after the June 12-15 rainfall of 96.2 mm was higher than observed. The mismatch in magnitude could be due to the location of the SE-inlet, which was used as inflow forcing for this simulation and Dam #1. In the 296 m between the SE-inlet and Dam#1, there are eight ponds (average area of 179 m^2) that might play a bigger role in the water retention along the stream, given the differences between the measured and modeled flow peak. The following flow peaks (July 4 and August 15) did not present the mismatch in the same magnitude because the upstream ponds could have been full. In hindsight, it would have been useful to install a stream gauging station immediately upstream of the pond associated with Dam #1, which then would have provided an unaltered input to the simulations.
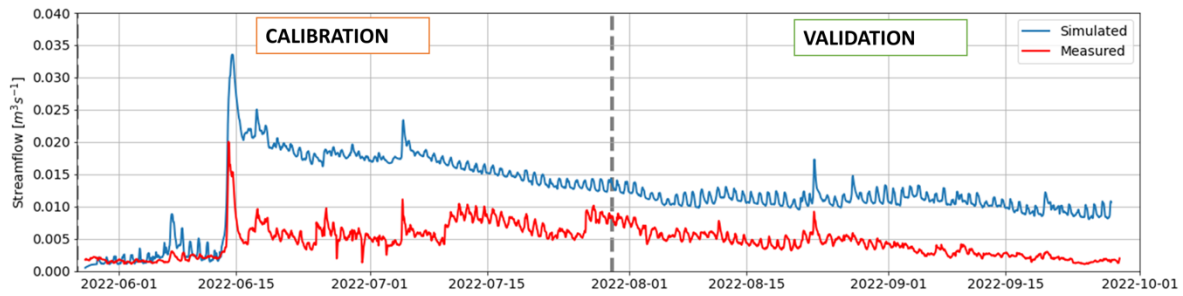
Figure 4-14 Modelled (blue) and measured (red) stream discharge downstream of Sibbald Fen Dam #1. The simulated result successfully represented the frequency of change and timing; however, a mismatch on magnitude is observed after the 96.2 mm rainstorm. Overall, both results are within the same magnitude scale. The peak streamflow after the rainstorm in mid-June and the steady descending streamflow trend in late summer are visible. The grey lines separate the calibration and validation periods.

Table 4-3 Discharge analysis metrics for the single dam simulation. RMSE and MB values are in m^3s^{-1}.

Metric	Dam #1		Dam #3	
	Calibration	Validation	Calibration	Validation
RMSE	0.01	0.01	0.06	0.05
NRMSE	0.50	0.86	0.55	5.21
MLE	0.01	0.01	0.06	0.05
NSE_m	-2.74	-4.07	-3.25	-18.22
KGE	-1.20	-0.77	-1.87	-7.85
MB	1.49	1.72	2.78	8.78

In addition, BeaverPy was run using the same single-beaver approach but with Dam #3. This dam was located in a downstream position within the studied beaver dam sequence (Figure 4-15; Table 4-3). Dam #3 was 68 m long and had an effective hydrologic height of 2.1 m. Beavers also built it using branches and mud. The dam had several large gaps (diameter larger than 0.2 m) that released water during the gapflow state. The most frequent flow state in this dam was underflow (44 % of the observed time) followed by gapflow (14%), and then a mixed state formed by overflow and gapflow (8%) (Chapter 3). Given the technical difficulties in measuring pond depth at Dam #3, and the dams' similarity to Dam #1, the pond depth of Dam #1 (1.69 m) was assumed for Dam #3.

It was used the discharge observed in the outflow of Dam #2 as inflow for the Dam #3 simulation to reduce the impacts of routing between dams. The outflow gauge for Dam #3 was impacted on June 27 when beavers constructed a new beaver dam (Dam #4; Chapter 3). The construction of new dams or their alteration by biotic, hydrologic, or geomorphic triggers

is expected in beaver-dominated landscapes. Dam #4 was 1.1 m long and was composed of 0.7 m of mud on the bottom with a layer of branches on top and was in a throughflow state on June 27 and August 8. Despite efforts to remove Dam #4 on August 8, it was quickly rebuilt overnight by beavers. To assess the discharge, it was developed a rating curve for the period pre-construction of Dam #4 and another for post-construction, given the associated reduction in velocity from 0.153 m/s to 0.04 m/s.

For Dam #3, the simulated series matched the timing of observations, for example, accurately representing the June 12-15 storm. Similar to observations at Dam #1, there was a decreasing trend in observed discharge during the late summer and early fall that the model captured. The discrepancy in volume between the modeled and measured might be explained by 1) the lack of an updated pond depth which resulted in an underestimation of the pond storage volume behind Dam #3, which explains the large difference in peak flow in response to the 96.2 mm in June; and 2) the construction of the new beaver dam (i.e., Dam #4) and, therefore, the uncertainty of using two rating curves. For instance, it was measured a discharge of 0.058 m3/s before the construction of Dam #4. Discharge after its construction was immediately reduced to 0.01 m3/s. Increasing the streamflow measurements once beavers build a new dam to have rating curves capturing a broad range of conditions is strongly suggested.
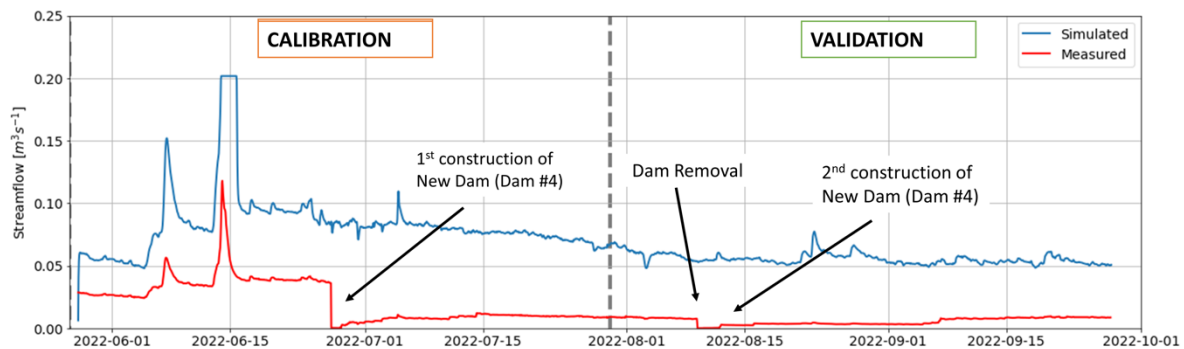
Figure 4-15 Modelled (blue) and measured (red) streamflow at Sibbald Fen Dam #3. Note that a new dam (coded Dam #4) was built by beavers downstream of this station, thus affecting its measurements on June 27. Dam #4 was removed on August 8, and beaver rebuilt it that night; it remained in place thereafter. There is a rating curve for the stream for before Dam #4 construction, and another after Dam #4. The grey lines separate the calibration and validation periods.

4.5.2. Multiple beaver dams in sequence at Sibbald Fen

The influence of multiple beaver dam in sequence on streamflow was simulated with BeaverPy. Used were the same parameters for the single simulation of Dams #1 and #3 but with the addition of Dam #2, an on-stream dam built with branches and mud, with a length of 22 m and an effective hydrologic height of 0.8 m positioned between Dams #1 and #3. From May to October 2022, Dam #2 was in the underflow state for 40% of the total number of days, overflow for 29%, and seep flow for 8% (Chapter 3). Eight percent of the changes in flow state resulted from rainfall and 0% from biotic agents (Chapter 3). The pond depth of Dam #2 was 1.2 m, obtained from field measurements with a ruler close to the dam's center.

Model evaluation during the calibration, validation and overall phases was determined using several metrics (Table 4-4), time-series plots, (Figure 4-16), and 1:1 simulated versus observed plots (Figure 4-17). BeaverPy matched the peaks in streamflow produced by the rainfall events and their timing, but not the magnitude as indicated by the poor NSE and KGE metrics. The mismatches were not systematic (Figure 4-17), for example, the simulated values of Dam #1 were larger than the observed one and the opposite occurred at Dam #2. There were both under- and over-estimates of simulated discharge at Dam #3. For Dam #2, the metrics describing model fit poor; MLE and MB were negative, indicating volume was overestimated (Figure 4-17).
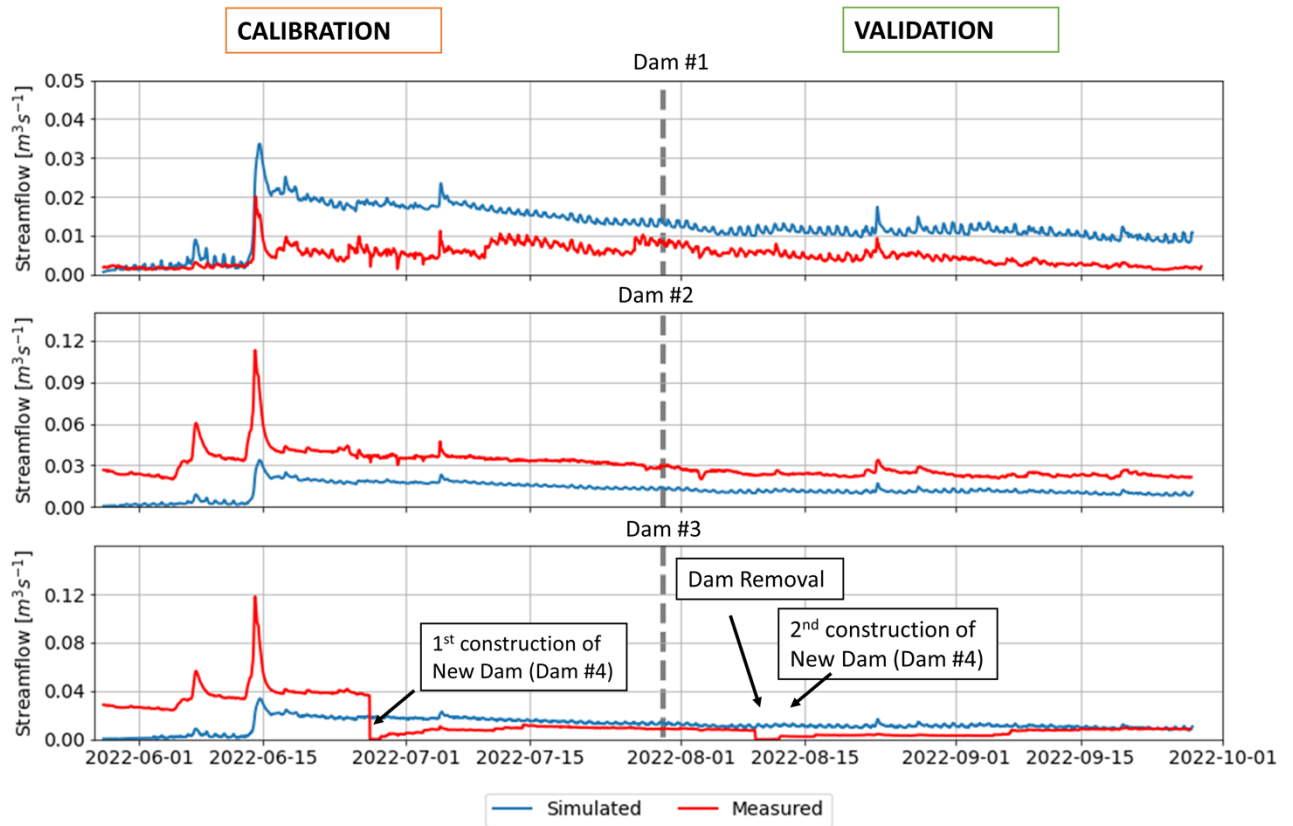
Figure 4-16 Modelled (blue) and measured (red) stream discharge downstream of each dam in the studied sequence. The input for Dam #1 simulation was the inlet gauge, and for dam #2 and #3 the upstream dam. The construction of Dam #4 impacted the gauge records for Dam #3 and the major events were mentioned in the plot. The grey lines separate the calibration and validation periods.
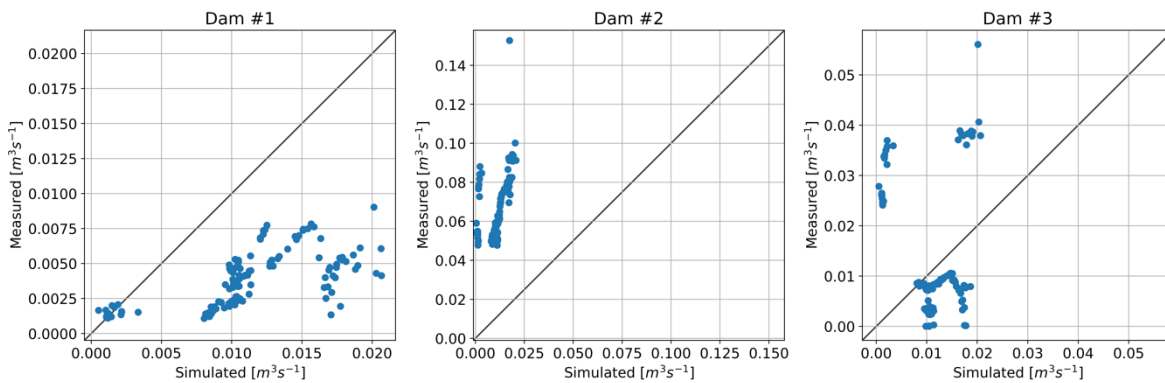
Figure 4-17 Scatterplot of modelled versus measured stream discharge downstream of each dam in the studied sequence. Results were aggregated daily. Values that fall on the 1:1 line indicate simulated discharge was equal to measured discharge.

81

Table 4-4 Discharge analysis metrics for the in-sequence simulation. RMSE and MB values are in m^3s^{-1}.

Metric	Dam #1		Dam #2		Dam #3	
	Calibration	Validation	Calibration	Validation	Calibration	Validation
RMSE	0.01	0.01	0.08	0.04	0.02	0.01
NRMSE	0.50	0.86	0.23	1.50	0.18	0.65
MLE	0.01	0.01	-0.07	-0.04	-0.01	0.01
NSE_m	-2.72	-4.07	-3.70	-12.78	-0.17	-1.02
KGE	-1.20	-0.77	-0.27	-0.19	-0.28	-0.75
MB	1.49	1.72	-0.84	-0.80	-0.40	0.92

To assess the ability of BeaverPy to simulate pond evapotranspiration, daily streamflow amplitude, i.e. the difference between the maximum and minimum Q excluding the period of the two largest rainfall events, was examined as a surrogate (Figure 4-18). Observed vs. simulated Q amplitude are scattered around the 1:1 line for Dam #1, are primarily concentrated at or above the line for Dam #2, and are primarily below the 1:1 line for Dam #3.
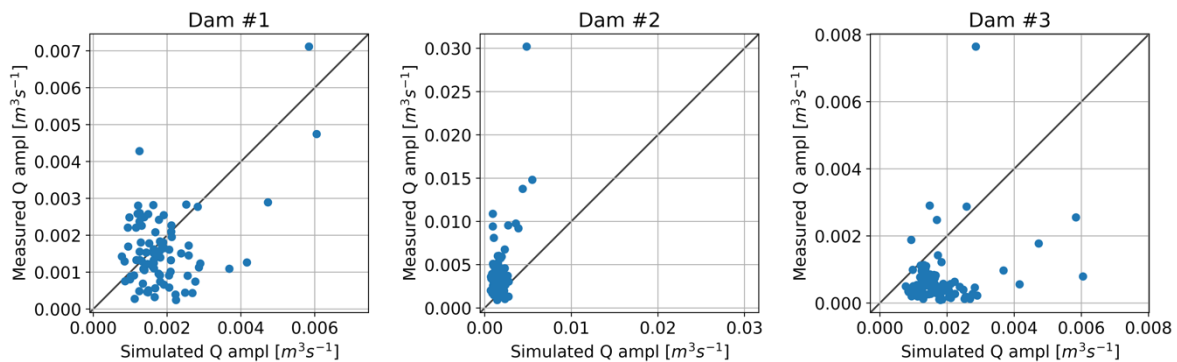
Figure 4-18 Daily streamflow (Q) amplitude (difference between daily minimum and maximum Q) for each beaver dam in the series for days between rains events. Values that fall on the 1:1 line indicate simulated change in evaporation (as approximated by daily amplitude of stream discharge) was equal to measured evaporation.

In addition, the simulated and measured pond water levels were compared (Figure 4-19 and Table 4-5). The relatively small values of RMSE, NRMSE, and MB for all three ponds indicate that the model was able to simulate the major hydrological process, such as direct pond rainfall and evapotranspiration, along with implementing a water-balance-based algorithm to handle inputs and outputs. This algorithm sums all the inputs and outputs and calculates a balance for each time step, and then saves the values for each element in a 2D

table. The magnitude of the MLE values is similar, which suggests a good fit between measured and modelled data. However, the negative values for Dam #2 indicated that the results of this simulation overestimated pond level.

For a time-series evaluation of model performance on pond level behavior, it was presented the modelled versus measured values in Table 4-5 and Figure 4-19 along with pond images. These images were captured on June 24, 2022, after the large storms when the ponds were close to being full. For Dam #1, it was observed that BeaverPy was able to capture the responses of the two large rainfall events in June. In summer, however, some differences in magnitude might result from the formation of a temporary second outflow from the dam, similar to an emergency release valve, which was not represented in the model. In mid-June, the measured pond level dropped and rose, which was explained by a 6 mm rainfall (Chapter 3), although it was also hypothesized that beavers repaired the dam, and that this beaver activity was not captured by the cameras (Chapter 3). Cameras traps were placed focused on the front of the dam to assess the flow state of the beave rather than wildlife activity.

For the pond associated with Dam #2, the model simulates the trend, timing, and pond level, as observed on the Table 4-5 metrics. The simulation matches the magnitude scale most of the time with the exception of a 0.2 m overestimation in pond level during the June 12-15 rainfall event response. As the photograph in Figure 4-19 shows, the pond contains emergent vegetation, which influences the volume available for water; those effects are not incorporated in the current version of the model. For the pond associated with Dam #3, the model reproduces the trend, magnitude, timing, and frequency of measured change. This pond was stable around 1.0 to 1.2 m during a significant part of the study period, a state which is reproduced by the model.

Pond hydrograph	Beaver ponds image
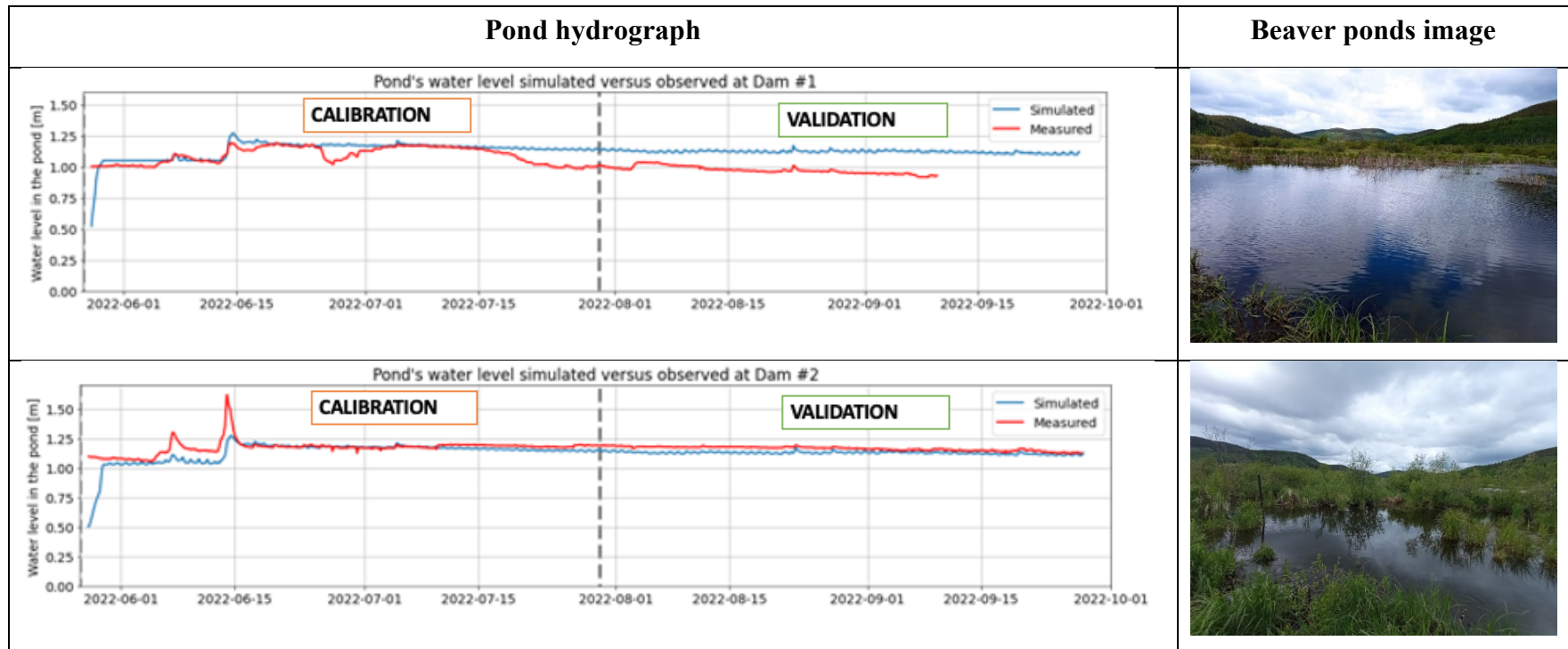
Figure 4-19 Simulated (blue) versus observed (red) pond level in the sequence of three ponds selected on Sibbald Fen. The left column presents BeaverPy results and observed water level. The observed line includes a correction to represent the bottom of the dam (between 0.7 to 0.9 m). The right column presents images of the ponds to illustrate the observed storage. The three images were captured on June 24, 2022. The observed series at Dam #1 was affected by animal activity in late September and it was removed.

Figure 4-19 (Continued)

Pond hydrograph	Beaver ponds image
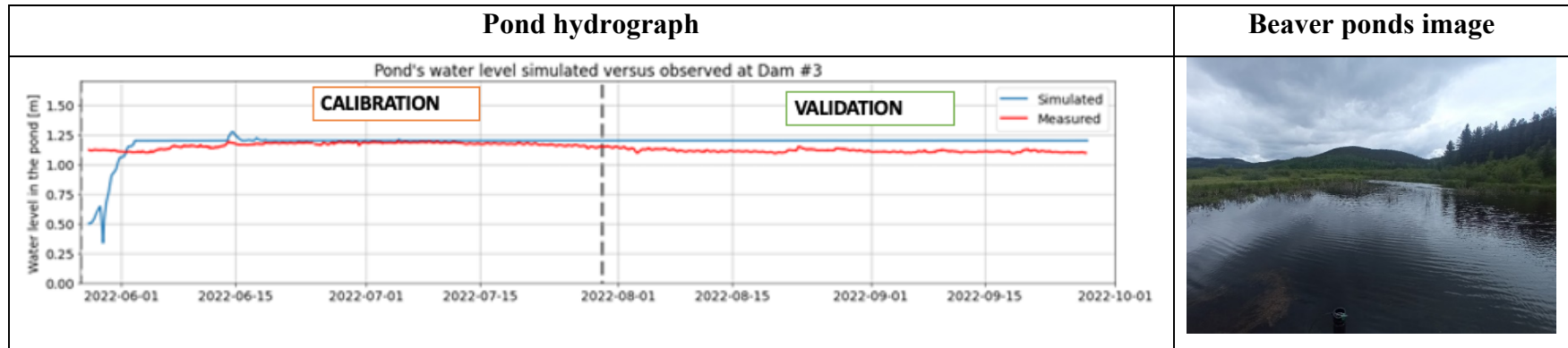
Table 4-5 Pond level analysis metrics for the in-sequence simulation. RMSE and MB values are in meters.

Metric	Pond associated with Dam #1		Pond associated with Dam #2		Pond associated with Dam #3	
	Calibration	Validation	Calibration	Validation	Calibration	Validation
RMSE	0.07	0.09	0.09	0.03	0.12	0.09
NRMSE	0.35	1.29	0.16	0.53	1.25	1.46
MLE	0.02	0.02	-0.02	-0.01	0.01	0.04
MB	0.04	0.16	-0.04	-0.03	0.01	0.08

The observed flow state of beaver dams (Chapter 3) and the modelled flow states are shown in Figure 4-20. The model was run using a rules-based approach. A set of rules was developed for each beaver dam based on how these beaver dams responded during the season of study, as captured with hydrometric measures and camera trap images. These rules were defined using only the water level in the pond, although there is the option to include more variables for future model users. This approach provides a solution to run the model with different inflow series and test precipitation change scenarios.

The results for Dam #1 (Figure 4-20) generally matched the field observations, especially during spring. During summer, there was an overestimation of the time of the mixed flow state, which suggest excess water in the model in line with the previous pond level results. For Dam #2, the model reproduces the overflow state but not the other states, which is also linked to excess water, as the MLE and MB results pointed out. For Dam #3, the model reproduces the overflow and underflow flow states and their dynamics but misses the period with gapflow and mixed flow states. There was a period without valid observations of flow state for Dam #2 and Dam #3 (see Chapter 3), which prevented a valid evaluation from July 16 to August 8. The current ecohydrological understanding of Sibbald suggests that overflow is a possible flow state for these dams during the observation data gap, considering the water storage dynamics.

For the three dams, the model followed the observed pattern of changing the flow state after the large rainstorm in June, although the flow state dynamics during low flows presented some differences between measured and modeled results. The limited version of the rules applied with only one variable, in this case pond level, needs a refined calibration process to accurately simulate flow state behavior, as shifts are frequently observed (Ronnquist &

Westbrook, 2021; Chapter 3). The model demonstration revealed that the model was able to shift from one flow state to another (Figure 4-20), but it could not fully capture the dynamics of observed flow states. There remain challenges in capturing the correct timing between different flow states that expressed themselves as different proportions of time each dam spent in a particular flow state. A longer time series of measured pond levels across various weather conditions might be useful in identifying thresholds triggering flow state changes.

Dynamics of the flow state of beaver dams	Photo and observed flow state
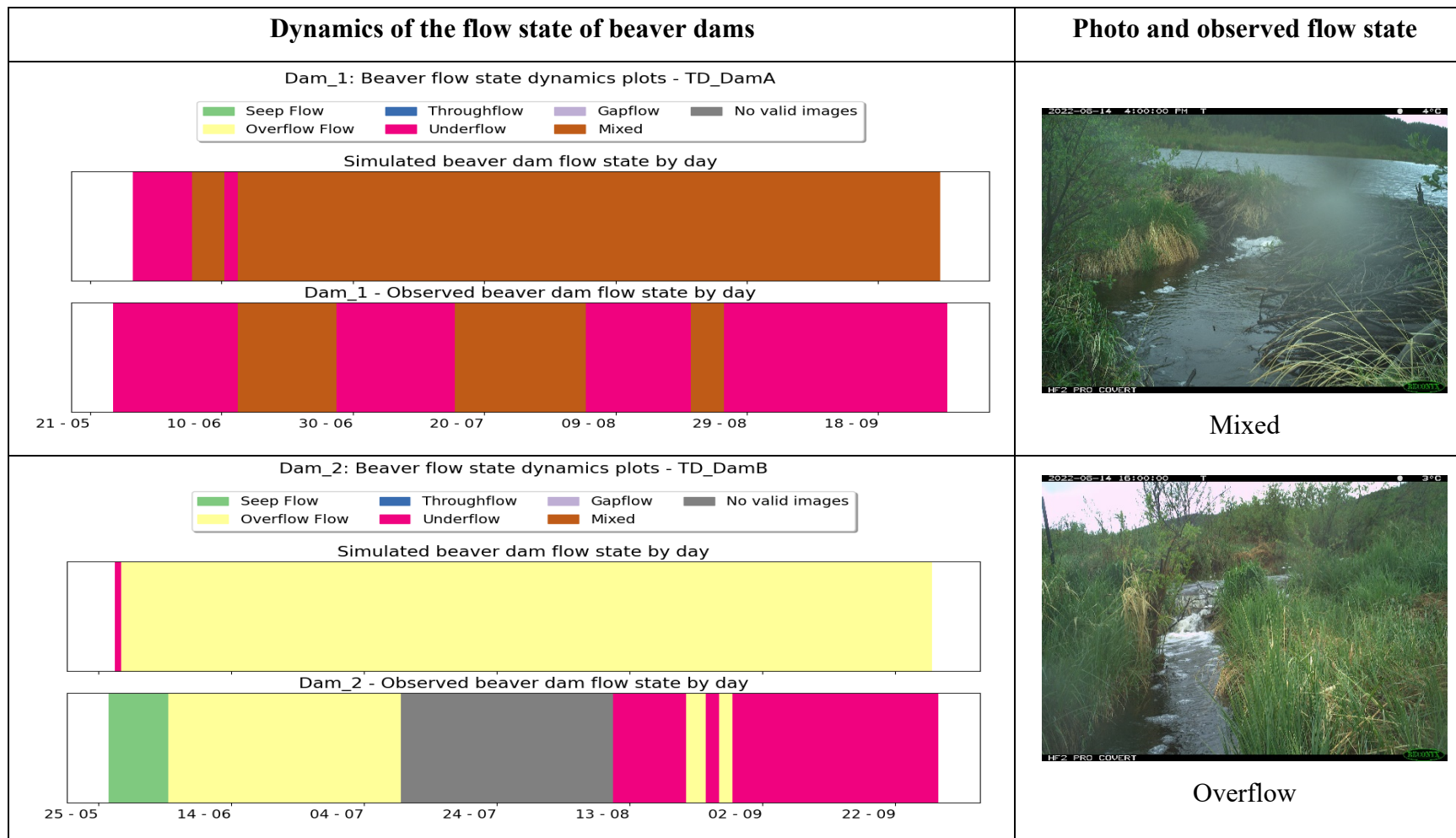
Figure 4-20   Simulated versus observed flow state of beaver dams in the studied sequence on Sibbald Fen. The left column includes a plot for each dam where the upper part of the output presents the simulated flow state based on rules (forecast option) and the lower part the observed flow state. The right column includes camera traps images of the flow state to illustrate the characteristics of dams. The three images were captured on June 14, 2022, triggered by timed triggers (not triggered by motion).

Figure 4-20 (Continued)

Dynamics of the flow state of beaver dams	Photo and observed flow state
Dam_3: Beaver flow state dynamics plots - TD_DamC	Overflow
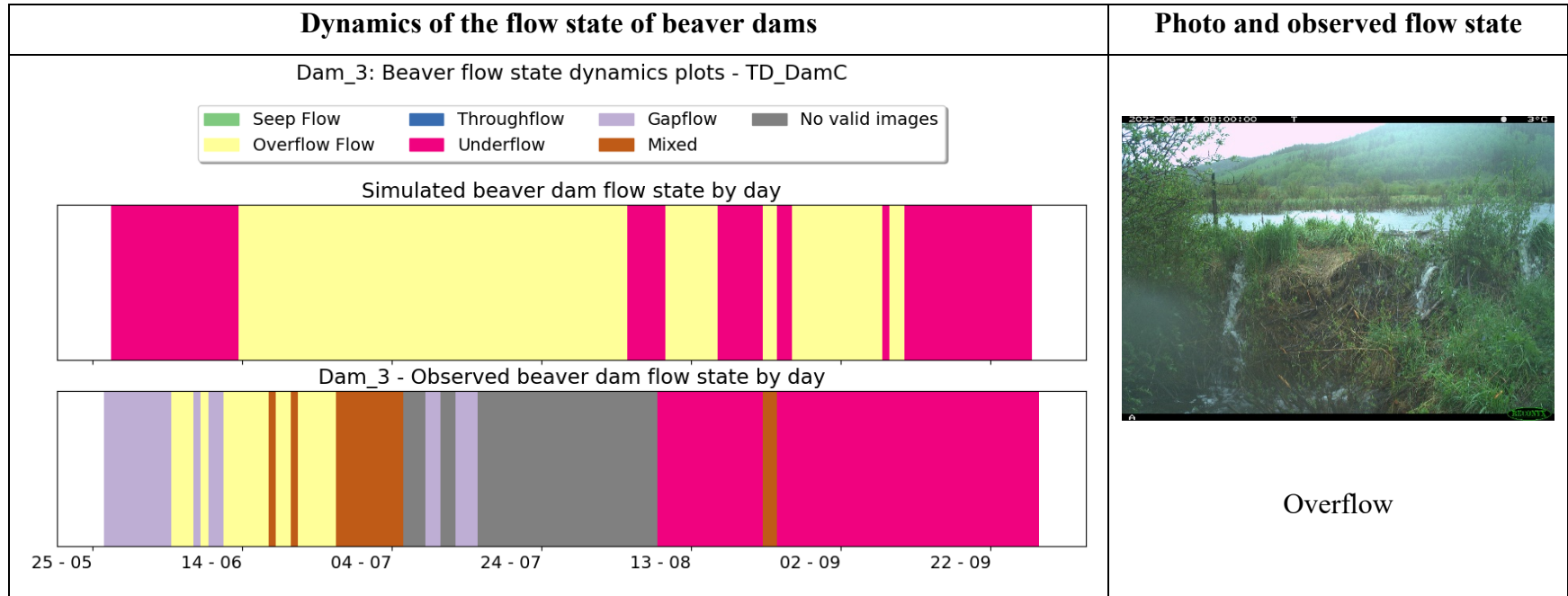
4.6. DISCUSSION

The BeaverPy model was specifically designed as an ecohydraulic model to be used with either an established catchment hydrology model or observational streamflow data to simulate streamflow routing through beaver-dominated areas. The objective was a flexible design that captures the structural and hydrological heterogeneity of beaver dams that exist in nature (Hafen et al., 2020; Ronnquist & Westbrook, 2021; Woo & Waddington, 1990).

Previous attempts to model the hydrological impact of beaver dams were limited in their capacities to represent the structural heterogeneity of beaver dams and the resulting variation in the paths streamflow take past them (Beedle, 1991; Caillat et al., 2014; Neumayer et al., 2020; Noor, 2021). However, the results from my case study indicate that incorporating the flow state of beaver dams in a dynamic manner permits capture of several key processes of beaver dam hydrology, specifically pond evapotranspiration, stormflow (hydrograph peaks), and pond storage of individual beaver dams and a short sequence of beaver dams.

Most of the model parameters were set from field observations and therefore not calibrated, with the exception of the thresholds for the beaver dams to change from one flow state to another. This process-based approach was adopted to represent Sibbald Fen from a fidelity-driven perspective rather than focus on the metrics following Pomeroy et al. (2007, 2022). Evaluating the parametrizations and testing the basin understanding are the strengths of this approach, and the limited prediction, given by the differences between the model results and the observed values (e.g., Table 4-3 and Table 4-4), indicate that increased field data are required for enhance calibration. Setting the small calibration budget was decided to keep the information from field-informed parameters. There is a large, yet uncalculated, uncertainty in the observed parameters due to the short field season; however, my approach reduced the perils of calibration (related to excessive tweaking) (Acero Triana et al., 2019), which highlights the utility of developing a model working in a wide range of beaver-dominated environments. This approach has been used in previous model development as it is useful in delineating a path for model progress (Fang et al., 2013; Fang & Pomeroy, 2007a, 2020; Krogh et al., 2017; Shook & Pomeroy, 2011). Despite the results of the metrics, the model was able to represent the process that controls streamflow modulation by beaver dams, the

pond storage, and the flow state dynamics. Longer observed time series would reduce uncertainty in the model parameters.

The timing of hydrograph peaks downstream of beaver dams in both individual and in-sequence runs generally matched observations because the dam overtopping module was able to represent how dams react to stormflow in the field (Westbrook et al., 2020; Chapter 3). During high flows, dams changed to overflow state, as represented by the broad-crest weir equation, which quickly releases streamflow via overtopping the dam crest. The overflow state is key to understanding the response of beaver dams to rainfall events (Ronnquist & Westbrook, 2021; Woo & Waddington, 1990).

Beaver pond levels and discharge downstream of beaver ponds tend to have diel fluctuations that have been attributed to evapotranspiration (Burns & McDonnell, 1998; He et al., 2023). The pond storage and stream discharge downstream of beaver dams simulated by BeaverPy replicate sub-daily oscillations in discharge downstream of dams, and to a lesser extent, pond storage (Figure 4-18). These results suggest that BeaverPy can simulate evapotranspiration without a systematic error; and that the daily amplitude in streamflow attributed to evapotranspiration (McMillan, 2020; Schwab et al., 2016) is also well-captured. Evapotranspiration in the model was estimated using the Priestly-Taylor approach. While the model simulates the daily patterns correctly, it would be helpful to also determine pond evapotranspiration via a direct method, such as eddy covariance, to evaluate the uncertainty in the volume of water evapotranspired.

While the BeaverPy model was able to adequately replicate diel evapotranspiration and the timing of rainfall event peaks, the model had challenges with adequately representing the hydrograph. The model reasonably well represents average (low) discharge conditions, as evidenced by RMSE and MLE scores of close to 0 in individual and in-sequence simulations. High flows, however, had negative NSE_m and KGE values, indicating that discharge is overestimated discharge for Dam #1 and underestimated it for Dams #2 and #3 during rainfall events. So, why did the model overestimate volume for some dams and not others? In cascade systems, downstream results are largely controlled by upstream elements (Wang et al., 2019). The inlet stream gauge, which was used as the surface inflow for pond associated with Dam #1, was 296 m upstream of the dam. There were several smaller beaver dams in this stream

reach. The presence of multiple beaver ponds, even if they are small, can cumulatively increase the volume of water stored in a site and has a significant flow attenuation impact (Lin & Rutten, 2016; Puttock et al., 2017; Tsoukalas & Makropoulos, 2015). As the model systematically underestimated streamflow volume downstream of Dam #1 throughout the time series, the most likely explanation is that it did not account for water storage in the ponds between the inlet and outlet. I decided not to adjust the inflow to account for this storage as I followed a basin understanding modeling approach (*sensu* Fang et al., 2013; Pomeroy et al., 2007). Although, to mitigate this issue, the model could be run for all beaver dams in the series or, alternatively, a stream gauge could be placed immediately upstream of the pond at Dam #1 to use as the inlet.

Hydrograph volume downstream of the two dams in the middle and downstream positions of the hydrograph was underestimated by the BeaverPy model likely due to a combination of uncertainties in pond storage and beaver activity. Pond storage was estimated via the V-A-h method (Karran et al., 2017), which requires maximum pond depth. Only the pond associated with Dam #1 had a full bathymetric map from which maximum pond depth was extracted. Maximum depth of the pond associated with Dam #2 was field measured by probing with a ruler in various spots, a method that introduces higher uncertainty. Since the pond associated with Dam #3 was too deep to safely probe, it was assigned the same maximum depth value as the pond associated with Dam #1. A future sensitivity analysis would reveal if improved maximum depth values might significantly improve model fit. One other factor to consider though is that beaver dam systems are dynamic as they are continuously being changed by beaver activity. While there were no recordings of beavers altering the structure any of the studied dams (Chapter 3), beavers were active in the dam series. For example, they built a new dam, Dam #4, that backed-up water in the channel downstream of Dam #3, which resulted in the need for a second rating curve at the stream gauge located downstream of Dam #3, which was consistent with guidance in the literature (Clark, 2020; Hamilton et al., 2019; McCullough et al., 2006). Guidance from the Water Survey of Canada is to remove beaver dams built near stream gauges as the dams produce an abrupt reduction in velocity for a given stream stage (Rainville et al., 2016). Given the relatively short study period, each rating curve was populated by only a few velocity-depth observations, which increase streamflow estimation uncertainty (Mcmillan & Westerberg, 2015; Sikorska et al., 2013; Tomkins,

2014). When there is higher rating curve uncertainty, measured values could be considered with a ±10% of variation (Tomkins, 2014), which would bring the simulated streamflow volumes downstream of the beaver dams into closer agreement with observations. One other mitigation to address the issue of the mismatch of simulated vs observed streamflow volume, especially at high flows, is to utilize longer inflow time series that capture a larger number of rainfall events of different magnitudes.

Two different hydrological phases were observed in the pond level time series that were replicated by the model. One of these phases was a period of relatively stable pond levels occurring between July and October. The other phase was a brief period of rapid pond level rise and fall in response to a large (96.2 mm) rainfall. There have been previous reports of dynamic beaver pond levels such as were observed. For instance, Westbrook et al. (2020) observed a 10 to 80 cm increase in beaver pond levels in response to a 195 mm rainfall event in the Canadian Rocky Mountains. Nyssen et al. (2011) observed an increase in beaver pond storage up to 310 m^3 given a discharge variation from 0.2 m^{3}s^{-1} to 0.76 m^{3}s^{-1}, and Devito & Dillon (1993) reported an increase in beaver pond level from 0.15 m to 0.35 m, exceeding dam crest at 0.3 after an increase discharge of 120 l s^{-1}. Periods of relatively stable pond levels, maintained at the dam crest or below it, have also been observed (Puttock et al., 2017; Ronnquist & Westbrook, 2021; Woo & Waddington, 1990). The simulated pond levels were never close to zero, which is rare to find in nature unless a beaver dam is breached to its maximum depth and beavers have abandoned the site (Hood & Bayley, 2008; Ronnquist & Westbrook, 2021). In addition, the model captured the sometimes subtle variations in pond level observed by this research and by Woo & Waddington (1990) in response to changes in the flow state of beaver dams. As BeaverPy was able to simulate beaver pond levels during both types of hydrological phases, it demonstrates that the model has the parametrizations necessary to predict pond storage.

One other output of the BeaverPy model is a time series of the flow state of each beaver dam in the series. The dynamics of flow states of beaver dams were modeled using the pond level rules approach, resulting in runs where the flow state simulated by the model was usually the same flow state observed on the camera traps (e.g., overflow was observed in both observed and simulated data). Although, the model does not simulate flow state changes as often as

they occurred; for example, the time during which overflow state was active was overestimated in the Dam #2 simulation. BeaverPy is the first ecohydraulic model that includes different flow states. Other ecohydraulic or ecohydrological models have represented beaver dams as having just one flow state, usually the overflow (Beedle, 1991; Caillat et al., 2014; Noor, 2021) or the mixed (Neumayer et al., 2020) flow state. Representing all flow states and their dynamics are critical, given that it is one of the key mechanisms affecting how much beaver dams attenuate streamflow (Ronnquist & Westbrook, 2021; Woo & Waddington, 1990; Chapter 3). BeaverPy was not able to replicate the observed flow state changes likely because the study period was not long enough to identify numeric thresholds for change of one dam flow state to another. For instance, there were few rain events in the study period to raise pond level. A longer observational time series of flow states recorded with pond level sensors, streamflow downstream of the dam, and camera traps is needed to assess robust thresholds.

Despite the advantages of the BeaverPy model in simulating streamflow routing through and water storage in beaver-dominated areas, some hydraulic/hydrological processes were purposely simplified. For example, the model does not capture overbank flooding of riparian areas, a process important in broad valleys during high flow periods (Westbrook et al., 2006). However, incorporation of this process would require high resolution (resolution < 1.0 m) topography, a mesh-based discretization, and additional computer power. One other potentially important process not well captured by the model is groundwater recharge beneath beaver ponds. Beaver dams increase the level (i.e., hydraulic head) of a stream reach, which can shift the reach from gaining to losing (Janzen & Westbrook, 2011; Lautz & Siegel, 2006). While likely a key control on the magnitude of groundwater recharge beneath beaver dams (Larsen et al., 2021), this is an area requiring in depth field study before it can be represented in BeaverPy.

As BeaverPy was devised to route water during ice-free periods, it should be useful for predictions during the snowmelt period, a critical hydrological period in cold regions (DeBeer & Pomeroy, 2017; Dornes et al., 2008; Fang & Pomeroy, 2007) where beavers live (Hood, 2020b), with minimal changes. During snowmelt periods, I hypothesize that rapid changes in flow states are likely, shifting from flow states flow of limited transmission (e.g.,

seep flow or underflow) to flow states able to deliver larger volumes and avoid breaching the dam (e.g., gapflow and overflow), but further fieldwork is needed to test the dynamics of flow state changes during snowmelt period and the transition to rainfall driven periods. BeaverPy has a module to change the flow state based on pond level, and as demonstrated here, it can conduct simulations under these conditions. However, the current version of the model was evaluated for only the ice -free period and does not currently include modules to handle snow over the pond, ice in the dams, or frozen ponds. To run the model under winter conditions, ice melt should be modeled by considering radiation and an energy bulk transfer approach (*sensu* Pomeroy et al., 2022; Shook et al., 2013). Given limited observations of the hydrology of beaver-dominated environments in winter or during snowmelt (Hillman, 1998; Pearce et al., 2021; Tape et al., 2018), further instrumentation, including loggers and cameras, is needed before model adjustments are made.

4.7.   CONCLUSION

The BeaverPy model was devised to simulate the influence of individual and sequences of beaver dams on streamflow and water storage. Three key principles guided its development: 1) represent the dam and pond heterogeneity as observed in the field, 2) provide explicit representations of each flow state and its dynamics, and 3) offer an open-source tool that can be coupled with other models and help ecohydrologists to provide reproducible solutions to a broad range of communities. Examples presented here demonstrated how the BeaverPy model could successfully simulate the timing, trend, peaks of streamflow modulation by beaver dams, as well the pond level variations. Several mismatches were present in the streamflow magnitude as the metric elicited, given parameter uncertainty, inflow uncertainty, rating curve (i.e., observation) uncertainty, and underestimation of pond depths. Flow state changes of beaver dams were simulated using a set of rules based on pond level and led to a satisfactory result matching observed patterns and the rate of change. Overall, the model was able to simulate the effects of beaver dams at high and low flows. As beavers are densifying in their native range in North America and Eurasia (Graham et al., 2022; Hood & Bayley, 2008; Naiman et al., 1988) and increasing their presence in new environments such as urban settings, the Arctic tundra, and southern Patagonia (García et al., 2022; Tape et al., 2018;

Westbrook & England, 2022), the BeaverPy model should be useful in predicting how much the streamflow and water storage might change, helping practitioners and communities to assess possible benefits and damages. Recommended is testing of the utility of the BeaverPy model in watersheds with contrasting bedrock, soils and landforms, land uses, and beaver histories.

5.   CONCLUSIONS

Beavers are expanding their global extent in Eurasia, Central North America, the Arctic tundra, and urban environments (England & Westbrook, 2021; Foster et al., 2022; Hood & Bayley, 2008; Johnston & Naiman, 1990; Naiman et al., 1988; Tape et al., 2018, 2022b). Additionally, following their release from fur farms, beavers have established robust populations in southern Patagonia, which presents challenges for an ecosystem ill-equipped to counter the impact of beavers (García et al., 2022; Huertas Herrera et al., 2020, 2021; Skewes et al., 2006; Westbrook et al., 2017). Given both the natural and human-facilitated expansion of beaver populations globally, it is critical to understand and predict hydrological changes in beaver-dominated landscapes. However, predictive modeling of these changes can be challenging because beavers readily adapt their behaviors to local environmental conditions (Beedle, 1991; Neumayer et al., 2020). For example, the construction of dams by beavers is location dependent and reflects local contexts (e.g., peatlands, minerotrophic wetlands, urban environments), which further affects beaver dam structure and streamflow attenuation (Green & Westbrook, 2009; Hood & Larson, 2015; Larsen et al., 2021; Ronnquist & Westbrook, 2021; Westbrook et al., 2020). Beaver dams have been classified by their flow state, which is how water flows past a beaver dam (Ronnquist & Westbrook, 2021; Woo & Waddington, 1990). The implementations of beaver dams in hydrological models have not yet incorporated two key elements of beaver dams – physical heterogeneity of beaver dams and their spatiotemporal variability – which affects model accuracy and fidelity. To address this gap, I studied the hydrological behavior of beaver dams and their incorporation into a hydrological model.

Flow state is a key factor determining how beaver dams affect hydrological processes because of its influence over water storage in the pond and the downstream hydrograph (Neumayer et al., 2020; Ronnquist & Westbrook, 2021; Woo & Waddington, 1990). To tackle the challenge, Chapter 3 explored changes in the flow state of beaver dams and variables driving its change. Integrating traditional field hydrometric data and analysis of images recorded on camera traps, I concluded that the flow state of beaver dams is highly dynamic. The flow state of a beaver dam can change multiple times over a short period. On average, I found beaver dams at the study site changed flow state every 9.7 days. The most common flow state found in the study was underflow, while rainfall triggered between 66%

and 80% of the changes in flow state (Chapter 3). I did not observe any changes in flow state driven by biota (considering abilities- or weight-driven changes). Nevertheless, given the camera placement oriented to capture key hydrology of the dam rather than wildlife, the entire length of the dam was not captured by the camera. Further, changes in flow state presented limited synchronicity between dams in the same sequence. After a large rainfall event of 96.4 mm, the one beaver dam not already in the overflow state changed to the mixed flow state, which included overflow conditions. I argued that these results expand the flow state perceptual model of Woo & Waddington (1990), which sets beaver as the main agent to modify dams and proposes a specific order between flow states over the beaver occupancy cycle, with beaver dams starting in the overflow state when dams are built, changing to the gapflow state as they age, and finally to a marked gapflow state when they are abandoned (Neumayer et al., 2020).

Once I assessed the dynamic behavior of beaver dams in Chapter 3, I reviewed the existing approaches used to represent beaver dams on hydrological models (Beedle, 1991; Caillat et al., 2014; Neumayer et al., 2020; Noor, 2021) and determined that they were inadequate for representing the heterogeneous and spatiotemporal dynamic behavior of beaver dams. To address this gap, I developed a Python model to represent the water storage dynamics and streamflow modulation by beaver dams, which I called BeaverPy (Chapter 4). BeaverPy is organized on three key principles: (a) it represents the heterogeneity of beaver dams and ponds as observed in the field, i.e., functions on a fidelity-oriented perspective; (b) it simulates each flow state of beaver dams explicitly, including the changes from one state to another, and the drivers of these changes, as described in the literature (Ronnquist & Westbrook, 2021; Woo & Waddington, 1990); and (c) it provide a FAIR compliance code (Barker et al., 2022) that will enable ecohydrologists working in environments dominated by beavers to inform decision-makers of how beaver dams might change the local hydrology.

Then, I demonstrated that BeaverPy was able to simulate water storage, streamflow modulation, and flow state by conducting a simulation of Sibbald Fen, a montane peatland in the Canadian Rocky Mountains (see Westbrook & Bedard-Haughn (2016) for a complete description of the site). The model accurately represented the trend and timing of changes in water storage and hydrograph peak. Overall, average values were best represented (RMSE,

MLE) than the high flow and peaks as demonstrated by KGE and NSE_m metrics. There are mismatches in streamflow magnitude attributed to several uncertainties that might be mitigated by additional field data over longer time periods that capture variable hydrological conditions. For example, the model simulated the rising and falling limbs after precipitation events and the sub-daily behavior in response to evapotranspiration. The root mean squared error (RMSE) metric for the in-sequence simulation was 0.007 m^3s^{-1} for Dam #1, 0.006 m^3s^{-1} for Dam #2, and 0.004 m^3s^{-1} for Dam #3, indicating good overall agreement between observed and simulated flows. The water storage results (i.e., beaver pond level) of model simulations accurately showed ponds filling after precipitation events and a steady pond level during the summer. The flow state dynamics of beaver dams were also simulated by BeaverPy, consistent with observed changes triggered by rainfall. There were several mismatches in flow states between modelled and measured data, such as during periods when the beaver dams were in a seep flow or underflow state, and overrepresentation of the mixed state, which might be explained by excess water in the system. Some limitations should be the focus of future studies including expanding the overbank flooding approach and investigating routing between dams. Despite these limitations, the results from Sibbald Fen simulation demonstrated that BeaverPy was able to represent the most important hydrological processes of beaver-dominated environments.

Overall, I addressed two interrelated key challenges of the hydrology of beaver dams. I provided new insights into the dynamic behavior of beaver dams on the scale of weeks, triggered by rainfall events, and then incorporated this dynamic behavior into a new model suitable for use in beaver-dominated environments. As a result, scientists can incorporate beaver dams into larger model implementations, a strategy widely used in other systems (e.g., Annand (2022) in the Canadian Prairies or Metcalfe et al. (2017) on other nature-based structures). The advances I made in understanding and predicting the impacts of dam building by beavers will allow for broad use of beavers as a nature-based solution to aid in flood mitigation and stream restoration plans, thereby increasing our resilience at various spatiotemporal scales (Albert & Trimble, 2000; Charnley et al., 2020; Conlisk et al., 2022; Jordan & Fairfax, 2022; Pollock et al., 2015).

6.   REFERENCES

Acero Triana, J. S., Chu, M. L., Guzman, J. A., Moriasi, D. N., & Steiner, J. L. (2019). Beyond model metrics: The perils of calibrating hydrologic models. *Journal of Hydrology*, *578*, 124032. https://doi.org/10.1016/J.JHYDROL.2019.124032

Addy, S., & Wilkinson, M. E. (2019). Representing natural and artificial in-channel large wood in numerical hydraulic and hydrological models. *WIREs Water*, *6*(6), 1–20. https://doi.org/10.1002/wat2.1389

Albert, S., & Trimble, T. (2000). Beavers are partners in riparian restoration on the Zuni Indian reservation. *Ecological Restoration*, *18*(2), 87–92. https://doi.org/10.3368/ER.18.2.87

Allers, D., & Culik, B. M. (1997). Energy requirements of beavers (*Castor canadensis*) swimming underwater. *Physiological Zoology*, *70*(4), 456–463.

Annand, H. (2022). *The influence of climate change and wetland management on prairie hydrology - Insights from Smith Creek, Saskatchewan* [Ph.D. Thesis]. University of Saskatchewan.

Auster, R. E., Barr, S. W., & Brazier, R. E. (2021). Improving engagement in managing reintroduction conflicts: learning from beaver reintroduction. *Journal of Environmental Planning and Management*, *64*(10), 1713–1734. https://doi.org/10.1080/09640568.2020.1837089

Auster, R. E., Barr, S. W., & Brazier, R. E. (2022). Beavers and flood alleviation: Human perspectives from downstream communities. *Journal of Flood Risk Management*, *15*(2). https://doi.org/10.1111/JFR3.12789

Aydin, I., Altan-Sakarya, A. B., & Sisman, C. (2011). Discharge formula for rectangular sharp-crested weirs. *Flow Measurement and Instrumentation*, *22*(2), 144–151. https://doi.org/10.1016/J.FLOWMEASINST.2011.01.003

Bagheri, S., & Heidarpour, M. (2010). Flow over rectangular sharp-crested weirs. *Irrigation Science*, *28*(2), 173–179. https://doi.org/10.1007/S00271-009-0172-1/FIGURES/9

Bailey, D. R., Dittbrenner, B. J., & Yocom, K. P. (2019). Reintegrating the North American beaver (*Castor canadensis*) in the urban landscape. *Wiley Interdisciplinary Reviews: Water*, *6*(1). https://doi.org/10.1002/WAT2.1323

Barker, M., Chue Hong, N. P., Katz, D. S., Lamprecht, A. L., Martinez-Ortiz, C., Psomopoulos, F., Harrow, J., Castro, L. J., Gruenpeter, M., Martinez, P. A., & Honeyman, T. (2022). Introducing the FAIR Principles for research software. *Scientific Data*, *9*(1). https://doi.org/10.1038/s41597-022-01710-x

Beedle, D. (1991). *Physical dimensions and hydrologic effects of beaver ponds on Kuiu Island*. Oregon State University. Department of Forest Engineering. Mater thesis . http://hdl.handle.net/1957/9343

Beery, S., Morris, D., & Yang, S. (2019). *Efficient Pipeline for Camera Trap Image Review*. http://arxiv.org/abs/1907.06772

Belvederesi, C., Zaghloul, M. S., Achari, G., Gupta, A., & Hassan, Q. K. (2022). Modelling river flow in cold and ungauged regions: a review of the purposes, methods, and challenges. In *Environmental Reviews* (Vol. 30, Issue 1, pp. 159–173). Canadian Science Publishing. https://doi.org/10.1139/er-2021-0043

Blersch, D. M., & Kangas, P. C. (2014). Signatures of self-assembly in size distributions of wood members in dam structures of *Castor canadensis*. *Global Ecology and Conservation*, *2*, 204–213. https://doi.org/10.1016/j.gecco.2014.08.011

Blöschl, G., & Sivapalan, M. (1995). Scale issues in hydrological modelling: A review. *Hydrological Processes*, *9*(3–4), 251–290. https://doi.org/10.1002/hyp.3360090305

Brazier, R. E., Puttock, A., Graham, H. A., Auster, R. E., Davies, K. H., & Brown, C. M. L. (2021). Beaver: Nature's ecosystem engineers. *Wiley Interdisciplinary Reviews: Water*, *8*(1), 1–29. https://doi.org/10.1002/wat2.1494

Burchsted, D., Daniels, M., Thorson, R., & Vokoun, J. (2010). The river discontinuum: Applying beaver modifications to baseline conditions for restoration of forested headwaters. *BioScience*, *60*(11), 908–922. https://doi.org/10.1525/BIO.2010.60.11.7

Burns, D. A., & McDonnell, J. J. (1998). Effects of a beaver pond on runoff processes: Comparison of two headwater catchments. *Journal of Hydrology*, *205*(3–4), 248–264. https://doi.org/10.1016/S0022-1694(98)00081-X

Butler, D. R., & Malanson, G. P. (2005). The geomorphic influences of beaver dams and failures of beaver dams. *Geomorphology*, *71*(1–2), 48–60. https://doi.org/10.1016/j.geomorph.2004.08.016

Caillat, A., Callaway, B., Hebert, D., Nguyen, A., & Petro, S. (2014). *Beaver (Castor canadensis) impact on water resources in the Jemez watershed, New Mexico*. University of California, Santa Barbara. Master thesis.

Charnley, S., Gosnell, H., Davee, R., & Abrams, J. (2020). Ranchers and beavers: Understanding the human dimensions of beaver-related stream restoration on western rangelands. *Rangeland Ecology and Management*, *73*(5), 712–723. https://doi.org/10.1016/J.RAMA.2020.04.008

Choi, Y. D., Goodall, J. L., Sadler, J. M., Castronova, A. M., Bennett, A., Li, Z., Nijssen, B., Wang, S., Clark, M. P., Ames, D. P., Horsburgh, J. S., Yi, H., Bandaragoda, C., Seul, M., Hooper, R., & Tarboton, D. G. (2021). Toward open and reproducible environmental modeling by integrating online data repositories, computational environments, and model Application Programming Interfaces. *Environmental Modelling and Software*, *135*, 104888. https://doi.org/10.1016/j.envsoft.2020.104888

Clark, T. (2020). *Impacts of beaver dams on mountain stream discharge and water temperature*. Utah State University. Civil and Environmental Engineering. Master thesis.

Clifford, H. F. (1978). Descriptive phenology and seasonality of a Canadian brown-water stream. *Hydrobiologia*, *58*, 213–231.

Cloutier, E. (1950). *Birds of Canada's. Mountain Parks*. http://parkscanadahistory.com/wildlife/birds-mountain-1950.pdf

Conlisk, E., Chamberlin, L., Vernon, M., & Dybala, K. E. (2022). *Evidence for the Multiple Benefits of Wetland Conservation in North America: Carbon, Biodiversity, and Beyond*

with funding from Natural Resources Defense Council. https://doi.org/10.5281/zenodo.7388321

Cordeiro, M. R. C., Wilson, H. F., Vanrobaeys, J., Pomeroy, J. W., & Fang, X. (2017). Simulating cold-region hydrology in an intensively drained agricultural watershed in Manitoba, Canada, using the Cold Regions Hydrological Model. *Hydrology and Earth System Sciences*, *21*(7), 3483–3506. https://doi.org/10.5194/hess-21-3483-2017

Costa-Luis, C. da, Larroque, S. K., Altendorf, K., Mary, H., richardsheridan, Korobov, M., Raphael, N., Ivanov, I., Bargull, M., Rodrigues, N., Chen, G., Lee, A., Newey, C., CrazyPython, JC, Zugnoni, M., Pagel, M. D., mjstevens777, Dektyarev, M., … Nordlund, M. (2023). *tqdm: A fast, Extensible Progress Bar for Python and CLI.* https://doi.org/10.5281/ZENODO.7697295

Cowell, D. W. (1984). The Canadian beaver, *Castor canadensis*, as a geomorphic agent in karst terrain. *Canadian Field-Naturalist*, *98*(2), 227–230.

Czerniawski, R., & Sługocki, Ł. (2018). *A comparison of the effect of beaver and human-made impoundments on stream zooplankton.* https://doi.org/10.1002/eco.1963

Das, A. (2004). Parameter Estimation for Muskingum Models. *Journal of Irrigation and Drainage Engineering*, *130*(2), 140–147. https://doi.org/10.1061/ASCE0733-94372004130:2140

DeBeer, C. M., & Pomeroy, J. W. (2017). Influence of snowpack and melt energy heterogeneity on snow cover depletion and snowmelt runoff simulation in a cold mountain environment. *Journal of Hydrology*, *553*, 199–213. https://doi.org/10.1016/j.jhydrol.2017.07.051

Demmer, R., & Beschta, R. L. (2008). Recent history (1988-2004) of beaver dams along Bridge Creek in Central Oregon. *Northwest Science*, *82*(4), 309–318. https://doi.org/10.3955/0029-344X-82.4.309

Devito, K. J., & Dillon, P. J. (1993). Importance of runoff and winter anoxia to the P and N dynamics of a beaver pond. *Canadian Journal of Fisheries and Aquatic Sciences*, *50*(10), 2222–2234. https://doi.org/10.1139/f93-248

Dingman, S. L. (2015). *Physical Hydrology* (3rd ed.). Waveland Press.

Dornes, P. F., Pomeroy, J. W., Pietroniro, A., Carey, S. K., & Quinton, W. L. (2008). Influence of landscape aggregation in modelling snow-cover ablation and snowmelt runoff in a sub-arctic mountainous environment. *Hydrological Sciences Journal*, *53*(4), 725–740. https://doi.org/10.1623/hysj.53.4.725

Dytkowicz, M., Hinds, R., Megill, W. M., Buttschardt, T. K., & Rosell, F. (2023). A camera trapping method for the targeted capture of Eurasian beaver (*Castor fiber*) tails for individual scale pattern recognition. *European Journal of Wildlife Research*, *69*(2). https://doi.org/10.1007/s10344-023-01654-6

Ellis, C. R., Pomeroy, J. W., Brown, T., & MacDonald, J. (2010). Simulation of snow accumulation and melt in needleleaf forest environments. *Hydrology and Earth System Sciences*, *14*(6), 925–940. https://doi.org/10.5194/hess-14-925-2010

England, K., & Westbrook, C. J. (2021). Comparison of beaver density and foraging preferences between urban and rural riparian forests along the South Saskatchewan river, Canada. *Journal of Urban Ecology*, *7*(1), 1–10. https://doi.org/10.1093/jue/juab021

Fairfax, E., & Small, E. E. (2018). Using remote sensing to assess the impact of beaver damming on riparian evapotranspiration in an arid landscape. *Ecohydrology*, *11*(7), 1–15. https://doi.org/10.1002/eco.1993

Fairfax, E., & Whittle, A. (2020). Smokey the Beaver: Beaver-dammed riparian corridors stay green during wildfire throughout the western United States. *Ecological Applications*, *30*(8). https://doi.org/10.1002/EAP.2225

Fang, X., & Pomeroy, J. (2007a). Snowmelt runoff sensitivity analysis to drought on the Canadian prairies. *Hydrological Processes*, *21*, 2594–2609. https://doi.org/10.1002/hyp.6796

Fang, X., & Pomeroy, J. (2020). Diagnosis of future changes in hydrology for a Canadian Rockies headwater basin. *Hydrology and Earth System Sciences*, *24*(5), 2731–2754. https://doi.org/10.5194/hess-24-2731-2020

Fang, X., & Pomeroy, J. W. (2007b). Snowmelt runoff sensitivity analysis to drought on the Canadian prairies. *Hydrological Processes*, *21*(19), 2594–2609. https://doi.org/10.1002/hyp.6796

Fang, X., Pomeroy, J. W., Ellis, C. R., MacDonald, M. K., Debeer, C. M., & Brown, T. (2013). Multi-variable evaluation of hydrological model predictions for a headwater basin in the Canadian Rocky Mountains. *Hydrology and Earth System Sciences*, *17*(4), 1635–1659. https://doi.org/10.5194/hess-17-1635-2013

Feiner, K., & Lowry, C. S. (2015). Simulating the effects of a beaver dam on regional groundwater flow through a wetland. *Journal of Hydrology: Regional Studies*, *4*, 675–685. https://doi.org/10.1016/j.ejrh.2015.10.001

Fenicia, F., Kavetski, D., & Savenije, H. H. G. (2011). Elements of a flexible approach for conceptual hydrological modeling: 1. Motivation and theoretical development. *Water Resources Research*, *47*(11). https://doi.org/10.1029/2010WR010174

Fennell, M., Beirne, C., & Burton, A. C. (2022). Use of object detection in camera trap image identification: Assessing a method to rapidly and accurately classify human and animal detections for research and application in recreation ecology. *Global Ecology and Conservation*, *35*. https://doi.org/10.1016/J.GECCO.2022.E02104

Foster, A. C., Wang, J. A., Frost, G. V., Davidson, S. J., Hoy, E., Turner, K. W., Sonnentag, O., Epstein, H., Berner, L. T., Armstrong, A. H., Kang, M., Rogers, B. M., Campbell, E., Miner, K. R., Orndahl, K. M., Bourgeau-Chavez, L. L., Lutz, D. A., French, N., Chen, D., … Goetz, S. (2022). Disturbances in North American boreal forest and Arctic tundra: Impacts, interactions, and responses. In *Environmental Research Letters* (Vol. 17, Issue 11). https://doi.org/10.1088/1748-9326/ac98d7

Gable, T. D., Stanger, T., Windels, S. K., & Bump, J. K. (2018). Do wolves ambush beavers? Video evidence for higher-order hunting strategies. *Ecosphere*, *9*(3). https://doi.org/10.1002/ECS2.2159

Gable, T. D., & Windels, S. K. (2018). Kill rates and predation rates of wolves on beavers. *Journal of Wildlife Management*, *82*(2), 466–472. https://doi.org/10.1002/JWMG.21387

Gable, T. D., Windels, S. K., Bruggink, J. G., & Homkes, A. T. (2016). Where and how wolves (*Canis lupus*) kill beavers (*Castor canadensis*). *PLoS ONE*, *11*(12). https://doi.org/10.1371/journal.pone.0165537

Gable, T. D., Windels, S. K., Romanski, M. C., & Rosell, F. (2018). The forgotten prey of an iconic predator: a review of interactions between grey wolves *Canis lupus* and beavers *Castor* spp. In *Mammal Review* (Vol. 48, Issue 2, pp. 123–138). Blackwell Publishing Ltd. https://doi.org/10.1111/mam.12118

García, V. J., Hotchkiss, E. R., & Rodríguez, P. (2022). Ecosystem metabolism in sub-Antarctic streams and rivers impacted by non-native beaver. *Aquatic Sciences*, *84*(4), 1–11. https://doi.org/10.1007/s00027-022-00876-1

Gibson, P. P., & Olden, J. D. (2014). Ecology, management, and conservation implications of North American beaver (*Castor canadensis*) in dryland streams. *Aquatic Conservation: Marine and Freshwater Ecosystems*, *24*(3), 391–409. https://doi.org/10.1002/aqc.2432

Gill, M. A. (1979). Critical Examination of the Muskingum Method. In *Nordic Hydrology* (Vol. 10). http://iwaponline.com/hr/article-pdf/10/4/261/9378/261.pdf?casa_token=hO6sKY4sHvcAAAAA:ZxqIyc7zqYCuKq3dypjpy_rOBzjdPu_d6fSuixUSUkb2MG

Graham, H. A., Puttock, A. K., Elliott, M., Anderson, K., & Brazier, R. E. (2022). Exploring the dynamics of flow attenuation at a beaver dam sequence. *Hydrological Processes*, *36*(11), 1–17. https://doi.org/10.1002/hyp.14735

Green, K. C., & Westbrook, C. J. (2007). Yield following loss of beaver dams. *Methods*, *10*(1), 68–79.

Green, K., & Westbrook, C. (2009). Changes in riparian area structure, channel hydraulics, and sediment yield following loss of beaver dams. *BC Journal of Ecosystem and Mangement*, *10*(1), 68–79. www.forrex.org/publications/jem/ISS50/vol10_no1_art7.pdf

Greenberg, S. (2020). *Automated image recognition for wildlife camera traps: making it work for you*. https://prism.ucalgary.ca/handle/1880/112416

Greenberg, S., Godin, T., & Whittington, J. (2019). Design patterns for wildlife-related camera trap image analysis. *Ecology and Evolution*, *9*(24), 13706–13730.

Gupta, H. V., Kling, H., Yilmaz, K. K., & Martinez, G. F. (2009). Decomposition of the mean squared error and NSE performance criteria: Implications for improving hydrological modelling. *Journal of Hydrology*, *377*(1–2), 80–91. https://doi.org/10.1016/j.jhydrol.2009.08.003

Gurnell, A. M. (1998). The hydrogeomorphological effect of beaver dam-building activity. *Progress in Physical Geography*, *22*(2), 167–189. https://doi.org/10.1177/030913339802200202

Hafen, K. C., Wheaton, J. M., Roper, B. B., Bailey, P., & Bouwes, N. (2020). Influence of topographic, geomorphic, and hydrologic variables on beaver dam height and persistence in the intermountain western United States. *Earth Surface Processes and Landforms*, *45*(11), 2664–2674. https://doi.org/10.1002/esp.4921

Halley, D., Rosell, F., & Saveljev, A. (2012). Population and Distribution of Eurasian Beaver (*Castor fiber*). *Baltic Forestry*, *June 2015*.

Hamilton, S., Watson, M., & Pike, R. (2019). The role of the hydrographer in rating curve development. *Confluence: Journal of Watershed Science and Management*, *3*(1). https://doi.org/10.22230/jwsm.2019v3n1a11

Han, Z., Long, D., Huang, Q., Li, X., Zhao, F., & Wang, J. (2020). Improving reservoir outflow estimation for ungauged basins using satellite observations and a hydrological model. *Water Resources Research*, *56*(9). https://doi.org/10.1029/2020WR027590

Harris, C. R., Millman, K. J., van der Walt, S. J., Gommers, R., Virtanen, P., Cournapeau, D., Wieser, E., Taylor, J., Berg, S., Smith, N. J., Kern, R., Picus, M., Hoyer, S., van Kerkwijk, M. H., Brett, M., Haldane, A., del Río, J. F., Wiebe, M., Peterson, P., … Oliphant, T. E. (2020). Array programming with {NumPy}. *Nature*, *585*(7825), 357–362. https://doi.org/10.1038/s41586-020-2649-2

He, H., Moore, T., Humphreys, E. R., Lafleur, P. M., & Roulet, N. T. (2023). Water level variation at a beaver pond significantly impacts net CO_2 uptake of a continental bog. *Hydrology and Earth System Sciences*, *27*(1), 213–227. https://doi.org/10.5194/hess-27-213-2023

Hillman, G. R. (1998). Flood wave attenuation by a wetland following a beaver dam failure on a second order boreal stream. *Wetlands*, *18*(1), 21–34. https://doi.org/10.1007/BF03161439

Hood, G. (2011). *The beaver Manifesto*. RMB.

Hood, G. (2020a). Not all ponds are created equal: Long-term beaver (*Castor canadensis*) lodge occupancy in a heterogeneous landscape. *Canadian Journal of Zoology*, *98*(3), 210–218. https://doi.org/10.1139/cjz-2019-0066

Hood, G. (2020b). *Semi-aquatic Mammals: Ecology and Biology.* Johns Hopkins University Press. https://ebookcentral.proquest.com/lib/usask/detail.action?docID=6367384#

Hood, G. (2023, November). Night and day: Spatial and temporal abundance of riparian wildlife [Paper presentation]. *TWS Annual Conference*.

Hood, G., & Bayley, S. (2008). Beaver (*Castor canadensis*) mitigate the effects of climate on the area of open water in boreal wetlands in western Canada. *Biological Conservation*, *141*(2), 556–567. https://doi.org/10.1016/j.biocon.2007.12.003

Hood, G., & Larson, D. (2015). Ecological engineering and aquatic connectivity: A new perspective from beaver-modified wetlands. *Freshwater Biology*, *60*(1), 198–208. https://doi.org/10.1111/fwb.12487

Hrachowitz, M., & Clark, M. P. (2017). HESS Opinions: The complementary merits of competing modelling philosophies in hydrology. *Hydrology and Earth System Sciences*, *21*(8), 3953–3973. https://doi.org/10.5194/hess-21-3953-2017

Huertas Herrera, A., Lencinas, M. V., Manríquez, M. T., Miller, J. A., & Pastur, G. M. (2020). Mapping the status of the North American beaver invasion in the Tierra del Fuego archipelago. *PLoS ONE*, *15*(4), 1–19. https://doi.org/10.1371/journal.pone.0232057

Huertas Herrera, A., Toro Manríquez, M. D. R., Lencinas, M. V., & Martínez Pastur, G. (2021). *The North American Beaver Invasion and the Impact Over the Ecosystem Services in the Tierra del Fuego Archipelago*. 213–226. https://doi.org/10.1007/978-3-030-69166-0_10

Hunter, J. D. (2007). Matplotlib: A 2D graphics environment. *Computing in Science & Engineering*, *9*(3), 90–95. https://doi.org/10.1109/MCSE.2007.55

Jacobs, C. E., & Ausband, D. E. (2018). An evaluation of camera trap performance – What are we missing and does deployment height matter? *Remote Sensing in Ecology and Conservation*, *4*(4), 352–360. https://doi.org/10.1002/rse2.81

Jain, S. (2001). *Open-channel flow*. John Wiley & Sons.

Janzen, K., & Westbrook, C. (2011). Hyporheic flows along a channelled peatland: Influence of beaver dams. *Canadian Water Resources Journal*, *36*(4), 331–347. https://doi.org/10.4296/cwrj3604846

Johnsgard, P. A. (2009). *Birds of the Rocky Mountains*. U of Nebraska Press. https://digitalcommons.unl.edu/cgi/viewcontent.cgi?article=1000&context=bioscibirds rockymtns

Johnson-Bice, S. M., Gable, T. D., Windels, S. K., & Host, G. E. (2022). Relics of beavers past: time and population density drive scale-dependent patterns of ecosystem engineering. *Ecography*, *2022*(2). https://doi.org/10.1111/ecog.05814

Johnston, C. A., & Naiman, R. J. (1987). Boundary dynamics at the aquatic-terrestrial interface: The influence of beaver and geomorphology. In *Landscape Ecology* (Vol. 1, Issue 1). SPB Academic Publishing.

Johnston, C. A., & Naiman, R. J. (1990). The use of a geographic information system to analyze long-term landscape alteration by beaver. In *Landscape Ecology* (Vol. 4, Issue 1). SPB Academic Publishing bv.

Jordan, C. E., & Fairfax, E. (2022). Beaver: The North American freshwater climate action plan. *Wiley Interdisciplinary Reviews: Water*, *9*(4). https://doi.org/10.1002/WAT2.1592

Karran, D. J., Westbrook, C. J., & Bedard-Haughn, A. (2018). Beaver-mediated water table dynamics in a Rocky Mountain fen. *Ecohydrology*, *11*(2), 1–11. https://doi.org/10.1002/eco.1923

Karran, D. J., Westbrook, C. J., Wheaton, J. M., Johnston, C. A., & Bedard-Haughn, A. (2017). Rapid surface-water volume estimations in beaver ponds. *Hydrology and Earth System Sciences*, *21*(2), 1039–1050. https://doi.org/10.5194/hess-21-1039-2017

Keys, T. A., Govenor, H., Jones, C. N., Hession, W. C., Hester, E. T., & Scott, D. T. (2018). Effects of large wood on floodplain connectivity in a headwater Mid-Atlantic stream. *Ecological Engineering*, *118*(March), 134–142. https://doi.org/10.1016/j.ecoleng.2018.05.007

Kluyver, T., Ragan-Kelley, B., Pérez, F., Granger, B., Bussonnier, M., Frederic, J., Kelley, K., Hamrick, J., Grout, J., Corlay, S., Ivanov, P., Avila, D., Abdalla, S., & Willing, C. (2016). Jupyter Notebooks—a publishing format for reproducible computational workflows. *Positioning and Power in Academic Publishing: Players, Agents and Agendas - Proceedings of the 20th International Conference on Electronic Publishing, ELPUB 2016*, 87–90. https://doi.org/10.3233/978-1-61499-649-1-87

Knoben, W. J. M., Clark, M. P., Bales, J., Bennett, A., Gharari, S., Marsh, C. B., Nijssen, B., Pietroniro, A., Spiteri, R. J., Tang, G., Tarboton, D. G., & Wood, A. W. (2022). Community workflows to advance reproducibility in hydrologic modeling: Separating model-agnostic and model-specific configuration steps in applications of large-domain hydrologic models. *Water Resources Research*, *58*(11). https://doi.org/10.1029/2021WR031753

Knoben, W. J. M., Freer, J. E., & Woods, R. A. (2019). Technical note: Inherent benchmark or not? Comparing Nash-Sutcliffe and Kling-Gupta efficiency scores. *Hydrology and Earth System Sciences*, *23*(10), 4323–4331. https://doi.org/10.5194/hess-23-4323-2019

Krause, P., Boyle, D. P., & Bäse, F. (2005). Comparison of different efficiency criteria for hydrological model assessment. In *Advances in Geosciences* (Vol. 5).

Krogh, S. A., Pomeroy, J. W., & Marsh, P. (2017). Diagnosis of the hydrology of a small Arctic basin at the tundra-taiga transition using a physically based hydrological model. *Journal of Hydrology*, *550*, 685–703. https://doi.org/10.1016/j.jhydrol.2017.05.042

Larsen, A., Larsen, J. R., & Lane, S. N. (2021). Dam builders and their works: Beaver influences on the structure and function of river corridor hydrology, geomorphology, biogeochemistry and ecosystems. *Earth-Science Reviews*, *218*(October 2020), 103623. https://doi.org/10.1016/j.earscirev.2021.103623

Lautz, L. K., & Siegel, D. I. (2006). Modeling surface and ground water mixing in the hyporheic zone using MODFLOW and MT3D. *Advances in Water Resources*, *29*(11), 1618–1633. https://doi.org/10.1016/j.advwatres.2005.12.003

Lhomme, J. P. (1997). An examination of the Priestley-Taylor equation using a convective boundary layer model. *Water Resources Research*, *33*(11), 2571–2578. https://doi.org/10.1029/97WR01897

Lin, N. M., & Rutten, M. (2016). Optimal operation of a network of multi-purpose reservoir: A review. *Procedia Engineering*, *154*, 1376–1384. https://doi.org/10.1016/j.proeng.2016.07.504

Lundmark, C., & Ball, J. P. (2008). Living in snowy environments: Quantifying the influence of snow on moose behavior. *Arctic, Antarctic, and Alpine Research*, *40*(1), 111–118. https://doi.org/10.1657/1523-0430(06-103)[LUNDMARK]2.0.CO;2

Macfarlane, W. W., Wheaton, J. M., Bouwes, N., Jensen, M. L., Gilbert, J. T., Hough-snee, N., & Shivik, J. A. (2017). Modeling the capacity of riverscapes to support beaver dams. *Geomorphology*, *277*(November 2017), 72–99. https://doi.org/10.1016/j.geomorph.2015.11.019

McCarthy, G. T. (1938). The unit hydrograph and flood routing. *Conf. North Atlantic Division, U.S.*

McCullough, M., Eisenhauer, D., Dooskey, M., & Admiraal, D. (2006). Hydraulic characteristics of beaver dams in a Midwestern U.S. agricultural watershed.

Proceedings of the World Environmetal & Water Resources Congress, 10. https://www.srs.fs.usda.gov/pubs/ja/ja_mccullough002.pdf

McMillan, H. (2020). Linking hydrologic signatures to hydrologic processes: A review. *Hydrological Processes*, *34*(6), 1393–1409. https://doi.org/10.1002/hyp.13632

Mcmillan, H. K., & Westerberg, I. K. (2015). Rating curve estimation under epistemic uncertainty. *Hydrological Processes*, *29*(7), 1873–1882. https://doi.org/10.1002/hyp.10419

Medin, D. (1990). *Bird Populations in and Adjacent to a Beaver Pond Ecosystem in Idaho*. U.S. Department of Agriculture, Forest Service, Intermountain Forest and Range Experiment Station.

Metcalfe, P., Beven, K., Hankin, B., & Lamb, R. (2017). A modelling framework for evaluation of the hydrological impacts of nature-based approaches to flood risk management, with application to in-channel interventions across a 29-km^2 scale catchment in the United Kingdom. *Hydrological Processes*, *31*(9), 1734–1748. https://doi.org/10.1002/hyp.11140

Monteith, J. L. (1981). Evaporation and surface temperature. In *Quart. J. R. Met. SOC* (Vol. 107, Issue 451).

Morrison, A., Westbrook, C. J., & Bedard-Haughn, A. (2015). Distribution of Canadian Rocky Mountain wetlands impacted by beaver. *Wetlands*, *35*(1), 95–104. https://doi.org/10.1007/s13157-014-0595-1

Myhrvold, N. P., Baldridge, E., Chan, B., Sivam, D., Freeman, D. L., & Ernest, S. K. M. (2015). An amniote life-history database to perform comparative analyses with birds, mammals, and reptiles. *Ecology*, *96*(11), 3109–000. https://doi.org/10.1890/15-0846R.1

Naiman, R. J., Johnston, C. A., Kelley, J. C., Naiman, R. J., Johnston, C. A., & Kelley, J. C. (1988). Alteration of North American streams by beaver. *American Institute of Biological Sciences*, *38*(11), 753–762.

Nash, J. E. (1959). A note on the Muskingum flood-routing method. *Journal of Geophysical Research*, *64*(8), 1053–1056. https://doi.org/10.1029/jz064i008p01053

Nash, J. E., & Sutcliffe, J. V. (1970). River flow forecasting through conceptual models part I - A discussion of principles. *Journal of Hydrology*, *10*(3), 282–290. https://doi.org/10.1016/0022-1694(70)90255-6

Nature Alberta. (2018). *Shorebirds of Alberta*. https://naturealberta.ca/wp-content/uploads/2020/10/2019_NatureAlberta_ShorebirdsChecklist_web.pdf

Neitsch, S. L., Arnold, J. G., Kiniry, J. R., & Williams, J. R. (2011). Soil & Water Assessment Tool Theoretical Documentation Version 2009. *Texas Water Resources Institute*, 1–647. https://doi.org/10.1016/j.scitotenv.2015.11.063

Neumayer, M., Teschemacher, S., Schloemer, S., Zahner, V., & Rieger, W. (2020). Hydraulic modeling of beaver dams and evaluation of their impacts on flood events. *Water (Switzerland)*, *12*(1), 1–23. https://doi.org/10.3390/w12010300

Niedballa, J., Sollmann, R., Courtiol, A., & Wilting, A. (2016). camtrapR: an R package for efficient camera trap data management. *Methods in Ecology and Evolution*, *7*(12), 1457–1462. https://doi.org/10.1111/2041-210X.12600

Noor, S. M. (2021). *Hydrological Impact of Beaver Habitat Restoration in the Milwaukee River Watershed*. University of Wisconsin Milwaukee. Master thesis.

Nyssen, J., Pontzeele, J., & Billi, P. (2011). Effect of beaver dams on the hydrology of small mountain streams: Example from the Chevral in the Ourthe Orientale basin, Ardennes, Belgium. *Journal of Hydrology*, *402*(1–2), 92–102. https://doi.org/10.1016/j.jhydrol.2011.03.008

Osner, N. (2022). *MegaDetector Version 5*. *June*, 1–7. https://wildeyeconservation.org/megadetector-version-5/

Paine, R. T. (1966). Food web complexity and species diversity. *The American Naturalist*, *100*(910), 65–75. https://www.jstor.org/stable/2459379

Paine, R. T. (1969). The Pisaster-Tegula interaction: Prey patches, predator food preference, and intertidal community structure. *Ecology*, *50*(6), 950–961. http://www.jstor.org/stable/193688

Pandas Development team. (2020). *pandas-dev/pandas: Pandas*. Zenodo. https://doi.org/10.5281/zenodo.3509134

Pearce, C., Vidon, P., Lautz, L., Kelleher, C., & Davis, J. (2021). Impact of beaver dam analogues on hydrology in a semi-arid floodplain. *Hydrological Processes*, *35*(7). https://doi.org/10.1002/hyp.14275

Perumal, M., & Price, R. K. (2013). A fully mass conservative variable parameter McCarthy-Muskingum method: Theory and verification. *Journal of Hydrology*, *502*, 89–102. https://doi.org/10.1016/j.jhydrol.2013.08.023

Pollock, M., Lewallen, G., Woodruff, K., Jordan, C., & Castro, J. (2015). The Beaver Restoration Guidebook: A Practitioners Guide to Working with Beaver to Restore Streams, Wetlands and Floodplains. *United States Fish and Wildlife Service*, *June*. http://www.fws.gov/oregonfwo/ToolsForLandowners/RiverScience/Beaver.asp%5Cnp apers2://publication/uuid/F5CC7199-5304-42F2-8C26-50AF48FC1A31

Pomeroy, J., Gray, D., Brown, T., Hedstrom, N., Quinton, W., Granger, R., & Carey, S. (2007). The cold regions hydrological model: a platform for basing process representation and model structure on physical evidence. *Hydrological Processes*, *21*(19), 2650–2667. https://doi.org/https://doi.org/10.1002/hyp.6787

Pomeroy, J. W., Brown, T., Fang, X., Shook, K. R., Pradhananga, D., Armstrong, R., Harder, P., Marsh, C., Costa, D., Krogh, S. A., Aubry-Wake, C., Annand, H., Lawford, P., He, Z., Kompanizare, M., & Lopez Moreno, J. I. (2022). The cold regions hydrological modelling platform for hydrological diagnosis and prediction based on process understanding. *Journal of Hydrology*, *615*(May), 128711. https://doi.org/10.1016/j.jhydrol.2022.128711

Pontius, R. G., Thontteh, O., & Chen, H. (2008). Components of information for multiple resolution comparison between maps that share a real variable. *Environmental and Ecological Statistics*, *15*(2), 111–142. https://doi.org/10.1007/s10651-007-0043-y

Priestley, C. H. B., & Taylor, R. J. (1972). On the assessment of surface heat flux and evaporation using large-scale parameters. *Monthly Weather Review*, *100*(2), 81–92.

Prieto, L. (2009). *Soil / Rock Mechanics and Foundations Engineering* . Florida International University.

Puttock, A., Graham, H. A., Ashe, J., Luscombe, D. J., & Brazier, R. E. (2020). Beaver dams attenuate flow: A multi-site study. *Hydrological Processes*, *October*, 1–18. https://doi.org/10.1002/hyp.14017

Puttock, A., Graham, H. A., Cunliffe, A. M., Elliott, M., & Brazier, R. E. (2017). Eurasian beaver activity increases water storage, attenuates flow and mitigates diffuse pollution from intensively-managed grasslands. *Science of the Total Environment*, *576*, 430–443. https://doi.org/10.1016/j.scitotenv.2016.10.122

R Core Team. (2023). *R: A Language and Environment for Statistical Computing*. https://www.R-project.org/

Rainville, F., Hutchinson, D., Stead, A., Moncur, D., & Elliott, D. (2016). *Hydrometric Manual-Data Computations Stage-Discharge Model Development and Maintenance*. Water Survey of Canada.

Rasouli, K., Pomeroy, J. W., Janowicz, J. R., Carey, S. K., & Williams, T. J. (2014). Hydrological sensitivity of a northern mountain basin to climate change. *Hydrological Processes*, *28*(14), 4191–4208. https://doi.org/10.1002/hyp.10244

Ronnquist, A. (2021). *Dam different! How the physical properties of beaver dams influence water storage dynamics*. University of Saskatchewan. Department of Geography. Master thesis.

Ronnquist, A., & Westbrook, C. (2021). Beaver dams: How structure, flow state, and landscape setting regulate water storage and release. *Science of the Total Environment*, *785*. https://doi.org/10.1016/j.scitotenv.2021.147333

Rosell, F., Bozsér, O., Collen, P., & Parker, H. (2005). Ecological impact of beavers *Castor fiber* and *Castor canadensis* and their ability to modify ecosystems. *Mammal Review*, *35*(3–4), 248–276. https://doi.org/10.1111/j.1365-2907.2005.00067.x

Safarzadeh, A., & Mohajeri, S. H. (2018). Hydrodynamics of rectangular broad-crested porous weirs. *Journal of Irrigation and Drainage Engineering*, *144*(10), 1–12. https://doi.org/10.1061/(asce)ir.1943-4774.0001338

Scheffer, P. M. (1938). The beaver as an upstream engineer. *Soil Conservation*, *3*(7), 178–181.

Schwab, M., Klaus, J., Pfister, L., & Weiler, M. (2016). Diel discharge cycles explained through viscosity fluctuations in riparian inflow. *Water Resources Research*, 8744–8755. https://doi.org/10.1111/j.1752-1688.1969.tb04897.x

Scrafford, M. A., & Boyce, M. S. (2018). Temporal patterns of wolverine (*Gulo gulo luscus*) foraging in the boreal forest. *Journal of Mammalogy*, *99*(3), 693–701. https://doi.org/10.1093/jmammal/gyy030

Shariq, A., Hussain, A., & Ahmad, Z. (2022). Flow over gabion weir under free and submerged flow conditions. *Flow Measurement and Instrumentation*, *86*(July 2021), 102199. https://doi.org/10.1016/j.flowmeasinst.2022.102199

Shaw, E. L. (2009). *Lateral exchange of water and nitrogen along a beaver-dammed stream draining a Rocky Mountain valley*. University of Saskatchewan. Master thesis.

Shook, K., Pomeroy, J. W., Spence, C., & Boychuk, L. (2013). Storage dynamics simulations in prairie wetland hydrology models: Evaluation and parameterization. *Hydrological Processes*, *27*(13), 1875–1889. https://doi.org/10.1002/hyp.9867

Shook, K. R., & Pomeroy, J. W. (2011). Memory effects of depressional storage in Northern Prairie hydrology. *Hydrological Processes*, *25*(25), 3890–3898. https://doi.org/10.1002/hyp.8381

Shook, K., Spiteri, R., Pomeroy, J., Liu, T., & Sharomi, O. (2021). WDPM: the Wetland DEM Ponding Model. *Journal of Open Source Software*, *6*(64), 2276. https://doi.org/10.21105/joss.02276

Sikorska, A. E., Scheidegger, A., Banasik, K., & Rieckermann, J. (2013). Considering rating curve uncertainty in water level predictions. *Hydrology and Earth System Sciences*, *17*(11), 4415–4427. https://doi.org/10.5194/hess-17-4415-2013

Singh, V. P., & McCann, R. C. (1980). Some notes on Muskingum method of flood routing. *Journal of Hydrology*, *48*, 343–361.

Skewes, O., Gonzalez, F., Olave, R., Ávila, A., Vargas, V., Paulsen, P., & König, H. E. (2006). Abundance and distribution of American beaver, *Castor canadensis* (Kuhl 1820), in Tierra del Fuego and Navarino islands, Chile. *European Journal of Wildlife Research*, *52*(4), 292–296. https://doi.org/10.1007/s10344-006-0038-2

St. Clair, C. C. (2003). Comparative permeability of roads, rivers, and meadows to songbirds in Banff National Park. *Conservation Biology*, *17*(4), 1151–1160. https://doi.org/10.1046/J.1523-1739.2003.02156.X

Stoll, N. L., & Westbrook, C. J. (2020). Beaver dam capacity of Canada's boreal plain in response to environmental change. *Scientific Reports*, *10*(1), 1–12. https://doi.org/10.1038/s41598-020-73095-z

Streich, S. (2019). *The hydrological function of a mountain valley-bottom peatland under drought conditions*. University of Saskatchewan. Department of Geography. Master thesis. https://harvest.usask.ca/handle/10388/12188

Streich, S., & Westbrook, C. (2020). Hydrological function of a mountain fen at low elevation under dry conditions. *Hydrological Processes*, *34*(2), 244–257. https://doi.org/10.1002/hyp.13579

Swinnen, K. R. R., Hughes, N. K., & Leirs, H. (2015). Beaver (*Castor fiber*) activity patterns in a predator-free landscape. What is keeping them in the dark? *Mammalian Biology*, *80*(6), 477–483. https://doi.org/10.1016/j.mambio.2015.07.006

Swinnen, K. R. R., Reijniers, J., Breno, M., & Leirs, H. (2014). A novel method to reduce time investment when processing videos from camera trap studies. *PLoS ONE*, *9*(6). https://doi.org/10.1371/journal.pone.0098881

Swinnen, K. R. R., Rutten, A., Nyssen, J., & Leirs, H. (2019). Environmental factors influencing beaver dam locations. *Journal of Wildlife Management*, *83*(2), 356–364. https://doi.org/10.1002/jwmg.21601

Tabak, M. A., Falbel, D., Hamzeh, T., Brook, R. K., Goolsby, J. A., Zoromski, L. D., Boughton, R. K., Snow, N. P., VerCauteren, K. C., & Miller, R. S. (2022). CameraTrapDetectoR: Automatically detect, classify, and count animals in camera trap images using artificial intelligence. *BioRxiv*. https://doi.org/10.1101/2022.02.07.479461

Talukdar, P., & Dey, A. (2019). Hydraulic failures of earthen dams and embankments. *Innovative Infrastructure Solutions*, *4*(1). https://doi.org/10.1007/s41062-019-0229-9

Tape, K. D., Clark, J. A., Jones, B. M., Kantner, S., Gaglioti, B. V., Grosse, G., & Nitze, I. (2022a). Expanding beaver pond distribution in Arctic Alaska, 1949 to 2019. *Scientific Reports*, *12*(1). https://doi.org/10.1038/s41598-022-09330-6

Tape, K. D., Clark, J. A., Jones, B. M., Kantner, S., Gaglioti, B. V., Grosse, G., & Nitze, I. (2022b). Expanding beaver pond distribution in Arctic Alaska, 1949 to 2019. *Scientific Reports*, *12*(1). https://doi.org/10.1038/s41598-022-09330-6

Tape, K. D., Clark, J. A., Jones, B. M., Wheeler, H. C., Marsh, P., & Rosell, F. (2021). *Beaver Engineering: Tracking a New Disturbance in the Arctic*. https://doi.org/10.25923/0jtd-vv85

Tape, K. D., Jones, B. M., Arp, C. D., Nitze, I., & Grosse, G. (2018). Tundra be dammed: Beaver colonization of the Arctic. *Global Change Biology*, *24*(10), 4478–4488. https://doi.org/10.1111/gcb.14332

Thompson, S., Vehkaoja, M., Pellikka, J., & Nummi, P. (2021). Ecosystem services provided by beavers *Castor* spp. *Mammal Review*, *51*(1), 25–39. https://doi.org/10.1111/MAM.12220

Tomkins, K. M. (2014). Uncertainty in streamflow rating curves: Methods, controls and consequences. *Hydrological Processes*, *28*(3), 464–481. https://doi.org/10.1002/hyp.9567

Touihri, M., Labbé, J., Imbeau, L., & Darveau, M. (2018). North American beaver (*Castor canadensis* Kuhl) key habitat characteristics: Review of the relative effects of

geomorphology, food availability and anthropogenic infrastructure. *Ecoscience*, *25*(1), 9–23. https://doi.org/10.1080/11956860.2017.1395314

Tsoukalas, I., & Makropoulos, C. (2015). Multiobjective optimisation on a budget: Exploring surrogate modelling for robust multi-reservoir rules generation under hydrological uncertainty. *Environmental Modelling and Software*, *69*, 396–413. https://doi.org/10.1016/j.envsoft.2014.09.023

U.S. Army Corps of Engineers, H. E. C. (2022). *HEC-HMS Hydrologic Modeling System*.

Van Rossum, G., & Drake, F. L. (2009). *Python 3 Reference Manual*. CreateSpace.

Vélez, J., Castiblanco-Camacho, P. J., Tabak, M. A., Chalmers, C., Fergus, P., & Fieberg, J. (2022). *Choosing an Appropriate Platform and Workflow for Processing Camera Trap Data using Artificial Intelligence*. 1–30. http://arxiv.org/abs/2202.02283

Wade, J., Lautz, L., Kelleher, C., Vidon, P., Davis, J., Beltran, J., & Pearce, C. (2020). Beaver dam analogues drive heterogeneous groundwater–surface water interactions. *Hydrological Processes*, *34*(26), 5340–5353. https://doi.org/10.1002/hyp.13947

Wang, B., Zhang, H., Liang, X., Li, X., & Wang, F. (2019). Cumulative effects of cascade dams on river water cycle: Evidence from hydrogen and oxygen isotopes. *Journal of Hydrology*, *568*, 604–610. https://doi.org/10.1016/j.jhydrol.2018.11.016

Wang, X., Shaw, E. L., Westbrook, C. J., & Bedard-Haughn, A. (2018). Beaver dams induce hyporheic and biogeochemical changes in riparian areas in a mountain peatland. *Wetlands*, *38*(5), 1017–1032. https://doi.org/10.1007/s13157-018-1059-9

Watters, J. R., & Stanley, E. H. (2007). Stream channels in peatlands: The role of biological processes in controlling channel form. *Geomorphology*, *89*(1-2 SPEC. ISS.), 97–110. https://doi.org/10.1016/j.geomorph.2006.07.015

Westbrook, C., Cooper, D., & Baker, B. (2006). Beaver dams and overbank floods influence groundwater-surface water interactions of a Rocky Mountain riparian area. *Water Resources Research*, *42*(6), 1–13. https://doi.org/10.1029/2005WR004560

Westbrook, C. J., & Bedard-Haughn, A. (2016). Sibbald Research Wetland: Mountain peatland form and ecohydrologic function as influenced by beaver. *Forestry Chronicle*, *92*(1), 37–38. https://doi.org/10.5558/tfc2016-011

Westbrook, C. J., Cooper, D. J., & Anderson, C. B. (2017). Alteration of hydrogeomorphic processes by invasive beavers in southern South America. *Science of the Total Environment*, *574*, 183–190. https://doi.org/10.1016/j.scitotenv.2016.09.045

Westbrook, C. J., & England, K. (2022). Relative effectiveness of four different guards in preventing beaver cutting of urban trees. *Environmental Management*, *70*(1), 97–104. https://doi.org/10.1007/s00267-022-01658-z

Westbrook, C., Ronnquist, A., & Bedard-Haughn, A. (2020). Hydrological functioning of a beaver dam sequence and regional dam persistence during an extreme rainstorm. *Hydrological Processes*, *34*(18), 3726–3737. https://doi.org/10.1002/hyp.13828

Whitfield, C., Baulch, H., Chun, K., & Westbrook, C. (2015). Beaver-mediated methane emission: The effects of population growth in Eurasia and the Americas. *Ambio*, *44*(1), 7–15. https://doi.org/10.1007/s13280-014-0575-y

Wikar, Z., & Ciechanowski, M. (2023). Beaver dams and fallen trees as ecological corridors allowing movements of mammals across water barriers—A case study with the application of novel substrate for tracking tunnels. *Animals*, *13*(8). https://doi.org/10.3390/ani13081302

Wilman, H., Belmaker, J., Simpson, J., de la Rosa, C., Rivadeneira, M. M., & Jetz, W. (2014). EltonTraits 1.0: Species-level foraging attributes of the world's birds and mammals. *Ecology*, *95*(7), 2027–2027. https://doi.org/10.1890/13-1917.1

Wohl, E. (2021). Legacy effects of loss of beavers in the continental United States. *Environmental Research Letters*, *16*(2). https://doi.org/10.1088/1748-9326/abd34e

Woo, M., & Waddington, J. (1990). Effects of beaver dams on subarctic wetland hydrology. *Arctic*, *43*(3), 223–230. https://doi.org/10.14430/arctic1615

Yarmey, N. T., & Hood, G. A. (2020). Resident perceptions of human-beaver conflict in a rural landscape in Alberta, Canada. *Human-Wildlife Interactions*, *14*(3), 476–486.

APPENDICES

APPENDIX A – CODE TO RENAME CAMERA TRAPS IMAGES

This appendix includes a Python script to rename camera traps images and build a database with camera id, location, and date-time.

The code is available in the Rocky Mountain Ecohydrology group GitHub https://github.com/Ecohydrology-westbrook/camera_traps_rename

APPENDIX B – TIMELAPSE TEMPLATES

This appendix includes all the custom templates used in *Timelapse* to identify the family and species (where possible) of the images recorded by the camera traps that had positive animal detections.

A shared folder is available in the Rocky Mountain Ecohydrology group GitHub https://github.com/Ecohydrology-westbrook/timelapse_templates

APPENDIX C - TAXA OF OBSERVED ANIMALS IN SIBBALD FEN

Animal	Family	Scientific Name (where identified)	Mean Body Mass (kg)	Body Mass Source
mallard	Anatidae	*Anas platyrhynchos*	0.84	Wilman et al. (2014)
kingfisher	Alcedinidae	*Alcedo atthis*	0.03	Wilman et al. (2014)
great-blue heron	Ardeidae	*Ardea herodias*	2.52	Wilman et al. (2014)
grouse sp.	Phasianidae		0.53	Wilman et al. (2014)
yellow-bellied sapsucker	Picidae	*Sphyrapicus varius*	0.05	Wilman et al. (2014)
shorebird	Scolopacidae		0.11	Wilman et al. (2014)
gull	Laridae		0.52	Wilman et al. (2014)
raptor	Accipitridae		1.10	Wilman et al. (2014)
raven	Corvidae	*Corvus corax*	0.93	Wilman et al. (2014)
songbird	Sittidae		0.01	Wilman et al. (2014)
red-winged black bird	Icteridae	*Agelaius phoeniceus*	0.05	Wilman et al. (2014)
beaver	Castoridae	*Castor canadensis*	21.82	Wilman et al. (2014)
muskrat	Cricetidae	*Ondatra zibethicus*	1.07	Wilman et al. (2014)
weasel	Mustelidae		0.12	Wilman et al. (2014)
mink	Mustelidae	*Neovison vison*	1.15	Wilman et al. (2014)
river otter	Mustelidae	*Lontra canadensis*	8.09	Wilman et al. (2014)

Animal	Family	Scientific Name (where identified)	Mean Body Mass (kg)	Body Mass Source
domestic cattle	Bovidae	*Bos taurus*	900.00	Wilman et al. (2014)
white-tailed deer	Cervidae	*Odocoileus virginianus*	55.51	Wilman et al. (2014)
chipmunk	Sciuridae		0.04	Myrhvold et al. (2016)

APPENDIX D - CHANGES ON FLOW STATE OF BEAVER DAMS AND TRIGGERS PRESENT.

Changes between flow states are valid if the flow state was determined before and after. Non-determined periods are marked with (NDP)

which were caused by vegetation obscuring the camera lens.

Dam	Valid	Change N°	Flow State Before	Flow State After	Date	Biotic Presence	Rainfall Presence	Rainfall total amount [mm]
Dam #1	1	1	Underflow	Mixed (Gapflow & Underflow)	13-Jun	0	1	59.4
Dam #1	1	2	Mixed (Gapflow & Underflow)	Underflow	27-Jun	0	1	6
Dam #1	1	3	Underflow	Mixed (Underflow & Seep flow)	16-Jul	0	0	0
Dam #1	1	4	Mixed (Underflow & Seep flow)	Underflow	5-Aug	0	0	0.1
Dam #1	1	5	Underflow	Mixed (Gapflow & Underflow)	25-Aug	0	1	10.1
Dam #1	1	6	Mixed (Gapflow & Underflow)	Underflow	26-Aug	0	1	1.7
Dam #2	1	1	Seep flow	Overflow	5-Jun	0	1	19.5
Dam #2	0	NA	Overflow	NDP	10-Jul	NA	NA	0
Dam #2	0	NA	NDP	Underflow	11-Aug	NA	NA	0
Dam #2	1	2	Underflow	Overflow	22-Aug	0	1	22.5
Dam #2	1	3	Overflow	Underflow	25-Aug	0	1	3.1

Dam	Valid	Change N°	Flow State Before	Flow State After	Date	Biotic Presence	Rainfall Presence	Rainfall total amount [mm]
Dam #2	1	4	Underflow	Overflow	27-Aug	0	1	11.2
Dam #2	1	5	Overflow	Underflow	29-Aug	0	0	0.1
Dam #3	1	1	Gapflow	Overflow	5-Jun	0	1	19.5
Dam #3	1	2	Overflow	Gapflow	8-Jun	0	1	17.5
Dam #3	1	3	Gapflow	Overflow	9-Jun	0	0	0
Dam #3	1	4	Overflow	Gapflow	10-Jun	0	0	0
Dam #3	1	5	Gapflow	Overflow	12-Jun	0	1	8.1
Dam #3	1	6	Overflow	Mixed (Overflow & Gapflow)	18-Jun	0	1	9.7
Dam #3	1	7	Mixed (Overflow & Gapflow)	Overflow	19-Jun	0	1	7.2
Dam #3	1	8	Overflow	Mixed (Overflow & Gapflow)	21-Jun	0	1	2.2
Dam #3	1	8	Mixed (Overflow & Gapflow)	Overflow	22-Jun	0	0	0
Dam #3	1	10	Overflow	Mixed (Overflow & Gapflow)	27-Jun	0	0	0
Dam #3	0	NA	Mixed (Overflow & Gapflow)	NDP	6-Jul	NA	NA	0.2
Dam #3	0	NA	NDP	Gapflow	9-Jul	NA	NA	0
Dam #3	0	NA	Gapflow	NDP	12-Jul	NA	NA	0
Dam #3	0	NA	NDP	Gapflow	13-Jul	NA	NA	0

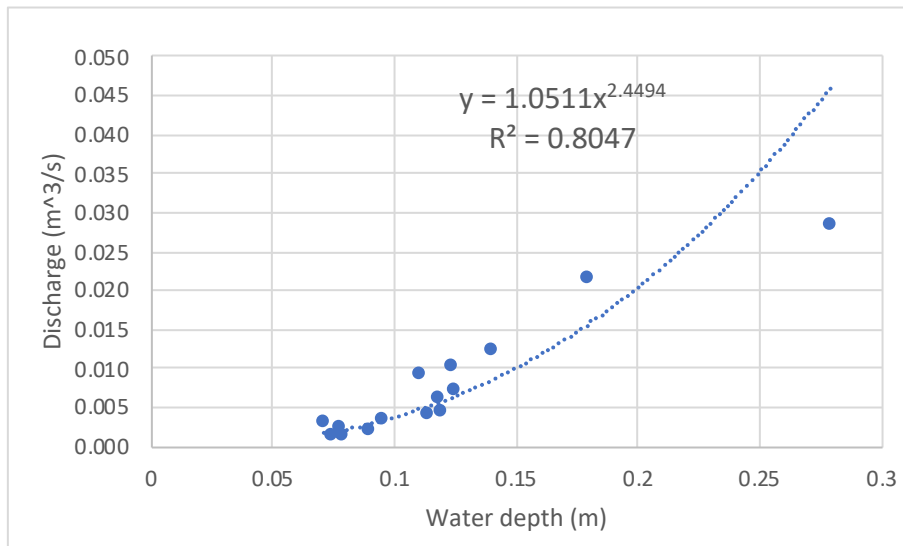| Dam	Valid	Change N°	Flow State Before	Flow State After	Date	Biotic Presence	Rainfall Presence	Rainfall total amount [mm]
Dam #3	0	NA	Gapflow	NDP	16-Jul	NA	NA	0
Dam #3	0	NA	NDP	Underflow	9-Aug	NA	NA	0
Dam #3	1	11	Underflow	Mixed (Gapflow-Underflow)	23-Aug	0	1	25.2
Dam #3	1	12	Mixed (Gapflow-Underflow)	Underflow	25-Aug	0	1	3.1

APPENDIX E – BEAVERPY CODE

This appendix includes the BeaverPy model code, including installation instruction, license, and examples. The code is available at https://github.com/ijaguirre/beaverpy_model and https://github.com/ijaguirre/beaverpy_model_dev. A shared folder with the examples is available at https://github.com/Ecohydrology-westbrook/beaverpy_sibbald_fen
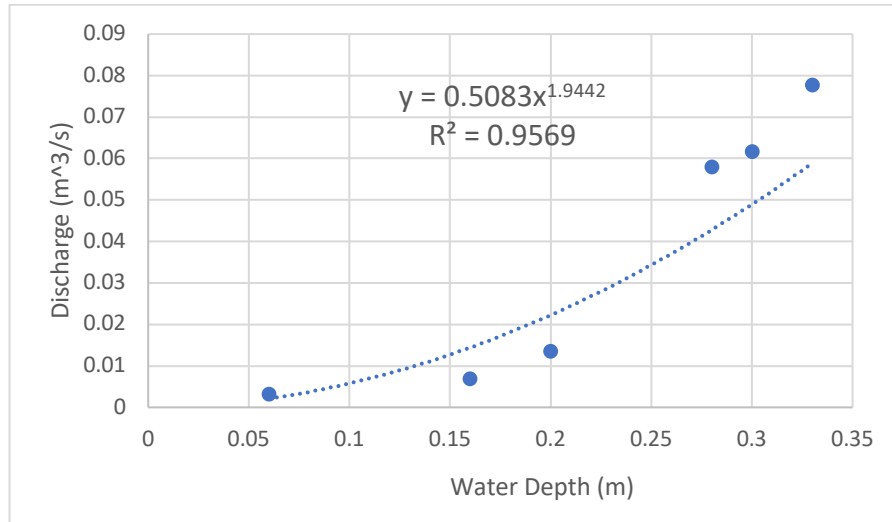
APPENDIX F – RATING CURVES

This Appendix includes the rating curve for each gauge station and a photograph to show the stream's shape. The inlet station had records from previous June to August 2017 fieldwork (Streich, 2019). The inlet and Dam #3 images were captured on August 10, and for Dams #1 and 2 on June 24, 2022
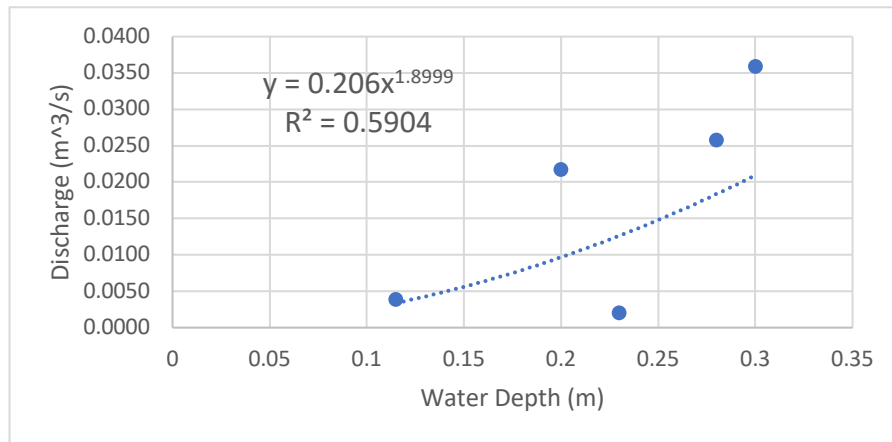
Inlet station

$y = 1.0511x^{2.4494}$
$R^2 = 0.8047$

Gauge station downstream Dam #1

$y = 0.5083x^{1.9442}$
$R^2 = 0.9569$

Discharge (m^3/s) vs Water Depth (m)

Gauge station downstream Dam #2

$y = 0.206x^{1.8999}$
$R^2 = 0.5904$

Discharge (m^3/s) vs Water Depth (m)

Gauge station downstream Dam #3